Analysis of GNSS point locations in forested areas

by

TAEYOON LEE

(Under the Direction of Pete Bettinger and Chris Cieszewski)

ABSTRACT

Thanks to recent developments in GNSS technologies, affordable consumer-grade GNSS receivers have been available for use in general forest activities. Especially, non-traditional consumer-grade GNSS receivers, which include smartphones and GPS watches, have garnered attention due to their usability and price range. However, there are still knowledge gaps regarding the positional error of non-traditional consumer-grade GNSS receivers, its effect on spatial point pattern analysis, and how nearby environmental conditions influence positional error. Therefore, three studies were developed to address this knowledge gap. The first study investigated the positional accuracy of a GPS watch by comparing it to a mapping-grade GNSS in different forest types, seasons, and meteorological conditions. The positional accuracy of the GPS watch was not significantly different in different forest types but was significantly different across seasons. The GPS watch provided a similar level of positional accuracy as the mapping-grade GNSS receiver during the leaf-off season. This study also confirmed a weak but significant correlation between positional accuracy and meteorological conditions (air temperature and absolute humidity). The second study was conducted to evaluate the feasibility of common methods to establish tree locations, and used spatial point pattern analysis to assess whether the pattern of trees in a forest, described by GNSS data, was consistent with the original pattern of

trees. This study confirmed that spatial information of trees collected by GNSS technology, without offending practicality of the data collection effort, failed to represent the original point pattern of trees in a real-world environment. This study also suggested that the inherent positional error of GNSS receivers might then mislead the results of spatial point pattern analysis if data are collected using normal field data collection protocols. The third study was conducted to assess the effect of nearby forest variables on positional accuracy of data collected by GNSS receivers. Correlation analysis was used to determine whether positional accuracy of data collected by various GNSS receivers was based on the vicinity and size of nearby trees. Some of statistically significant correlations were observed, but it was confirmed that the problem may be much more complicated to allow a generalization of the effects of forest conditions on positional accuracy, as the results were not consistent across GNSS receivers tested. Results of these studies expand upon the possibilities and limitations of using consumer-grade GNSS receivers in forested areas without significant augmentation methods.

INDEX WORDS: Consumer grade receiver, spatial point pattern analysis, horizontal positional accuracy, root mean square error, root square error of the mean

ANALYSIS OF GNSS POINT LOCATIONS IN FORESTED AREAS

by

TAEYOON LEE

M.Sc., University of Seoul, South Korea, 2016

A Dissertation Submitted to the Graduate Faculty of The University of Georgia in Partial Fulfillment of the Requirements for the Degree

DOCTOR OF PHILOSOPHY

ATHENS, GEORGIA

2022

ANALYSIS OF GNSS POINT LOCATIONS IN FORESTED AREAS

by

TAEYOON LEE

Major Professor:	Pete Bettinger
	Chris Cieszewski
Committee:	Marguerite Madden
	Jacek Siry
	Tripp Lowe
	Bogdan Strimbu

Electronic Version Approved:

Ron Walcott
Vice Provost for Graduate Education and Dean of the Graduate School
The University of Georgia
August 2022

DEDICATION

To my parents, *Yunchul Lee* and *Jungae Park* who always pray for me, to my delights *Josphe Eunsu Lee* and *Lydia Eunyu Lee*, who give me joy and rest, and to my wife, *Bokeum Won* who supports me with unconditional love and strong mind.

ACKNOWLEDGEMENTS

But God chose the foolish things of the world to shame the wise; God chose the weak things of the world to shame the strong. 1 Cor 1:27

I thank my Lord Jesus Christ for his abundant grace in getting me through this process. Tracking my doctoral degree has been a humbling experience where I have seen my weakness and rely on his authority.

I would like to express my gratitude to Dr. Bettinger who gave me the opportunity to continue the study and kept supporting me with patience. I feel like being privileged under your guidance, which is always helpful to proceed the research. I also thank Dr. Cieszewski who always suggested interesting research ideas. The conversation with you always finishes with open questions and lots of suggestions which make me obtain different research ideas. Additionally, I would like to thank my committee members, Drs. Marguerite Madden, Jacek Siry, Tripp Lowe, and Bogdan Strimbu for their time and comments on my dissertation. I also express my gratitude to my office mates, Shingo Obata, Alba Rocio Gutierrez Garzon, Volkan Bektas, and Joshua Temiofe Uzu. I always gain ideas and energy from conversations we had in room 4-321.

Lastly, Bokeum, thank you for your support and love; Eunsu and Eunyu, you are the biggest motivation to make me move forward. I love you, Bokeum, Eunsu, and Eunyu.

TABLE OF CONTENTS

Page

LIST OF TABLES

Page

LIST OF FIGURES

Page

CHAPTER 1

Introduction

Global Navigation Satellite Systems (GNSS) assist society in understanding where a person, animal, or vehicle may be located on Earth. The term Global Navigation Satellite Systems (GNSS) represents the broader collection of satellites used for navigating and determining locations on Earth. Nowadays, GNSS is considered as important infrastructure to our society as it has been incorporated into various systems and user applications, including transportation systems, power grid systems, communication systems, banking operations, safety of life, and advanced technologies (timing, scientific survey, earth observation, network synchronization) (Ioannides et al. 2016, Sanou 2013). As GNSS becomes integrated into more expansive applications, it is expected that its importance will continue to increase. Pham (2011) estimated its direct economic benefit on commercial usage was over $67.6 billion per year in the United States alone. The entire market of GNSS products and services is also expected to grow, with world-wide revenue expected to increase to about $300 billion in 2029 (GSA, 2019).

In North America, GNSS is colloquially referred to as GPS, which refers to the United States' NAVSTAR Global Positioning System. GNSS represents therefore the broader collection of satellite constellations that allow navigation, timing, and positioning on Earth. A person's location on Earth is determined using the electromagnetic waves emitted from the satellites and a method similar to trilateration, where the signals are decoded, and distances and directions are used to determine positions. Each satellite constellation emits electromagnetic waves at the speed

of light, with 19-25 cm wavelengths and frequencies (1.2 and 1.6 GHz) not overlapping other constellations (Teunissen and Montenbruck 2017). GNSS signals are unique and are modulated harmonic radio waves that contain a characteristic pseudorandom noise (PRN) code. The PRN code is a unique binary sequence of values that are repeated continuously with a certain interval. In addition, a set of information (ephemeris and signal propagation time) is embedded within each signal. As it has a unique pattern, each electromagnetic wave of energy emitted by a GNSS satellite plays a role as a fingerprint to help not only distinguish the satellite from which it came, but also to trilaterate a position on Earth. Based on the information contained within the signals from orbiting GNSS satellites, the distance between a GNSS receiver and a GNSS satellite is calculated. Theoretically, at least three of satellites are necessary to determine the location on the Earth, yet to determine a position accurately, information from a fourth satellite is necessary to distinguish between two alternative scenarios described by the intersection of three satellite signals, and to compensate for the receiver clock error (Figure 1.1). The GNSS receivers calculate the signal travel time using a “tracking loop” process which compares signals interpreted by a GNSS receiver to the signals emitted by a GNSS satellite (Teunissen and Montenbruck 2017).

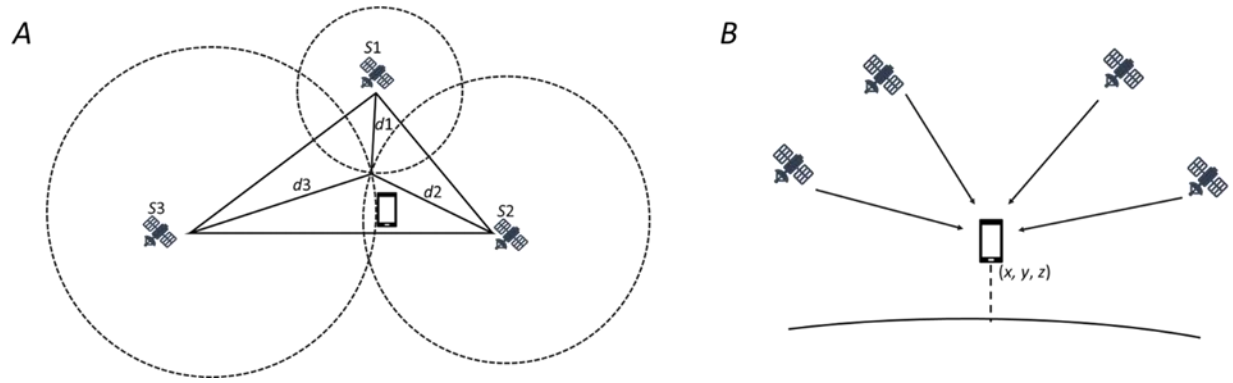

Figure 1.1 Concept of trilateration. The location of GNSS receiver determined using trilateration (range-based positioning) (*A*). The distance between satellites and receiver is calculated by multiplying signal propagation time by its velocity. Since there are two alternative positions determined through the signals of three orbiting satellites, at least four of satellites are necessary to locate the actual ground position (*x, y, z*) (*B*).

A general GNSS constellation system consists of three components: space segment, control segment, and user segment. The space segment refers to the groups of satellites transmitting the electromagnetic signals. For example, the NAVSTAR GPS program (operated by the United States) currently includes 30 of operational satellites, and each satellite orbits Earth twice a day at an altitude of about 20,200 km. The control segment includes ground facilities tracking the satellites, analyzing the information collected, and providing guidance to adjust satellite paths. The control segment of the NAVSTAR GPS program is now operated by the U.S. Space Force in Colorado Springs. The user segment refers to the multitude of GNSS receivers that access the signals emitted by these satellites. Nowadays, various kinds of GNSS receivers are available and they are generally classified into three groups: survey-grade, mapping-grade, and consumer-grade (Danskin et al. 2009b, Bettinger and Merry 2011, Lee et al. 2020). The more expensive

GNSS receivers generally guarantee higher horizontal positional accuracy, but the less-expensive, lower-grade GNSS receivers also provide relatively good horizontal position accuracy (5-10 m) in certain conditions thanks to continuous developments in GNSS technologies (Lee et al. 2022). Indeed, consumer-grade GNSS receivers such as smartphones and GPS watches have garnered attention due to their accessibility and price range (Keefe et al. 2019, Paziewski 2020).

Several GNSS satellite constellations have been deployed by different countries, including NAVSTAR GPS, GLONASS (Russia), BDS (BeiDou, China), Galileo (Europe), NavIC (India), and QZSS (Japan). Before the deployment of NAVSTAR GPS, the "Transit" system was developed in the United States. Transit, which became operational in 1964, was perhaps the world's first satellite-based positioning system that had a global reach (Parkinson et al. 2010). When its last pair of satellites were launched in 1988, there were 24 satellites in the Transit system, and it operated until 1996.

NAVSTAR GPS was developed for military and civilian purposes by the US Department of Defense, and until recently, it was managed by the U.S. Air Force. The first Block I NAVSTAR GPS satellites were launched in 1978. By 1995, 24 satellites were deployed and were fully operational. The system originally was designed to utilize two different frequencies, L1 (1575.42 MHz) and L2 (1227.6 MHz). The L1 frequency contains encrypted precision (P) code for authorized users and Coarse/Acquisition (C/A) code for civilian users. The L2 frequency is used only for authorized users. The C/A code was once intentionally degraded through selective availability (SA) until it was effectively turned off in 2000 (Keefe et al. 2019, Teunissen and

Montenbruck 2017). In more recent NAVSTAR GPS satellites, three new signals have been designed for civilian use: L2C, L5, and L1C. The program continuously deploys a new generation of satellites to replace the old satellites, and at any one time there are about 30 operational satellites in the constellation (U.S. Department of Commerce, National Oceanic Atmospheric Administration 2022). With regard to the control segment, the NAVSTAR GPS program has 29 ground control facilities that include the master control station in Colorado, an alternative master control station (California), 11 command and control antennas, and 16 monitoring sites.

The GLONASS (*Global'naya Navigatsionnaya Sputnikovaya Sistema*) program refers to the Russian satellite constellation. Although Russia launched its first satellite in 1957, their first navigation satellite was launched in 1967 (Roskosmos State Corporation, n.d.). Later, the "Cicada" system consisted of four satellites, which were deployed in 1979 to allow people to receive signals from one of the satellites every hour and a half or two hours. The first satellite in the GLONASS program was launched in 1982. The program became fully operational, with 24 of satellites, in 1996. Due to economic difficulties encountered in Russia, however, the number of operational satellites decreased over time so that only 7 were operational in 2002 (Roskosmos State Corporation, n.d.). With the advent of federal program "Global navigation system for 2002-2011", the program has since recovered to 24 operating satellites (Li et al. 2015). Satellites in the GLONASS program orbit at an altitude of 19,100 km and transmit signals on two different frequencies that include L1 (1620-1615.5 MHz) and L2 (1246-1256.5 MHz). The satellites that were launched from 2011 and 2014 also provide a new L3 frequency (1202.025 MHz). In addition, GLONASS satellites use frequency division multiple access and code division multiple

access methods to transmit information over a broad frequency range (Teunissen and Montenbruck 2017).

The Galileo program is a joint initiative of the European Commission (EC) and the European Space Agency (ESA). The program was developed due to a perceived need for independence from the NAVSTAR GPS and GLONASS programs (Bettinger and Merry, 2011, Teunissen and Montenbruck 2017). The first Galileo satellite was launched in 2011, and currently there are 26 of satellites in the constellation (European Space Agency, 2019). Satellites in the Galileo program are designed to orbit at an altitude of 23,222 km. Galileo became operational in 2016 and its satellites transmit signals across five frequencies: E1 (1575.46 MHz), E6 (1278.75 MHz), E5 (1191.795 MHz), E5a (1176.45 MHz) and E5b (1207.14 MHz)) (Keefe et al. 2019, Teunissen and Montenbruck 2017).

The Chinese navigational system, BeiDou (BDS), was initiated in 1980. Initially, the BeiDou program was a regional navigational system that consisted of four GEO (Geostationary) satellites that were launched between 2003 and 2007. The BeiDou-1 program was eventually replaced by the BeiDou-2 program to provide service to the Asia-Pacific region. The BeiDou-2 program was formerly known as COMPASS. The current BeiDou satellite navigation program, BDS-3, consists of 30 satellites that have provided global service since 2020 (China Satellite Navigation Office 2020, Keefe et al. 2019, Liu et al. 2022). The current program consists of three GEO satellites (35,786 km), three IGSO (inclined geosynchronous orbit) satellites (35,786 km), and 24 MEO (medium Earth orbit) satellites (21,528 km). Satellites in the BeiDou-3 program can

transmit signals in the L1/E1 and L5/E5 frequencies in addition to a B3 (1268.52 MHz) band (Teunissen and Montenbruck 2017).

In addition to the global navigation satellite systems mentioned above, there are two important regional navigation satellite systems, QZSS (Japan) and NavIC (India). The QZSS (Quasi-Zenith satellite system) program has been operational since 2018, and contains four of satellites called "Michibiki." It was designed to work as a complementary system to NAVSTAR GPS to ensure that a sufficient number of satellite signals were available in the urban canyons (cities with tall buildings) of the Asia-Oceania region (Cabinet Office, Government of Japan 2022). The QZSS satellites transmit signals that include: L1-C/A (1575. 42 MHz), L1C (1575.42 MHz), L2C (1227.6 MHz), L5 (1176.45 MHz), L1-SAIF (1575.42 MHz), and LEX (L-band Experiment, 1278.75 MHz), a QZSS experimental signal for high precision (3 cm level) service, sharing a frequency of the Galileo E6 signal. The NavIC (Indian Regional Navigation Satellite System) program provides two services: standard positioning service (SPS) and restricted service (RS). There are eight satellites orbiting in the system, including three GEO satellites and five GSO (Geosynchronous orbit) satellites (Department of Space, Indian Space Research Organisation 2022). NavIC satellites transmit dual frequency signals using 1176.45 MHz and 2492.028 MHz frequencies (Teunissen and Montenbruck 2017). In addition to these, South Korea also is developing its own satellite system, KPS (Korea positioning system), and plans to operate a regional program for East Asia and Oceania with seven geosynchronous satellites (Ji et al. 2021). Several signal augmentation processes may be used to enhance the accuracy of GNSS-determined positions on Earth. These processes can be classified as satellite-based augmentation systems (SBAS) and ground-based augmentation systems (GBAS) (Bettinger and Merry 2011,

Keefe et al. 2019). A SBAS refers systems where reference stations transmit a correction message to SBAS satellites, which then broadcast these to end users (Keefe et al. 2019). SBASs include WAAS (Wide Area Augmentation System), SDCM (System for Differential Correction and Monitoring), EGNOS (European Geostationary Navigation Overlay Service), MSAS (Multifunctional Transport Satellite (MTSAT) Satellite-based Augmentation System), and GAGAN (GPS-aided GEO Augmented Navigation System). WAAS is a regional SBAS program, and covers the continental United States, Alaska, Canada and Mexico. The WAAS program is managed by the U.S. Federal Aviation Administration and consists of three geo-stationary satellites, and multiple ground facilities that include 38 wide-area reference stations, three master stations, six ground uplink stations, and two operational control centers (U.S. Department of Commerce, National Oceanic Atmospheric Administration 2022). It utilizes the L1 and L5 bands to transmit correction messages to end users. The EGNOS program is maintained by the ESA and contains fours satellites that transmit correction messages using the L1 and L5 bands. The MSAS program was developed and maintained by Japan, and has one satellite broadcasting on the L1 band. The GAGAN program is maintained by the government of India, and three satellites in the system transmit correction messages using the L1 and L5 bands. The Russian program, SDCM, will use the L1 band when its three satellites are fully operational (Teunissen and Montenbruck 2017).

GBAS programs provide correction messages directly to end users from reference stations through radio or mobile data networks (Keefe et al. 2019). A GBAS is a form of differential GNSS that provides near real-time correction information between satellite pseudoranges and the generated pseudoranges by local base station (Bettinger and Merry 2011, Teunissen and

Montenbruck 2017). The correction messages are broadcast to end users directly via very high frequency (VHF, 30-300 MHz) or ultrahigh frequency (UHF, 300 MHz and 3 GHz) signal ranges (Teunissen and Montenbruck 2017). Perhaps the best examples of GBAS programs are Differential Global Positioning System (DGPS) and Real-Time Kinetic (RTK) augmentation. DGPS is a classic technique that was developed in the 1980s using fixed location reference stations. It compares data collected by a reference station to a true reference station ground position, then provides correction values that improve the positional accuracy of roving GPS receivers by reducing residual satellite and receiver clock error, satellite orbit error, and atmospheric propagation delay error (Teunissen and Montenbruck 2017). Information from DGPS base stations can be used in near real time or well after ground data have been collected, and base stations as far as 320 km from a field location may provide useable correction information. An RTK program is similar to a DGPS program, but is more localized (the base station is usually within 16 km of the field locations), and it receives and transmits carrier phase signals in addition to pseudoranges (Keefe et al. 2019). With either system, the effect of augmentation on position accuracy generally degrades with increasing distance between the reference station and end user (receiver) (Teunissen and Montenbruck 2017).

Error sources that deteriorate the accuracy of positions determined by GNSS receivers can be divided into two categories, depending on whether they are related to user equipment error (UEE) or signal-in-space range error (SISRE) (Liu et al. 2022, Teunissen and Montenbruck 2017). The error sources related to UEE include signal noise, multipath, and uncorrected atmospheric error (ionospheric and tropospheric delay) (Liu et al. 2022, Montenbruck et al. 2015). The error sources related to signal-in-space range error (SISRE) include errors in

ephemeris and clock conditions which, while periodically present, may be ameliorated by the space and ground segments of a GNSS program (Liu et al. 2022, Montenbruck et al. 2015). Atmospheric conditions propagate delays in GNSS signals, by changing their speed and direction of travel. These issues create signal noise (distortion) that occurs as satellite signals travel from about 20,000 km above Earth, through Earth's ionosphere and troposphere, to GNSS receivers. Some suggest that more than 50% of positional error occurs due to atmospheric propagation delays (Paziewski 2020). The neutral atmosphere is the part of atmosphere that is electrically neutral and stretches from ground level up to a height of 50 km and beyond (Teunissen and Montenbruck 2017). As most of the neutral atmospheric effects occur in the troposphere, it is referred to as tropospheric propagation delay. The resulting effects are different depending various factors such as the location or height of GNSS receivers, the weather conditions (temperature, pressure, and humidity), and the elevation angle (Bettinger and Merry 2011, Teunissen and Montenbruck 2017). Otherwise, the ionosphere is the upper atmosphere where free electrons exist ionized by radiations such as solar extreme ultraviolet (EUV) and x-rays (Guerova et al. 2016, Teunissen and Montenbruck 2017). The ionosphere is a dispersive medium for electromagnetic waves that attempt to pass through, and its effect is different depending on the frequency of electromagnetic waves and the electron density (total electron content, TEC) (Teunissen and Montenbruck 2017). In addition, its effect can be influenced by geographic location, local time, season, solar EUV flux, and magnetic activity as signals are affected the electrons existing in ionosphere. However, dual- or multi-frequency receivers can compensate ionosphere delay relatively easily (Paziewski 2020, Tomaštík and Varga 2021, Tomaštík et al. 2021, Zangenehnejad and Gao 2021).

Multipath error occurs when the signals from GNSS satellites are distorted by reflection or bouncing off of other objects. Therefore, the potential for multipath error depends on environment conditions (Teunissen and Montenbruck 2017), and it has been suggested to be the largest source of error in forested conditions (Danskin et al. 2009a). As long as a GNSS receiver is used in a forested area or urban canyon, multipath cannot easily be resolved. Various equipment can be employed to mitigate the impact of multipath error, such as an anechoic chamber, a choke ring antenna, or a radio frequency shield box or plate (Danskin et al. 2009, Fortunato et al. 2019, Gogoi et al. 2019, Li and Geng 2019, Tomaštík and Varga 2021), but these are not common and are often cumbersome to carry over long distances and long periods of time. Errors attributable to SISRE involve deviations in satellite position from the predicted ephemeris of satellite, due to the Earth's gravitational attraction, tidal forces, and solar radiation pressure (Teunissen and Montenbruck 2017). Clock errors can occur when a receiver clock does not synchronize exactly with the satellite clock (Bettinger and Merry 2011). This could happen because the clock in a GNSS receiver is not as stable as the atomic clock in a satellite. However, these SISRE effects are usually relatively small (i.e., represent less than a meter of positional error) (Teunissen and Montenbruck 2017).

The data obtained by GNSS receivers inherently contains a certain amount of positional error due to various error sources mentioned above. There are several common methods to evaluate the accuracy of positions determined by GNSS receivers, and they are often divided into two types: static positional accuracy and dynamic positional accuracy. Static accuracy assessments are conducted by comparing the observed positional information to known controls (true positions) while the GNSS receiver is held over the control point (Bettinger and Merry 2011).

Common measures to assess static positional accuracy include the root mean square error (RMSE), the root squared error of the mean (RSEM), and the circular error probable (CEP). The RMSE associated with field-collected GNSS data is the most frequently presented in accuracy assessments; it is calculated as the square root of the mean squared distance between a GNSS-determined position and a control point or true position (Lee et al. 2020, Ransom et al. 2010, Weaver et al. 2015). However, a general RMSE provides no information regarding direction of the error as it represents the deviation from the truth. The RSEM can be generated by calculating the distance between the average position of GNSS-determined points and their related control point (Bettinger and Fei 2010, Lee et al. 2020, Ransom et al. 2010). Here, the average position is equivalent to the mean center of observed points. Therefore, RSEM is useful for tracking directional trends in the distribution of observed points. The CEP is reported as the radius of a circle centered on the control point that contains a certain percentage of GNSS-determined positions (i.e., CEP_{50} is the radius of a circle containing 50% of GNSS-determined positions) (Bettinger and Merry 2011, Teunissen and Montenbruck 2017). Dynamic accuracy assessments are more complex and are evaluated by comparing the route or area observed by GNSS receivers to a real route (truth) or area. The difficulty lies in marking the real route or area in forest conditions, and then ensuring GNSS data is collected directly on top of the line defining the route or area boundary. In assessing dynamic accuracy, one can estimate the percentage of GNSS-determined points (vertices of lines or areas) that fall within specific buffers (e.g., 1 m, 2 m, etc.) that are created around the real route or area (i.e., Schipperijn et al. 2014, Ucar et al. 2014).

Objectives of the Dissertation

GNSS technology is an essential component of forest management, and it is used for various purposes that include navigation and position determination (Bettinger at al. 2019). The application of GNSS technology in forestry can be further described based on its use as a geofence or for activity recognition (Keefe et al. 2019). A geofence refers the application of GNSS technology to inform or influence the movement of a person or a machine based on a pre-defined boundary of acceptable activity. Activity recognition refers to the use of GNSS technology to simply track the movement of a person or animal. This application also includes the tracking harvest equipment or logging trucks as well as crews working in forested area. The popularity of using GNSS technology in forestry is also recognized by an increasing number of job descriptions requiring job candidates to have a knowledge of GNSS technologies (Bettinger and Merry 2018). In addition, recent developments in GNSS technologies have resulted in the miniaturization of GNSS chipsets and the lowering of their cost, which allows the technology to be more widely used in practice and academia. For example, miniaturized GNSS chipsets have been incorporated into various forms of GNSS receivers such as watches and smartphones (Lee et al. 2020). Smartphones are considered to be the most prevalent GNSS receivers these days based on number of sales (Gogoi et al. 2019, Paziewski 2020). Forestry professionals also seem to prefer lower-grade receivers (mapping-grade and consumer-grade) for general forestry activities rather than the survey-grade receivers (Bettinger et al. 2019, Keefe et al. 2019).

GNSS receivers have been widely studied in the forestry field, but the spatial aspect of positional error has rarely been considered (Bettinger and Merry 2012). Further, the accuracy of positions determined by GNSS receivers under forest canopies is often nowhere near that which is described in associated manufacturer's specification materials. This may be due to the complex environment within which practicing foresters must work is not the same as a manufacturer's test conditions, as satellite signals in forested areas suffer due to the interference by topography and canopy cover (Edson and Wing 2012). There have been many attempts to evaluate the positional error of GNSS receivers in forested conditions (i.e., Danskin et al. 2009b, Edson and Wing 2012). However, the results often lack consideration of directional error inherent in the data. One knowledge gap which has not yet been confirmed is whether the effects of nearby vegetation or environmental conditions on GNSS-determined positional error is random or systematic. Therefore, this dissertation was conducted to: (1) to evaluate the positional error of consumer-grade GNSS receivers (GPS watch and smartphone) in various environmental conditions (open area, hardwoods, pine forest); (2) to investigate the ability of GNSS-determined positions to effectively represent real tree patterns using spatial point pattern analysis; and (3) to assess whether develop the forest variables might be able to explain spatial aspects of positional error in GNSS-determined positions.

Chapters 2 and 3 contain work that has already been published, and are presented in this dissertation with permission from each publisher. Chapter 4 is in the process of being submitted to an international peer-reviewed journal. Each chapter is formatted following the author guidelines for each journal. Chapter 5 summarizes the key findings of each study and their contribution to science.

References

Bettinger, P. and Fei, S. 2010. One year's experience with a recreation-grade GPS receiver. Mathematical and Computational Forestry & Natural-Resource Sciences, 2(2): 153-160.

Bettinger, P. and Merry, K.L. 2011. Global navigation satellite system research in forest management: A summary of horizontal, vertical, static, and dynamic accuracy assessments. LAP Lambert Academic Publishing, Saarbrücken, Germany.

Bettinger, P. and Merry, K.L. 2012. Influence of the juxtaposition of trees on consumer-grade GPS position quality. Mathematical and Computational Forestry & Natural-Resource Sciences, 4(2): 81-91.

Bettinger, P. and Merry, K. 2018. Follow-up study of the importance of mapping technology knowledge and skills for entry-level forestry job postings, as deduced from recent job advertisements. Mathematical and Computational Forestry & Natural-Resource Sciences, 10(1): 15-23.

Bettinger, P., Merry, K., Bayat, M. and Tomaštík, J. 2019. GNSS use in forestry – A multi-national survey from Iran, Slovakia and southern USA. Computers and Electronics in Agriculture, 158: 369-383.

Cabinet Office, Government of Japan. 2022. Overview of the Quasi-Zenith Satellite System (QZSS). https://qzss.go.jp/en/overview/services/sv01_what.html (accessed June 2, 2022).

China Satellite Navigation Office. 2020. BeiDou Navigation Satellite System Signal in space interface control document. version 1. http://en.beidou.gov.cn/was5/web/search?channelid=249204 (accessed June 2, 2022)

Danskin, S., Bettinger, P. and Jordan, T. 2009a. Multipath mitigation under forest canopies: A choke ring antenna solution. Forest Science, 55(2): 109-116.

Danskin, S.D., Bettinger, P., Jordan, T.R. and Cieszewski, C. 2009b. A comparison of GPS performance in a southern hardwood forest: Exploring low-cost solutions for forestry applications. Southern Journal of Applied Forestry, 33(1): 9-16.

Department of Space, Indian Space Research Organisation. 2022. Indian Regional Navigation Satellite System (IRNSS) : NavIC. https://www.isro.gov.in/irnss-programme (accessed June 2, 2022).

Edson, C. and M.G. Wing. 2012. Tree location measurement accuracy with a mapping-grade GPs receiver under forest canopy. Forest Science, 58(6): 567-576.

European Space Agency. 2019. What is Galileo? https://www.esa.int/Applications/Navigation/Galileo/What_is_Galileo (accessed June 2, 2022).

Fortunato, M., Critchley-Marrows, J., Siutkowska, M., Ivanovici, M.L., Benedetti, E. and Roberts, W. 2019. Enabling high accuracy dynamic applications in urban environments using PPP and RTK on android multi-frequency and multi-GNSS smartphones. In 2019 European navigation conference (ENC). IEEE, New York. pp. 1-9.

Gogoi, N., Minetto, A., Linty, N. and Dovis, F. 2019. A controlled-environment quality assessment of android GNSS raw measurements. Electronics, 8(1), Article 5.

GSA. 2019. GNSS Market Report Issue 6, European GNSS Agency (GSA) Publications, Luxembourg. doi:10.2878/031762.

Guerova, G., Jones, J., Douša, J., Dick, G., de Haan, S., Pottiaux, E., Bock, O., Pacione, R., Elgered, G., Vedel, H. and Bender, M. 2016. Review of the state of the art and future

prospects of the ground-based GNSS meteorology in Europe. Atmospheric Measurement Techniques, 9(11): 5385-5406.

Ioannides, R.T., Pany, T. and Gibbons, G., 2016. Known vulnerabilities of global navigation satellite systems, status, and potential mitigation techniques. Proceedings of the IEEE, 104(6): 1174-1194.

Ji, G.-H., Shin, H. and Won, J.-H. 2021. Analysis of multi-constellation GNSS receiver performance utilizing 1-st side-lobe signal on the use of SSV for KPS satellites. IET Radar, Sonar & Navigation, 15(5): 485-499.

Keefe, R.F., Wempe, A.M., Becker, R.M., Zimbelman, E.G., Nagler, E.S., Gilbert, S.L. and Caudill, C.C. 2019. Positioning methods and the use of location and activity data in forests. Forests, 10(5): Article 458.

Lee, T., Bettinger, P., Cieszewski, C.J. and Gutierrez Garzon, A.R. 2020. The applicability of recreation grade GNSS receiver (GPS watch, Suunto Ambit Peak 3) in a forested and an open area compared to a mapping-grade receiver (Trimble Juno T41). PLoS ONE, 15(3): e0231532.

Li, G. and Geng, J. 2019. Characteristics of raw multi-GNSS measurement error from Google Android smart devices. GPS Solutions, 23(3): Article 90.

Li, X., Zhang, X., Ren, X., Fritsche, M., Wickert, J. and Schuh, H. 2015. Precise positioning with current multi-constellation global navigation satellite systems: GPS, GLONASS, Galileo and BeiDou. Scientific Reports, 5: Article 8328.

Liu, W., Jiao, B., Hao, J., Lv, Z., Xie, J. and Liu, J., 2022. Signal-in-space range error and positioning accuracy of BDS-3. Scientific Reports, 12: Article 8181.

Montenbruck, O., Steigenberger, P. and Hauschild, A. 2015. Broadcast versus precise ephemerides: a multi-GNSS perspective. GPS Solutions, 19(2): 321-333.

Parkinson, B.W., S.T. Powers, G. Green, H. Fruehauf, B. Strom, S. Gilbert, W. Melton, B. Huston, E. Martin, J. Spilker, F. Natali, J. Strada, B. Glazer, D. Schwartz, T. Stansell and others. 2010. The origins of GPS, and the pioneers who launched the system. GPS World, 21(6): 8-18.

Paziewski, J. 2020. Recent advances and perspectives for positioning and applications with smartphone GNSS observations. Measurement Science and Technology, 31(9): Article 091001.

Pham, N.D. 2011. The economics of disruption: $96 billion annually at risk, GPS World, Jul. 2011. https://www.gpsworld.com/gnss-systemthe-economics-disruption-96-billion-annually-risk-11825/ (accessed June 2, 2022).

Ransom, M.D., Rhynold, J. and Bettinger, P. 2010. Performance of mapping-grade GPS receivers in southeastern forest conditions. RURALS: Review of Undergraduate Research in Agricultural and Life Sciences, 5(1): Article 2.

Roskosmos State Corporation. n.d. About GLONASS. https://www.glonass-iac.ru/en/about_glonass/ (accessed June 2, 2022).

Sanou, D.A. 2013. Analysis of GNSS interference impact on society and evaluation of spectrum protection strategies. Positioning, 4(2): 169-182.

Schipperijn, J., Kerr, J., Duncan, S., Madsen, T., Klinker, C.D. and Troelsen, J. 2014. Dynamic accuracy of GPS receivers for use in health research: a novel method to assess GPS accuracy in real-world settings. Frontiers in Public Health, 10(2): Article 21.

Teunissen, P.J. and Montenbruck, O. 2017. Springer handbook of global navigation satellite systems (Vol. 10). New York, NY, USA. Springer International Publishing.

Tomaštík, J., Chudá, J., Tunák, D., Chudý, F. and Kardoš, M. 2021. Advances in smartphone positioning in forests: dual-frequency receivers and raw GNSS data. Forestry, 94(2): 292-310.

Tomaštík, J. and Varga, M. 2021. Practical applicability of processing static, short-observation-time raw GNSS measurements provided by a smartphone under tree vegetation. Measurement, 178: Article 109397.

Ucar, Z., Bettinger, P., Weaver, S., Merry, K.L. and Faw, K. 2014. Dynamic accuracy of recreation-grade GPS receivers in oak-hickory forests. Forestry, 87(4): 504-511.

U.S. Department of Commerce, National Oceanic Atmospheric Administration. 2022. GPS: The Global Positioning System. www.GPS.gov (accessed June 2, 2022).

Weaver, S.A., Ucar, Z., Bettinger, P. and Merry, K. 2015. How a GNSS receiver is held may affect static horizontal position accuracy. PLoS ONE, 10(4): e0124696.

Zangenehnejad, F. and Gao, Y., 2021. GNSS smartphones positioning: Advances, challenges, opportunities, and future perspectives. Satellite Navigation, 2: Article 24.

CHAPTER 2

The applicability of recreation-grade GNSS receiver (GPS watch, Suunto Ambit Peak 3) in a forested and an open area compared to a mapping-grade receiver (Trimble Juno T41)[1]

[1] Lee, T., Bettinger, P., Cieszewski, C. J., & Gutierrez Garzon, A. R. 2020. Published by PLoS ONE, 04/17/2020.

Abstract

Due to developments in global navigation satellite systems (GNSS) and the miniaturization of their components, the usage of Global Positioning System (GPS) is no longer restricted to professional applications, but has become available in various consumer type devices, such as wristwatches. These commercial devices, however, were primarily designed for tracking activities in predominately urban settings and their accuracy has not been tested in forested areas. In this study, we present an assessment of the positional accuracy of a GPS watch (Ambit Peak 3, Suunto, Finland) under different forest cover types, seasons and meteorological conditions within the Whitehall Forest GPS Test Site located in Athens, Georgia, USA. As a standard of comparison, the performance of the GPS watch measurements was juxtaposed to that of a mapping-grade receiver (Juno T41, Trimble Inc., USA). In this study, we analyzed the differences between the determined and control positions using root-mean-square-error (RMSE), along with the distribution of observed positions through the standard deviational ellipse. The results suggest that the seasonal variations contributed to a statistically significant impact on the RMSE values for the GPS watch. However, there were no statistically significant differences in horizontal position accuracy by forest cover-type when using the GPS watch. Furthermore, no significant differences were found in horizontal position accuracy during the leaf-off period between the RMSE values for the GPS watch and those of the mapping-grade receiver. Lastly, the positional accuracies for both types of receivers were found to be weakly, but significantly correlated with fluctuations in air temperature and absolute humidity.

Introduction

Although some discussions concerning the development of global navigation satellite systems (GNSS) occurred before the 1980s, their notable development began in earnest on the NAVSTAR GPS (United States) and GLONASS (Russia) systems during the 1980s. In the most recent years, there have been further developments by other entities, such as China's BeiDou/COMPASS and European Union's GALILEO projects. Each of these four systems provide publicly available signals, which hardware technology manufacturers can subsequently use to develop commercially available GNSS receivers. Consequently, since around the turn of the millennium there has been a rapid development in GNSS software and hardware. These developments have led not only to improvements in the reliability of GNSS, but also to its widespread commercial availability. For instance, the miniaturization of GNSS antennas and chips has allowed them to be incorporated into various types of digital devices, ranging from smartphones or smart wearables to wristwatches (1, 2). These types of non-traditional GNSS receivers allow people to become accustomed to the use of GNSS technology in their daily lives yet they provide very little information on the quality of data they generate. For instance, while many people may use smartphones to navigate unfamiliar territories, knowledge on the accuracy by which these devices portray horizontal positions on Earth is slowly forthcoming (e.g., (3)). Furthermore, many in the general public are beginning to use GPS watches to navigate or track their activities while exercising, without proper understanding of the impact that various meteorological conditions may have on GPS functionality. Currently, it is uncertain whether the positional information derived from non-traditional types of GNSS receivers can serve as a

reliable substitute in non-ideal circumstances, relative to the reliable information collected by traditional mapping-grade, which are often used to acquire sufficient quality positional information demanded by forest management or forestry research professionals (4).

In the forestry literature, GNSS receivers are generally classified into three groups: survey-grade, mapping-grade, and recreation or consumer-grade. In a general sense, the capability of horizontal position accuracy of individual receivers has been positively correlated with their prices (5, 6). From this perspective, cellular phones and tablets that act as GNSS receivers would fall within the recreation-grade class from both a cost and a horizontal accuracy perspective (7). Although survey-grade GPS receivers typically provide the highest positional accuracy in forests (8), the cost, knowledge, and skill required to operate these receivers, as well as the residence time required to determine a position (perhaps 20 minutes) hinder their use in typical forestry applications. Concerning mapping-grade receivers, this group typically achieves good static horizontal position accuracy under relatively open sky conditions (sub-meter) and in forests (2-5 meters) (9, 10). Moreover, due to their moderate price range and the high degree of accuracy that they provide, mapping-grade receivers are commonly used for both forest management and forestry research purposes (4). On the other hand, recreation-grade receivers generally provide the lowest accuracies, often in the 5-15 m range (11, 12), but are compensated by their low purchase price. This affordability of recreation-grade receivers makes them a relatively accessible and attractive option for non-professional applications. GPS watches can be classified as recreation or consumer-grade receivers because of their price and observed levels of positional accuracy.

As there are few notable brands which produce GPS watches, vigorous debate exists about their accuracy and reliability among the increasing number of people who use them. Since the GPS watch acts as an attractive alternative to a traditional GNSS receiver, its application and limitations should be documented. For instance, GPS watches have been used to monitor children and elderly people in urban areas and to track vehicle speed in motorsports (1, 2). Although researchers have already attempted to evaluate the usefulness of GPS watches currently offered on the consumer market, the methodology employed has been limited by either addressing the positional accuracy without conducting formal tests, or by conducting tests that failed to include a precise control.

Although some GPS watches have been designed for outdoor recreational purposes, their positional accuracies in forested areas have not yet been evaluated. Similar to urban areas, where artificial structures may interfere with GNSS signals, forested areas are also considered very challenging due to the interference by the topography and canopy cover, which mask and block signals (13-15). While many studies have examined the accuracy of recreation-grade and mapping-grade GNSS receivers in forested areas (9-11, 16, 17), the horizontal position accuracy of GPS watches in forested areas has yet to be evaluated. Furthermore, while a few studies have investigated the relationship between meteorological conditions and recreation-grade and mapping-grade GNSS receiver accuracy, no study to date has investigated the relationship between meteorological conditions and the accuracy of a GPS watch (11, 16-18).

Therefore, this study was conducted to evaluate the static horizontal position accuracy of a GPS watch when used under different cover types, seasons, and meteorological conditions. The

performance of the GPS watch was also compared to that of a mapping-grade GNSS receiver under identical environmental conditions. The hypotheses of this research are as such:

H1: The static horizontal position accuracy of the GPS watch is not significantly different between the leaf-on and the leaf-off seasons.

H2: The static horizontal position accuracy of the GPS watch is not significantly different between its uses in a coniferous forest, deciduous forest, and an open field.

H3: The static horizontal position accuracy of the GPS watch does not significantly change with variations in meteorological conditions (air temperature, relative/absolute humidity, atmospheric pressure, and wind speed).

H4: The static horizontal position accuracy of the GPS watch does not significantly differ from that of a mapping-grade GNSS receiver.

Materials and Methods

We conducted this study to assess the quality of static horizontal position data as measured by two GNSS receivers: a Suunto GPS watch (Ambit Peak 3, Suunto, Finland) and a Trimble GNSS device (Juno T41, Trimble Inc., USA). The Suunto GPS watch is much lighter than most other GNSS receivers, weighing approximately 89 grams. The watch is equipped with the GPS L1 patch antenna (15×15×4 mm) made by Patron Co. Ltd (Korea), which is relatively small and contained inside the watch. Furthermore, the watch contains a rechargeable battery, which can last up to 200 hours depending on the amount and type of activity. For static horizontal data collection, the display of the GPS coordinate system and compass declination was set to UTM

NAD1983 and as 5.5º degrees west, respectively. Although the watch allows users to change the GPS fixed intervals with three different levels, namely a “Best” interval (~ 1 sec), a “Good” interval (~ 5 sec), and an “OK” interval (~ 60 sec), this is only possible when it is tracking activities (dynamic horizontal data collection). Unlike many higher-grade receivers, the Suunto GPS watch did not allow for defining masks for the maximum positional dilution of precision (PDOP) and the minimum signal-to-noise ratio (SNR, the ratio between received power of signal and noise power).

The Trimble GNSS unit (Juno T41, Trimble Inc., USA) is considered a mapping-grade GNSS receiver with a wide range of operating temperatures (-30℃ to 60 ℃). It is equipped with a multi-function antenna (GPSGLONASS08N-S3-03-A, Inpaq technology Co., Ltd., Taiwan) that is larger than that of the GPS watch (70×43.18×9 mm). SOLO Forest software (Trimble Forestry Automation 2009) is used to collect and save the data. The maximum PDOP level on this receiver was set to 8, a moderate setting for the satellite geometric arrangement, and the minimum SNR was set to 4. The real-time, space-based augmentation was enabled using the wide area augmentation system (WAAS) satellite signal. Although the Suunto GPS watch and Trimble GNSS receiver are fundamentally different, a comparison between their accuracies would be helpful in ascertaining the current utility and limitations of recreation-grade GNSS receivers.

To assess the horizontal position accuracy of the two GNSS receivers under forested conditions, we conducted this study at the Whitehall Forest GPS Test Site (gps-test-site.uga.edu) located in Athens, Georgia (USA). This test site was established in 2004 by professional surveyors, and it

contains 3 monuments and 37 control points. The three monuments consist of an aluminum pin, about 9 cm in diameter and 1 m long, driven into the ground so that the top is flush with the ground level. The 37 control points each consist of a brass survey cap attached to a piece of rebar (about 0.5 m long), encased in cement (about 30 cm in diameter), where the survey cap is flush with the ground level. The positions of the three survey monuments were established using an Ashtech Locus survey-grade GNSS receiver. Data were collected for these three survey monuments over the span of four hours and subsequently processed using the Online Positioning User Service (OPUS), which is managed by the U.S. Department of Commerce, National Oceanic, and Atmospheric Administration (www.ngs.noaa.gov/OPUS). These three monuments have been accepted into the National Spatial Reference System (NSRS), with their positional precision certified to under 2 cm. Using the three monuments as a base, professional surveyors conducted a closed traverse survey of the 37 control points using a Topcon GTS-211D instrument. The resulting closure of the closed traverse network was estimated to be 1/92,137, and the positions of the 37 control points are estimated to have similar horizontal position accuracy of approximately 2 cm. It is considered, therefore, that the Whitehall Forest GNSS Test Site is a highly accurate model around which GNSS equipment could be tested.

Three of the control points that we selected for this study were located within an older coniferous forest, containing *Pinus echinata* and *Pinus taeda* which were 70 to 80 years age. The density of this area was estimated to be 223 trees ha-1, and the basal area was estimated to be 26.0 m^2 ha^{-1}. Three other control points we selected were located within an older deciduous forest consisting of *Quercus* spp., *Carya* spp., *Ostrya virginiana*, and other species, also 70 to 80 years age. The density in this area was estimated to be 126 trees ha^{-1}, and the basal area was estimated to be

23.0 m^2 ha^{-1} (Fig 2.1). These six control points were visited 17 times between 3:00 p.m. and 4:30 p.m. during the leaf-on season (September-October) and 17 times during the leaf-off season (December). In total, this resulted in 51 independent visits to control points in the coniferous forest and 51 independent visits to control points in the deciduous forest during each season. Furthermore, an open field NSRS monument was visited 17 times during each season.

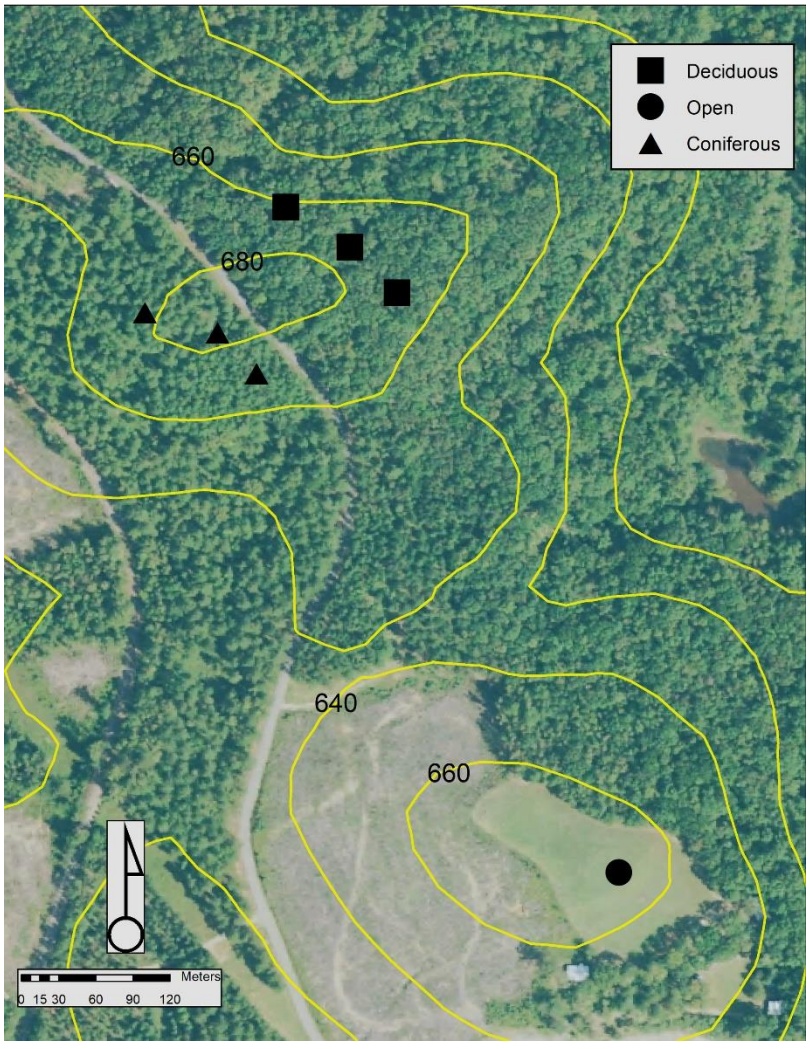

Figure 2.1 The surveyed area with control points, located at the Whitehall Forest GPS Test Site in Athens, Georgia (USA).

When the GNSS data were collected, we randomized the forest cover type (coniferous or deciduous), and further randomized the order of the three control points within each forest cover type, in an attempt to avoid potential biases. During each visit to a control point, each of the two GNSS receivers was positioned on top of a monopod (1.3 m) equipped with a leveling device. Researchers consistently positioned themselves on the north side of control points as the data were collected. Furthermore, an effort was made to ensure that the internal GNSS antenna of each device was positioned directly above the control points as the data were collected. The open field measurement was visited after the coniferous and deciduous control points were surveyed since it was about 1 km away by road. The Trimble GNSS receiver was allowed to warm-up (approximately 5 min) before its use. The Suunto GPS watch was always on and was therefore assumed to be ready for data collection purposes. The Suunto GPS watch collected a single waypoint at each control point during all visits. On the other hand, at each particular visit, about 15 position fixes per point were collected at 1-second intervals using the Trimble receiver. These position fixes were subsequently averaged, prior to downloading the data from the Trimble device, to produce a single position fix during each visit to each control point. We followed this protocol to be consistent with normal field data collection practices of foresters. Since the data collected by the Suunto GPS watch was saved in degrees (longitude and latitude to the specificity of the sixth decimal place) using the WGS 1984 coordinate system, this data was converted to UTM coordinates using ArcMap GIS software (version 10.6.1, Esri Inc., Redlands, CA, USA) for further processing. The Trimble GNSS device saved data in both formats of WGS and UTM coordinates. The difference (static horizontal position error) between each determined position and the associated control point position was computed using the root mean square error (RMSE), as has been done in many previous studies (i.e., Bettinger and Fei 2010, Bettinger and

Merry 2012, Danskin et al. 2009, Sigrist et al. 1999, Weaver et al. 2015). RMSE can be calculated as follows:

$$\text{RMSE} = \sqrt{\sum_{i}^{n}((x_i - x)^2 + (y_i - y)^2) \,/\, n}$$

Where n is the total number of observations in a visit; i is the i^{th} observation of the visit; x_i and y_i are respectively the easting and northing of the i^{th} observations; and x and y are the true easting and northing of the associated control point. Unlike the standard deviation which assesses accuracy using deviations from a mean value, the RMSE was considered as a good estimator to evaluate its accuracy because it represents the deviation from the truth, not the from the mean (19). In addition to the RMSE, the root squared error of the mean (RSEM) is calculated based on the mean center's coordinates as follows:

$$\text{RSEM} = \sqrt{\left(\frac{\sum_{i}^{n}(x_i - x)}{n}\right)^2 + \left(\frac{\sum_{i}^{n}(y_i - y)}{n}\right)^2}$$

Where n is the total number of observations in a visit; i is the i^{th} observation of the visit; x_i and y_i are the longitude and latitude of the i^{th} observations; and x and y are the true easting and northing of the associated control point. Standard deviational ellipses were also calculated to investigate the trends of determined positions, to assess whether these are related to cover type or season. Among standard deviational ellipses parameters, the anisotropic ratio was calculated as follows:

$$I_a = \frac{R - r}{R} \times 100\%$$

Where I_a is anisotropic ratio; R and r are the length of ellipse long and short axis, respectively.

Meteorological data, including air temperature, relative/absolute humidity, wind speed and barometric atmospheric pressure, were obtained for the relevant time period of each visit from a local weather station (Athens, Georgia airport). This data was used in statistical tests to determine their correlation with horizontal position error. In particular, these meteorological variables were selected due to their potential influence on GNSS signals as they pass through Earth's lower troposphere. The aforementioned local weather station reported these metrics in one-hour intervals, and thus a linear interpolation was performed to estimate their values at approximately the time of data collection. The absolute humidity, on the other hand, was calculated using a web-based calculator (https://planetcalc.com/2167/) because it was not directly monitored. Since the majority of RMSE values were normally distributed, we applied the one-way ANOVA, Kruskal-Wallis test, the Student's *t*-test and the Welch's *t*-test to test the hypotheses noted above using R Studio software (version 1.1.463, RStudio, Inc., Boston, MA, USA). The RSEM and parameters of standard deviational ellipses were calculated with ArcMap GIS software (version 10.6.1, Esri Inc., Redlands, CA, USA).

Results

Concerning H1, the observed RMSE values were analyzed using a Welch's *t*-test according to the season in which the data were collected. We found a significant difference in the mean RMSE values between the leaf-on and leaf-off seasons when using the GPS watch ($p\text{-}value < 0.001$) (Fig 2.2). For the Trimble GNSS receiver, meanwhile, no statistically significant differences were observed in the static horizontal position accuracy for either the leaf-off (mean = 3.50 m, standard deviation = 1.85 m) or leaf-on seasons (mean = 4.03 m, standard deviation =

2.34 m) (Student's *t*-test, *p-value* = 0.21). Therefore, we reject H1 and conclude that horizontal position accuracy of the GPS watch was significantly different between two seasons.

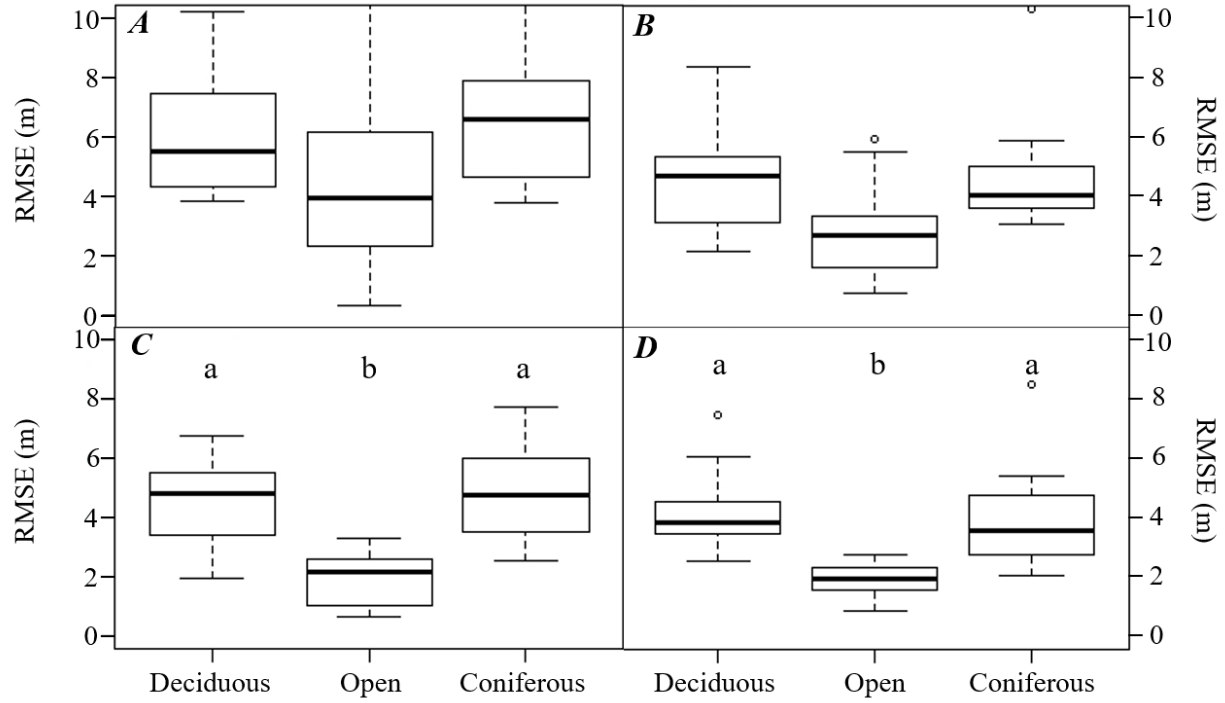

Figure 2.2 Boxplots for horizontal positional accuracy (RMSE) by equipment type (GPS watch: *A*, *B*; Mapping-grade GNSS receiver: *C*, *D*), cover type, and season (Leaf-on: *A*, *C*; Leaf-off: *B*, *D*). *Different letters* indicate significant differences (For *A* and *B*, Scheffe's Test at *p-value* < 0.05; for *C* and *D*, Dunn's Test at *p-value* < 0.05).

Table 2.1 The summary of elliptical parameters measured by different GPS equipment during different seasons (RSEM = root squared error of the mean; Mean X coordinate = the mean of difference between observed X coordinates and control X coordinate; Mean Y coordinate = the mean of difference between observed Y coordinates and control Y coordinate; I_a = the anisotropic ratio).

Metrics / Device	Leaf-on time period				Leaf-off time period			
	All three sites	Coniferous forest	Deciduous forest	Open field	All three sites	Coniferous forest	Deciduous forest	Open field
Suunto watch GPS								
RSEM (m)	12.21	10.06	15.81	15.01	2.70	3.11	2.20	3.94
Mean X coordinate (m)	-12.16	-9.17	-14.40	-14.43	-2.56	-2.77	-1.95	-3.72
Mean Y coordinate (m)	-1.04	4.13	-6.51	4.13	-0.85	-1.41	-1.01	1.29
Angle of rotation (°)	109.54	122.54	48.06	112.77	84.17	84.19	149.54	82.45
I_a (%)	17.27	37.61	18.04	65.35	59.07	63.01	12.66	83.95
Area of ellipse (m^2)	3525.6	2610.05	3881.4	2398.05	160.37	187.46	56.24	169.13
Trimble Juno T41								
RSEM (m)	2.82	2.93	2.49	1.65	2.27	2.39	1.72	1.69
Mean X coordinate (m)	-2.79	-2.85	-2.42	-0.65	-2.27	-2.39	-3.72	-1.20
Mean Y coordinate (m)	-0.35	-0.67	-0.57	1.52	0.06	0.13	1.29	1.19
Angle of rotation (°)	83.82	133.72	31.25	161.87	81.06	52.80	30.82	32.27
I_a (%)	41.78	19.96	18.26	38.16	48.20	4.46	20.61	21.50
Area of ellipse (m^2)	122.33	77.69	62.37	4.47	102.85	54.40	51.92	2.84

Table 2.2 Summary results of dataset, with outliers, of the horizontal position error of the GPS watch and mapping-grade GNSS receiver at the Whitehall Forest GPS Test Site in Athens, Georgia (USA).

Metrics / Device	Leaf-on time period				Leaf-off time period			
	All three sites	Coniferous forest	Deciduous forest	Open Field	All three sites	Coniferous forest	Deciduous forest	Open field
Suunto watch GPS								
Mean RMSE (m)	24.25	22.06	29.63	9.27	5.62	6.47	4.52	3.32
Minimum RMSE (m)	0.32	3.80	3.83	0.32	0.77	3.06	2.18	0.77
Maximum RMSE (m)	105.80	81.17	85.32	105.80	55.06	36.61	8.36	55.06
Standard deviation of RMSE (m)	27.48	23.72	25.91	32.86	8.59	7.95	1.63	12.76
n	119	51	51	17	119	51	51	17
Trimble Juno T41								
Mean RMSE (m)	4.03	5.40	4.81	1.87	3.50	4.33	4.29	1.88
Minimum RMSE (m)	0.66	2.58	1.96	0.66	0.89	2.05	2.53	0.89
Maximum RMSE (m)	10.33	10.33	9.56	3.29	10.00	10.00	7.46	2.77
Standard deviation of RMSE (m)	2.34	2.25	1.89	0.92	1.85	2.14	1.29	0.54
n	119	51	51	17	119	51	51	17

To represent how the determined GPS positions were spread around the control points, we used the standard deviational ellipse method for point data distribution analysis (Fig 2.3). The orientation angle of the GPS watch during the leaf-on season was 109.54°, and its I_a was 17.27% (Table 2.1). This small I_a value suggests that the GPS points might have been distributed in a circular spread rather than an elliptical distribution (Table 2.1). When considered in conjunction with the area of an ellipse, the observed GPS data points for the GPS watch during the leaf-on season were widely spread from the center of the standard deviational ellipse in a circular distribution area. In contrast, during the leaf-off season, the orientation angle of the GPS watch was 84.17°, and I_a was 59.07% (Table 2.1). The ascertained area of ellipse during the leaf-off season was smaller than the area during the leaf-on season. This indicates that the observed data points collected during the leaf-off season were more clustered and distributed more closely in relation to the control points.

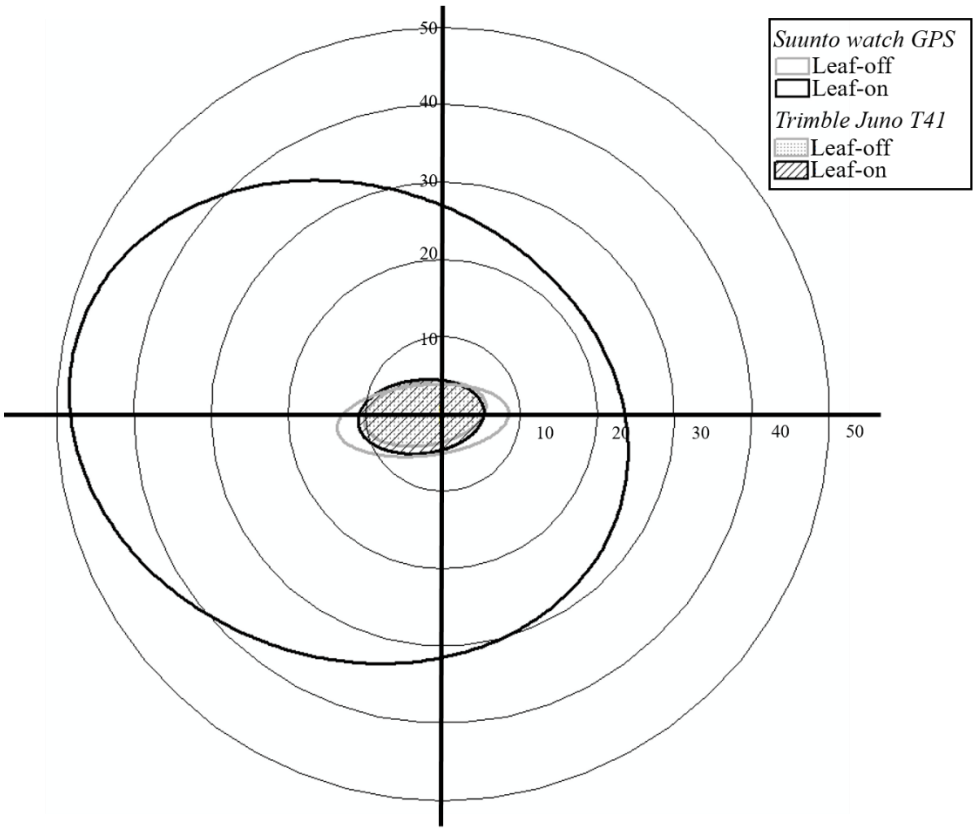

Figure 2.3 The distributions and standard deviational ellipses of translocated GPS points data obtained by different types of equipment during different seasons.

The point data distribution analysis for the Trimble receiver did not show any differences in response to the season. For this analysis, we obtained an orientation angle of 83.82°, and an I_a of 41.78% during the leaf-on season (Table 2.1). Similarly, the distribution of observed GPS points during the leaf-off season had an orientation angle of 81.06° and an I_a of 48.20%. Here, the I_a values were moderately substantial, suggesting that the GPS points were comparatively spread out on the longest axis of the ellipse (Fig 2.3). In both seasons, the areas of the ellipses were very similar to each other, and the centers of the ellipses were very close to the control point in every case.

Regarding H2, the RMSE values observed by GPS watch and Trimble receiver were analyzed using a one-way ANOVA and Kruskal-Wallis test, to determine whether cover type affected each instruments' horizontal position accuracy. It was found that there was no statistically significant difference between cover types using the GPS watch, as shown in the results ($F_{2,99}$= 0.242, *p-value* = 0.786) (Fig 2.4). Although the minimum (best) RMSE was observed in the open field (Table 2.2), there was no statistically significant difference in the response variable to the cover types in either the leaf-on season ($F_{2,48}$ = 0.485, *p-value* = 0.619) or the leaf-off season ($F_{2,48}$ = 0.224, *p-value* = 0.8). However, we found statistically significant differences in the accuracy of the Trimble GNSS receiver in the cover types regardless of the season (*p-value* < 0.01) (Fig 2.4). The lowest RMSE values were found in the open field, and this was significantly different compared to the RMSE values from the forested cover types. There was no significant difference in RMSE values observed in the deciduous and coniferous forest areas. In sum, for the GPS watch, we could not reject H2; however, for the Trimble GNSS receiver, we reject H2, as we found that static horizontal position accuracy varies significantly depending on the cover type.

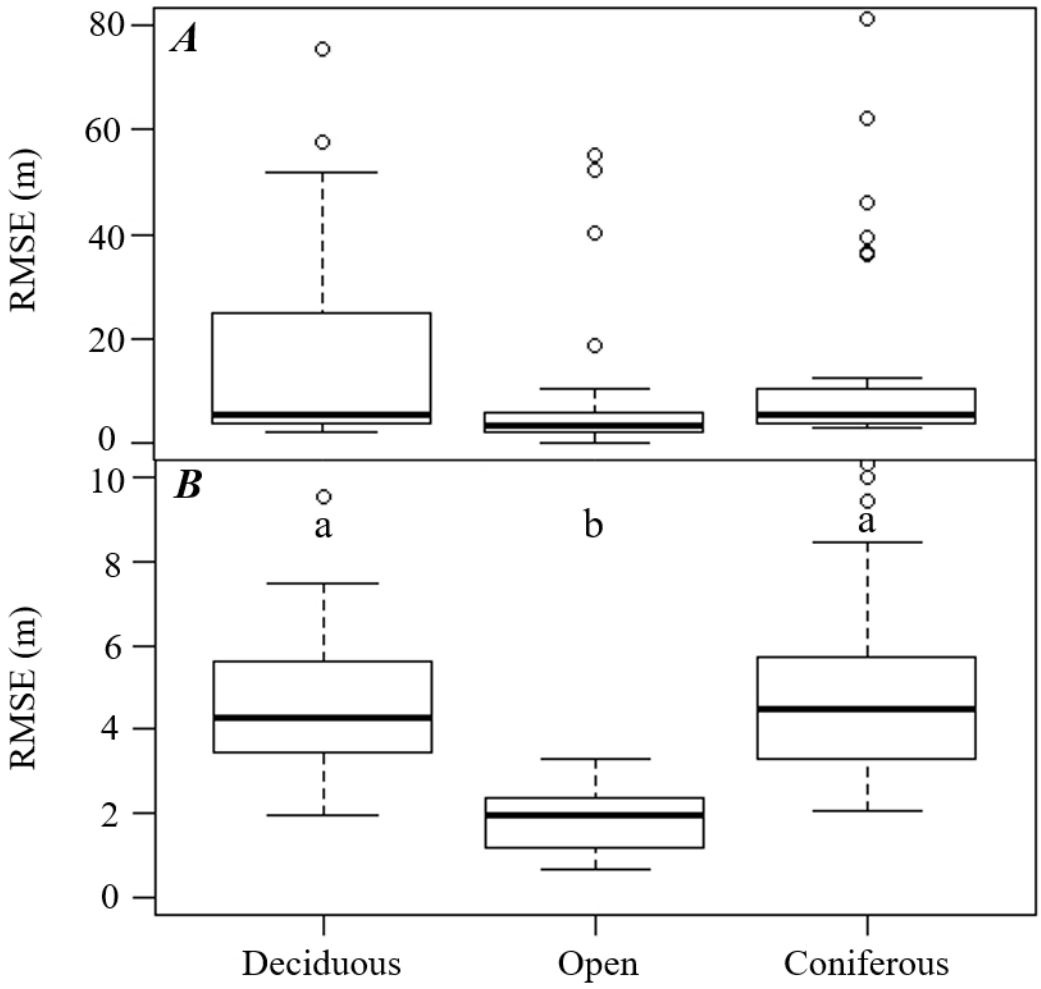

Figure 2.4 Boxplots describing horizontal positional accuracy (RMSE) by equipment type (GPS watch: *A*; Mapping-grade GNSS receiver: *B*) and cover type. *Different letters* indicate significant differences (Dunn's Test at *p-value* < 0.05).

The RSEM values for the GPS watch were much higher during the leaf-on season than during the leaf-off season. During the leaf-on season, the highest and lowest RSEM values were found in the deciduous forest and coniferous forest, respectively (Table 2.1). Otherwise, during the leaf-off season, the highest and lowest RSEM values were obtained in the open field and

deciduous forest, respectively. The mean X coordinate values were negative regardless of the season and cover type, indicating that the observed points were consistently located to the west of the control point (Table 2.1). Furthermore, the areas of the ellipses during the leaf-on season were much larger than during the leaf-off season. Meanwhile, the RSEM values for the Trimble receiver were found to be similar to the RSEM values for GPS watch during the leaf-off season. The highest and lowest RSEM values were found in the coniferous forest and open field respectively, regardless of the season. The mean X coordinate values were also negative regardless of season and cover type, and the areas of the ellipse were also similar to the those of the GPS watch during the leaf-off season.

For H3, the correlation coefficient *r* values were summarized in Table 2.3. These values indicate that air temperature and absolute humidity were significantly correlated with RMSE, regardless of equipment type. For both the Suunto watch and the Trimble receiver, weak positive correlations were found between the RMSE and the air temperature (0.26 and 0.20 for GPS watch and Trimble receiver, respectively) and between the RMSE and the absolute humidity (0.22 and 0.15 for GPS watch and Trimble receiver, respectively). Except for the temperature and absolute humidity, there were no other observed significant correlations between the horizontal position accuracy and meteorological factors. In sum, we only found weak positive correlation between RMSE values and air temperature or absolute humidity.

Table 2.3 Summary of Pearson correlation coefficients for RMSE and meteorological factors.

Env. factors / Device	Air temp. (°C)		Relative humidity (%)		Absolute humidity ($g \cdot m^{-3}$)		Wind speed (mph)		Barometric pressure (inches)	
	r	*p -value*	*r*	*p-value*	*r*	*p -value*	R	*p -value*	*r*	*p-value*
Suunto Watch GPS	0.26 ***	< 0.001	-0.07	0.2997	0.22 ***	< 0.001	-0.08	0.208	0.02	0.7984
Trimble Juno T41	0.20 **	0.002	-0.08	0.2246	0.15*	0.02	-0.02	0.801	0.05	0.4855

*** Statistically significant difference, *p-value* < 0.001
** Statistically significant difference, *p-value* < 0.01
* Statistically significant difference, *p-value* < 0.05

Table 2.4 Summary of the comparison between RMSE observed by different equipment type using a Welch's *t*-test (*p-value* < 0.05).

Forest cover type / Period	Coniferous Forest	Deciduous Forest	Open field
	p -value	*p -value*	*p -value*
Whole year	$p = 0.007$*	$p = 0.002$*	$p = 0.013$*
Leaf-on	$p = 0.011$*	$p = 0.001$*	$p = 0.029$*
Leaf-off	$p = 0.297$	$p = 0.648$	$p = 0.215$

* Statistically significant difference, *p-value* < 0.05

Finally, concerning H4, we applied the Welch's *t*-test to compare RMSE values observed by the GPS watch and the mapping-grade GNSS receiver, in response to the cover type and seasons. It was found that there were no significant differences observed during the leaf-off season regardless of the cover type (Table 2.4). Otherwise, there were significant differences during the leaf-on season, and across both seasons. In conclusion, we partially fail to reject H4 because there was no significant difference in RMSE values by GPS watch and mapping-grade GNSS receiver during the leaf-off season. However, we reject H4 with respect to the leaf-on season.

Discussion

Using a Trimble mapping-grade receiver as a basis of comparison, this study attempted to assess the accuracy of a recreation-grade GPS watch in response to the seasonal fluctuations and variations in the canopy cover and to investigate the correlation between the accuracy of the watch and meteorological factors that included humidity, air temperature, atmospheric pressure, and wind speed. The accuracy of the GPS watch was found to be significantly enhanced during the leaf-off season relative to the leaf-on season. In comparison, the accuracy of mapping-grade GNSS receiver was found to not be affected by seasonal fluctuations. One study (5) also had similar results, in that the significant effect in response to the change in season was only found when it was measured using the recreation-grade GNSS receiver, not with the mapping-grade GNSS receiver. Another study (17) conducted at the same site also found that the static horizontal accuracy was not affected by season using a mapping-grade GNSS receiver. Cumulatively, these results indicated that mapping-grade GNSS receivers might not be affected by the seasonal fluctuation, whereas the recreation-grade GNSS receivers do appear to be more

sensitive to the seasonal fluctuation. Although vegetation obstruction introduces a degree of error in the forested area through the blockage of satellite signals or through multipath signals (11, 20, 21), the defoliation during the winter season in the deciduous forests had a weak, but positive effect on enhancing the static horizontal position accuracy. Indeed, there was a significant increase in accuracy observed in every cover type (coniferous forest, deciduous forest, and open field) during the leaf-off season in this study. In other studies, the improvement in accuracy during leaf-off season in the deciduous forest was not observed (5, 11, 17). One possible explanation for the improvement of GPS watch accuracy during the leaf-off season, regardless of cover type, is the cumulative error caused by different meteorological conditions such as relatively low temperature and absolute humidity during leaf-off season that had a positive correlation with the RMSE values (negative correlation with accuracy) (16, 19, 22, 23). Furthermore, due to the improvements in accuracy observed during leaf-off seasons, there was no significant difference between accuracy of GPS watch and mapping-grade receiver during this season. This suggests that the GPS watch could be used to replace the mapping-grade receivers when considering cost efficiency, especially during leaf-off season.

Even though the outliers were also considered in this study, the static horizontal positions determined by the recreation-grade GNSS receiver and the mapping-grade GNSS receiver in the forested conditions had relatively low mean RMSE values in the range of 4.52 to 29.63 m and 4.29 to 5.40 m, respectively. These results were similar to other studies' results (recreation-grade GNSS receiver: 7 to 12 m, and mapping-grade GNSS receiver: 1 to 5 m) that were conducted at the same location (9, 11, 12, 17). These results confirm that our research was conducted reliably and indicate that the watch-type recreation-grade GNSS receiver maintained similar degree of

accuracy to the conventional handheld type of recreation-grade GNSS receiver in a forested area. The significant effects cover type had on static horizontal position accuracy were only observed when the mapping-grade GNSS receiver was used, not when the GPS watch was used due to the large variances observed. However, this significant difference was only found between the open field and forested area (coniferous and deciduous forest), not between the coniferous and deciduous forests. These results contrasted with other studies that have shown a significant difference in static horizontal position accuracy when using a recreation-grade GNSS receiver among varying forest cover type (5, 11, 12, 24). However, other studies (16, 17) did not find a significant difference in static horizontal position accuracy between forest cover types; yet, these studies employed mapping-grade GNSS receivers. These results indicate that the cover type itself is not the main factor affecting the static horizontal position accuracy. Rather, it suggests that canopy coverage might be the primary consideration when determining the GPS receiver accuracy (19). Indeed, the GPS accuracy was shown to be improved in a young coniferous forest relative to an old coniferous forest (11, 24, 25) and further accuracy improved in post-thinning conditions compared to the pre-thinning conditions (9).

We applied the standard deviational ellipse to investigate the direction or tendency of error, depending on the season and cover type; this study was the first of its type in forestry research to use GNSS data in this manner. As the standard deviational ellipse is a measure of the distribution of observed points, it provided information about the data concentration, including orientation (determined by the direction of the longest axis of observed points), anisotropic ratio (ratio of the longest and shortest axes), and the area of the ellipse intuitively through images and quantification (26). Although the area of ellipse was considerably smaller during leaf-off season

than during the leaf-on season regardless of GPS receiver type, a specific tendency in the orientation and the area of an ellipse was not observed in response to the cover type. However, the mean center of each ellipse was located on the western side of the control points regardless of the GPS receiver types. There have been a few studies considering the direction of the error (9, 11, 18). One study (9) using evaluations of rose diagrams confirmed that the bias in error changes in response to thinning. Our results showed that there were more points distributed on the western side of the control points as opposed to the eastern side. Although the location of nearby trees around control points was not investigated in our study, Bettinger and Merry (18) suggested that the vegetation near the control point influenced the direction and magnitude of the positional error. Another possible explanation for the biased distributions of the observed points is the movement of satellites within the constellation or the Earth's rotation. Finally, while we used the average value of 15 position fixes from the Trimble device to evaluate these, the use of the original 15 position fixes may have revealed some balanced error. However, at this time we are unable to determine whether the standard deviational ellipses would have been different had we evaluated them in this manner.

Prior studies have indicated that there was no correlation between meteorological variables of the lower troposphere and static horizontal position accuracy (11, 16-18). The only study (16), among the aforementioned studies, found a significant and negative correlation between air temperature and RMSE values at the deciduous forest using a mapping-grade GNSS receiver. In our study, however, we found a significant, but weakly positive correlation between air temperature and RMSE regardless of GPS receiver type. The air temperature appears to have receiver-specific effects on horizontal position accuracy, as there was no consistent correlation

between air temperature and RMSE values in other studies, regardless of GPS receiver types. Other studies have considered the correlation between relative humidity and RMSE (11, 16-18), but this study investigated the correlation between absolute humidity and RMSE, in which it found a significant, albeit weakly positive correlation. This phenomenon could be explained by the influence atmospheric water vapor has upon the travel of the GPS signal from the satellite. This could be achieved either by delaying the GPS signal propagation, thereby reducing the signal speed, or by causing additional multipath effects (16, 19, 23). Furthermore, the engrossing trend was observed that the RMSE values measured by the GPS watch were increased when the wind direction was suddenly changed. However, due to the limitations of this study, not all meteorological variables were precisely monitored at the forest, and the change in wind direction was not sufficiently quantified to determine the correlation between wind direction and RMSE values.

Conclusion

The study presented here investigated the static horizontal position accuracy of a GPS watch under varying forest cover types, seasonal fluctuations, and meteorological conditions. To evaluate the relative accuracy of the GPS watch, a mapping-grade GNSS receiver was used to compare coordinates outputs to those of the GPS watch. The key findings of this study were as follows: (1) the accuracy of the GPS watch was significantly affected by the season, but not by the cover type; (2) during the leaf-off season, the accuracy of the GPS watch did not differ significantly relative to the accuracy of the mapping-grade GNSS receiver; (3) the RMSE values of both GPS receivers had a significant but weakly positive correlation with air temperature and

absolute humidity. These results suggest that canopy coverage, rather than the forest cover type, might play a more critical role in governing the static horizontal position accuracy of GPS receivers in forested areas. Furthermore, the GPS watch showed improvements in static horizontal position accuracy during the leaf-off season, so that it had a similar level of accuracy to that of a mapping-grade GNSS receiver. Our results suggest that GPS watch might be able to provide an acceptable quality of locational information for forest management purposes during the leaf-off season. However, due to the limitations inherent to a small antenna, the quality of location information might not be able to guarantee acceptable static horizontal position accuracy during the leaf-on season. A recently released GPS watch (after our data collection process was completed) that is equipped with improved GPS antenna and the Assisted-GPS (A-GPS) technology, can determine location information from network stations and various technologies employed in the mobile terminals of the Differential GPS (D-GPS). This technology uses fixed and known positions to correct the GPS signal and might provide better static horizontal position accuracy in various conditions.

Regarding the effects of meteorological variables, the GPS watch and the mapping-grade GNSS receiver both indicated a significant correlation between positional accuracy and two environmental variables (air temperature and absolute humidity). Accordingly, air temperature and absolute humidity should be considered when these types of GPS receivers are used in forested areas. Our study had some limitations in that (1) the GPS watch used for this study was released in 2014, and may therefore not be a reliable indicator of the current technological state of GPS watches; (2) the locations of nearby trees were not measured to explain the distributions of observed points, and (3) the meteorological variables within the forest were not monitored in

an all-encompassing manner. Nevertheless, our study determined the accuracy of a GPS watch in various circumstances and illustrated the potential application of the GPS watch for forest management purposes, especially during the leaf-off season. Although users will need to decide whether the accuracy and reliability of a GPS watch is sufficient for their purposes, they should keep in mind that even mapping-grade GNSS receiver accuracy can vary depending on the working conditions, such as changes in canopy cover and meteorological conditions. Given falling prices and ease-of-accessibility, the GPS watch may serve as a circumstantially attractive replacement for the mapping-grade GNSS receivers. Further research exploring the technological developments in future GPS watches is therefore a relevant and useful endeavor.

Acknowledgements

We appreciate and value the thoughtful concerns and suggestions of the anonymous reviewers of this manuscript.

Author Contributions

All authors were involved in designing this research. TL carried out the experiments and performed the analysis. PB, CC and ARGG provided advice, comments and substantive input to the writing of the manuscript. All authors have read and agreed to the published version of the manuscript.

References

1. Gløersen ØN, Kocbach J, Gilgien M. Tracking performance in endurance racing sports: Evaluation of the accuracy offered by three commercial GNSS receivers aimed at the sports market. Frontiers in Physiology. 2018;9:1425.

2. Omr M, Georgy J, Noureldin A. Using multiple portable/wearable devices for enhanced misalignment estimation in portable navigation. GPS Solutions. 2017;21(2):393-404.

3. Merry K, Bettinger P. Smartphone GPS accuracy study in an urban environment. PLoS ONE. 2019;14(7).

4. Bettinger P, Merry K, Bayat M, Tomaštík J. GNSS use in forestry–A multi-national survey from Iran, Slovakia and southern USA. Computers and Electronics in Agriculture. 2019;158:369-83.

5. Danskin SD, Bettinger P, Jordan TR, Cieszewski C. A comparison of GPS performance in a southern hardwood forest: Exploring low-cost solutions for forestry applications. Southern Journal of Applied Forestry. 2009b;33(1):9-16.

6. Fauzi M, Idris N, Yahya M, Din A, Lau A, Ishak M. Tropical forest tree positioning accuracy: A comparison of low cost GNSS-enabled devices. International Journal of Geoinformatics. 2016;12(2):59-66.

7. Tomaštík JJ, Tomaštík JS, Saloň Š, Piroh R. Horizontal accuracy and applicability of smartphone GNSS positioning in forests. Forestry. 2016;90(2):187-98.

8. Ordoñez C, Martínez J, de Cos Juez JF, Lasheras FS. Comparison of GPS observations made in a forestry setting using functional data analysis. International Journal of Computer Mathematics. 2012;89(3):402-8.

9. Akbulut R, Ucar Z, Bettinger P, Merry K, Obata S. Effects of forest thinning on static horizontal positions collected with a mapping-grade GNSS receiver. Mathematical and Computational Forestry & Natural-Resource Sciences. 2017;9(1):14-21.
10. Bettinger P, Merry K. Global Navigation Satellite System Research in Forest Management: A Summary of Horizontal, Vertical, Static, and Dynamic Accuracy Assessments: LAP Lambert Academic Publishing; 2011.
11. Bettinger P, Fei S. One year's experience with a recreation-grade GPS receiver. Mathematical and Computational Forestry & Natural-Resource Sciences. 2010;2(2):153-60.
12. Bettinger P, Merry K. Static horizontal positions determined with a consumer-grade GNSS receiver: One assessment of the number of fixes necessary. Croatian Journal of Forest Engineering. 2012a;33(1):149-57.
13. Danskin S, Bettinger P, Jordan T. Multipath mitigation under forest canopies: A choke ring antenna solution. Forest Science. 2009a;55(2):109-16.
14. Edson C, Wing MG. Tree location measurement accuracy with a mapping-grade GPS receiver under forest canopy. Forest Science. 2012;58(6):567-76.
15. Pirti A. Using GPS near the forest and quality control. Survey Review. 2005;38(298):286-98.
16. Ransom MD, Rhynold J, Bettinger P. Performance of mapping-grade GPS receivers in southeastern forest conditions. RURALS: Review of Undergraduate Research in Agricultural and Life Sciences. 2010;5(1):Article 2.
17. Weaver SA, Ucar Z, Bettinger P, Merry K. How a GNSS receiver is held may affect static horizontal position accuracy. PLoS ONE. 2015;10(4):e0124696.

18. Bettinger P, Merry K. Influence of the juxtaposition of trees on consumer-grade GPS position quality. Mathematical and Computational Forestry & Natural-Resource Sciences. 2012b;4(2):81-91.
19. Sigrist P, Coppin P, Hermy M. Impact of forest canopy on quality and accuracy of GPS measurements. International Journal of Remote Sensing. 1999;20(18):3595-610.
20. Dussault C, Courtois R, Ouellet J-P, Huot J. Evaluation of GPS telemetry collar performance for habitat studies in the boreal forest. Wildlife Society Bulletin. 1999;27(4):965-972.
21. Klimánek M. Analysis of the accuracy of GPS Trimble JUNO ST measurement in the conditions of forest canopy. Journal of Forest Science. 2010;56(2):84-91.
22. Coster A, Williams J, Weatherwax A, Rideout W, Herne D. Accuracy of GPS total electron content: GPS receiver bias temperature dependence. Radio Science. 2013;48(2):190-196.
23. Bevis M, Businger S, Herring TA, Rocken C, Anthes RA, Ware RH. GPS meteorology: Remote sensing of atmospheric water vapor using the Global Positioning System. Journal of Geophysical Research: Atmospheres. 1992;97(D14):15787-801.
24. Wing MG. Consumer-grade global positioning systems (GPS) receiver performance. Journal of Forestry. 2008;106(4):185-190.
25. Wing MG, Eklund A, Kellogg LD. Consumer-grade global positioning system (GPS) accuracy and reliability. Journal of Forestry. 2005;103(4):169-173.
26. Yuill RS. The standard deviational ellipse; an updated tool for spatial description. Geografiska Annaler: Series B, Human Geography. 1971;53(1):28-39.

Supporting Information

S1 Data. Spreadsheet containing GPS data collected

S2 Data. Weather associated with data collection)

CHAPTER 3

Mission impossible: Positions determined by basic mapping-grade and recreation-grade GNSS receivers cannot emulate the actual spatial pattern of trees[2]

[2] Lee, T., Bettinger, P., Merry, K., Bektas, V., & Cieszewski, C. 2022. Published by Mathematical and Computational Forestry & Natural-Resource Sciences (MCFNS), 04/30/2022. Reprinted here with permission of the publisher 06/02/2022.

Abstract

Global navigation satellite systems (GNSS) can provide valuable spatial information for effectively mapping and navigating through complex terrain and forest conditions. Relatively accurate positional information is essential for certain algorithms and models that base analyses on the spatial arrangement of trees, and for management of forestry operations. The accuracy of GNSS receivers has been well-tested under many environmental conditions. Depending on the technology selected and conditions within which it is employed, different amounts of variation will occur in the determination of a horizontal position. However, studies involving the spatial pattern and distribution of tree locations (point positions) observed by independent GNSS receivers generally have not considered the horizontal position error inherent in the spatial data. We conducted this study to investigate whether tree locations determined by recreation- and mapping-grade GNSS receivers can adequately represent the real point pattern of trees in a forest. The study area was a pine seed orchard located at the Whitehall Forest in Athens, Georgia (USA), that consisted of a regular pattern of trees. We tested three different GNSS receivers: one mapping-grade receiver and two recreation-grade receivers (traditional, handheld-type, and non-traditional types, GPS watch). With each receiver we determined tree locations at cardinal points around the stems of 112 trees (at North, South, East, and West sides of the stems) and estimated the middle point measurement of two cardinal points (North-South, and East-West). In addition, we used the average of all cardinal points (All) to determine tree locations. We compared these observed tree locations to actual tree locations which were determined through precise field measurements and high-precision GPS base points. This study confirmed that the horizontal positional error of mapping grade receivers was significantly lower than those of recreation

grade receivers, regardless of measurement method. However, the observed point pattern of trees from the GNSS observations of both recreation- and mapping-grade receivers failed to adequately represent the actual regular point pattern of the trees, as the positional error observed was not consistently projected in the same direction and with the same magnitude.

Keywords: Global navigation satellite system, complete spatial randomness, regular pattern, clustered pattern, root mean squared error, GPS receivers

Introduction

The natural pattern of the location of trees is a result of ecological processes involving self-thinning and competition between trees and seed dispersal mechanisms. In planted forests, the pattern of the location of trees is operationally influenced yet can also be influenced by ecological processes involving pioneer and natural establishment of non-planted trees. For assessing patterns of trees, spatial point pattern analysis (SPPA) has become increasingly popular in ecological research (Gadow et al. 2012, Velázquez et al. 2016, Woodall 2002, Wiegand et al. 2013, Wiegand & Moloney 2013). As a way for analyzing the pattern of trees, SPPA allows one to characterize forest structure (i.e., dispersed, random, clustered) and test ecological hypotheses about underlying natural processes (Law et al. 2009, Ripley 1981, Velázquez et al. 2016, Wiegand & Moloney 2013). For example, SPPA has been used to investigate the effects of seed dispersal mechanisms (Garzon-Lopez et al. 2014, Seidler & Plotkin 2006) and to analyze the role of interactions and competition between trees (Dohn et al. 2017, Fajardo et al. 2006, Uria-Diez & Pommerening 2017).

SPPA compares the pattern of observed spatial data to a null model using various summary statistics. To evaluate the pattern of objects, SPPA uses point locations (i.e., locations trees, nests, or shrubs) and supplementary information (attributes) that characterize the object (i.e., surviving versus dead, species, size) (Velázquez et al. 2016). Further, the data can be classified as unmarked and marked spatial data based on its properties. For example, unmarked spatial data having a *priori* properties include such things as tree species, while marked spatial data having a *posteriori* properties including such things as status (surviving versus dead), size, or some other property from a marking process (Velázquez et al. 2016, Wiegand & Moloney 2013). SPPA provides a description of the spatial pattern of measured features using summary statistics, which are classified as either (a) numerical or functional or (b) location- or point-related (Illian et al. 2008, Wiegand & Moloney 2013). Outcomes of SPPA can represent spatial pattern as a value (e.g., intensity or the mean distance to the nearest neighbor) (Pommerening & Grabarnik 2019, Velázquez et al. 2016), and these have been widely used in modern point pattern analysis to represent a point pattern as a function of scale (Wiegand & Moloney 2013).

The null model (also referred to as the point process model or point process) associated with a SPPA analysis is a mathematical model representative of a certain point pattern (Wiegand & Moloney 2013). The null model plays an important role in SPPA because it is used to determine whether an observed spatial pattern can be statistically distinguished from it or not (Carrer et al. 2018, Diggle 2013, Wiegand & Moloney 2013). The simplest version of a null model is complete spatial randomness (CSR) following the homogeneous Poisson process, which assumes an equal intensity or distribution of objects across a study area (Carrer et al. 2018, Law et al.

2009, Wiegand & Moloney 2013). One might expect that a naturally regenerated or uneven-aged forest would possess CSR with respect to tree locations. Otherwise, a null model may also follow a heterogeneous Poisson process, which has a different intensity function that depends on the locations of objects within the study area (Carrer et al. 2018, Pommerening & Grabarnik 2019, Wiegand & Moloney 2013). SPPA compares an observed pattern to a confidence envelope, or group of null models generated by Monte Carlo simulation (Law et al. 2009). When an observed pattern of objects lies outside of a confidence envelope with a certain confidence level, this provides evidence of a departure from the null model (Wiegand & Moloney 2013). Otherwise, when an observed pattern of objects fails to prove departure from the null models, this indicates that there is no correlation between observed points, which is equivalent to saying that there are no ecological interactions evident in the data (Pommerening & Grabarnik 2019).

The result of SPPA is influenced by many factors. For example, spatial scale (size of sampling site) for the detection of tree patterns can be important, as larger sampling scales allow one to better detect a spatial pattern, such as clustering, that are not evident at smaller scales (Carrer et al. 2018, Garzon-Lopez et al. 2014). Further, using the heterogeneous Poisson model as a null model for emulating CSR may provide more reliable results than using the homogeneous Poisson model, since constant intensity across a study site may not be guaranteed (Carrer et al. 2018). Perry et al. (2006) and Hui et al. (2007) suggested that each summary statistic used in evaluating spatial pattern has limitations and strengths. Further, Gadow et al. (2012) and Pommerening (2008) pointed out that the application of spatial pattern analysis may be limited by the size of study area. Therefore, Velázquez et al. (2016) and Wiegand et al. (2013) suggested

that the various summary statistics should be applied together, to avoid omitting important meanings from spatial patterns.

In describing the distribution of trees in a forest, the positions (spatial coordinates) of tree boles are an essential input for SPPA (Aguirre et al. 2003, Pommerening 2002). For forest growth and yield purposes, the positions of tree boles are also needed for distance dependent tree growth models. However, collecting spatial data of tree bole positions can be very challenging due to the cost and time associated with the data collection effort, making the practical application of SPPA challenging (Aquirre et al. 2003, Gadow & Hui 2002, Gadow et al. 2012, Velázquez et al. 2016). For example, it might take more than 30 minutes to determine a tree's location if a survey-grade GNSS receiver is used. This is one reason why survey-grade GNSS receivers are not widely used in practice except to locate property corners or other important landscape positions. Further complicating the collection of tree bole locations, several studies that have been conducted to evaluate GNSS receiver accuracy in forested areas revealed that mapping grade and recreation-grade GNSS receivers have horizontal positional errors ranging on average more than 2 m (Danskin et al. 2009, Ransom et al. 2010, Sigrist et al. 1999) and more than 6 m (Danskin et al. 2009, Lee et al. 2020), respectively, in any direction from the true position. A greater positional error is often observed when using recreation-grade GNSS receivers (small inexpensive GNSS specific units, cellular phones, watches, etc.), yet recreation-grade receivers are still utilized frequently due to their applicability and accessibility. According to Bettinger et al. (2019), foresters in the southern United States commonly use cellular phones and tablets (70.6%) for positioning and navigation, followed by other recreation-grade receivers (49.4%) and mapping-grade receivers (43.8%). Bettinger et al. (2019) also indicated that only a few respondents used

survey-grade receivers (2.8%) and mapping-grade receivers with differential processes (DGPS) (15%) in their normal work activities. Platforms such as iNaturalist and iTree Eco have also allowed citizen observers to provide positional data using recreation-grade GNSS receivers (Fauzi et al. 2016a). Therefore, the quality of positions determined by GNSS for individual trees may be a great concern.

Compounding the issue of horizontal position accuracy, the physical direction of the position error is often unreported and assumed randomly distributed around a true position, yet the directionality of error may be influenced by nearby vegetation (Bettinger & Merry 2012b). Current SPPA studies do not consider the inherent error in positions determined by GNSS receivers, potentially leading to analysis error when spatial relationships are based on the distance between objects (i.e., distances between objects or counts of objects within certain distance). To overcome these challenges, different approaches to estimate the positions of trees have been explored, including the use of base maps facilitated by satellite images (Atkinson et al. 2007, Moustakas et al. 2008), aerial images from aircraft or unmanned vehicles (Garzon-Lopez et al. 2014, Moustakas et al. 2008, Xu et al. 2019), or LiDAR (light detection and ranging) including terrestrial and airborne laser scanning (Trochta et al. 2013). However, there are limitations in estimating the location of tree stems from these types of images, due to image quality, spatial resolution, and feature displacement. Specifically, when identifying the location of a tree bole, an interpreter is more commonly locating the centroid of a tree canopy as opposed to the location of a tree bole, and the corresponding pattern concerning centroids of tree crowns may differ from the pattern concerning the tree boles (Uria-Diez & Pommerening 2017, Vacchiano et al. 2011). Further, the crowns of some overtopped or suppressed trees may not be

evident in an analysis of satellite or aerial imagery. Additionally, the quality of images generated by LiDAR can be significantly deteriorated by weather conditions (water, dust, or wind) and the presence of rough terrain (Trochta et al. 2013).

Tree bole coordinates have been used in various studies to assess spatial pattern (Dohn et al. 2017, Hui et al. 2007, Law et al. 2009, Uria-Diez & Pommerening 2017), but the specific methods employed for collecting the coordinates of tree bole locations are often not described or it is suggested that the locations were determined using GNSS technology. Therefore, our objectives for this study are twofold. First, we evaluate the inherent positional error of tree bole locations using three different types of GNSS receivers and several assumptions regarding the data collection protocols. These data collection protocols emulate common practices employed by the typical forestry professional in the southern United States for capturing the position of resources of interest. Therefore, survey-grade GNSS receivers and the use of real-time kinematic (RTK) positioning were not tested. In RTK positioning, the mobile unit (the one used by the professional collecting data) relies on the acquisition and use of real-time position correction information that is supplied by an independent reference station (or base station) or a virtual reference station positioned over a known location. Second, we compare the observed spatial patterns of tree boles to the actual spatial pattern of trees measured using ground surveying methods, to determine whether tree bole coordinate positions determined from GNSS receivers can retain the fidelity of the real-world spatial pattern of trees.

Materials and Methods

This study was conducted in a loblolly pine (*Pinus taeda*) seed orchard within the Whitehall Forest in Athens, GA. Trees were planted in a regular grid arrangement, with an average spacing of about 6.15 m. At the time of this study, the trees were 34 years old (Figure 3.1). While representative of a regular pattern, the distances between the trees along and between rows are not exact, due to the natural growth and development forces on the trees. The density of the seed orchard was estimated to be 193 trees ha^{-1}, with a basal area of 26.4 m^2 ha^{-1}. It is uncommon to use a seed orchard as study site for SPPA because the distribution (pattern) of trees is uniformly dispersed. However, by using the seed orchard we were able to avoid influence associated with the spatial placement of plots having environmental heterogeneity and potential clustering characteristics (Garzon-Lopez et al. 2014). A total 112 trees were used across the study site (0.61 hectare), which is generally comparable to area required to reliably assess spatial pattern (Carrer et al. 2018). Therefore, this study site serves as a control pattern for evaluating the point pattern of tree bole positions determined using GNSS technology.

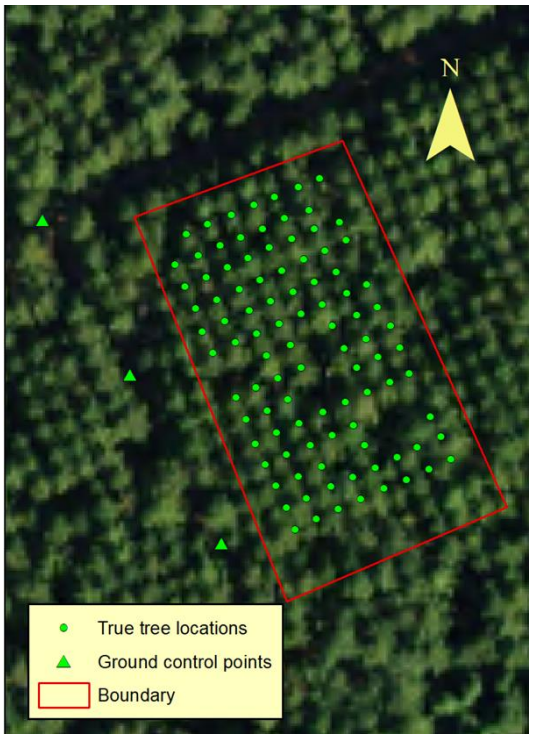

Figure 3.1 The study plot with 26 control points. These control points were determined based on the surveyed control points (#7, #20, CP1, and CP2) using trilateration. Each control points apart from each other in 6 meters.

To determine the spatial locations of tree boles in the study area, three different GNSS receivers were used: a Trimble GNSS receiver (Juno T41, Trimble Inc., USA), a Garmin GNSS receiver (Oregon 700, Garmin, Olathe, KS, USA), and a Suunto GPS watch (Ambit Peak 3, Suunto, Finland). The Trimble Juno T41 GNSS receiver is classified as a mapping-grade receiver based on an estimated horizontal accuracy of 1 to 5 m (Lee et al. 2020) and a general price range of $1,000 to $9,000 (Bettinger & Merry 2011). The Garmin Oregon 700 GNSS receiver and the Suunto GPS watch are classified as recreation grade receivers based on an estimated horizontal accuracy between 6 to 12 m (Danskin et al. 2009, Lee et al. 2020) and a general price range of

$100 to $700. These horizontal accuracy statements are based on common, practical use of the devices, which consist of an average of a collection of position fixes (all determined within about 30 seconds or less) from the mapping-grade device, and one waypoint from the recreation-grade devices to determine a horizontal position.

The Trimble GNSS receiver was equipped with a relatively large GPS antenna manufactured by Inpaq technology Co. Ltd (Taiwan) (70×43.18×9 mm), which has the ability to utilize both GPS (United States) and GLONASS (Russian Federation) commercially available satellite signals. The receiver uses SOLO Forest software (Trimble Inc., USA) to facilitate data collection with masks limiting the maximum PDOP (positional dilution of precision) and minimum SNR (signal to noise ratio), and allowing the use of the Wide Area Augmentation System (WAAS) for near-real time signal augmentation. The maximum PDOP and minimum SNR values were set to 8 and 4, respectively, and WAAS augmentation was enabled. A PDOP value reflects the quality of satellite constellation arrangement; a lower PDOP value suggests a preferable satellite geometry (wider satellite spacing), which can help to minimize trilateration error and perhaps provide more accurate position descriptions (Lewis et al. 2007). A PDOP value of 4 or less suggests rather good satellite geometry has been obtained, and a PDOP value greater than 9 suggests rather poor satellite geometry. So, the maximum PDOP value of 8 assumed represents a moderate setting for satellite geometric arrangement in this study. A position was determined by the Trimble receiver by averaging around 15 position fixes (one per second) during each visit to each tree, which is typical in practice when using this device.

The Garmin GNSS receiver was equipped with a GPS antenna made by Cirocomm Technology Corp. (Taiwan) (size: 15×15×4 mm). Like the Trimble receiver, the Garmin receiver can utilize both GPS and GLONASS satellite signals. The Garmin receiver has limited configuration options and does not allow one to set the maximum PDOP and minimum SNR values. However, the WAAS augmentation system was employed. The Garmin receiver has a function to determine a position by averaging multiple position fixes, but this function was not used in this study. Positions were determined using a single position fix (waypoint), which is common in practice when using this device. Data was collected and stored using the WGS84 coordinate system, and data were downloaded using "basecamp" software (Garmin International, USA).

The Suunto GPS watch is considered a non-traditional recreation-grade receiver. It is equipped with a GPS antenna equal in size to the Garmin GNSS receiver's (size: 15×15×4 mm) made by Patron Co. Ltd (Korea). Similar to the Garmin receiver, the Suunto GPS watch has limited configuration options. A user can only change the GPS coordinate system specified for data collection. Here, the GPS coordinate system for data collection was set to UTM NAD1983. The Suunto GPS watch has no function for averaging multiple position fixes to determine a location, so a position was recorded as one point per each visit to each tree. Prior analysis of this GPS watch (Lee et al. 2020) suggested that it can provide an average horizontal position accuracy of 29.6 m in an uneven-aged deciduous forest during the leaf-on conditions, and 22.1 m in an older pine forest in the southern United States.

In prior observational studies, average horizontal position accuracy has been estimated for various types of GPS devices in forested conditions. However, the direction of the error around a

control point was not assessed except in one study (Bettinger & Merry 2012b). The combination of horizontal and directional error could affect the pattern of individual trees if mapping them were the main purpose. This interplay has yet to be researched and represents an area of novelty of this study. If one assumed that the direction of error of point locations for features such as trees was consistent within a short period of time, then the determined point positions should represent well the point pattern of the trees that they represent. Unaugmented GNSS position fixes collected with autonomous recreation-grade GNSS receivers have been used to develop databases of urban tree locations (Green et al. 2016, Tait et al. 2009) and rural forest tree locations (Fauzi et al. 2016b), yet in the latter case the data were deemed unsuitable for adequately describing individual tree locations. Alternative technologies such as RTK GNSS (Khot et al. 2006), differential GNSS, or simultaneous localization and mapping (SLAM) algorithms (Fan et al. 2018) may help improve horizontal position accuracy for individual trees in forests. However, as we noted earlier, we did not employ these augmentations during our tests as they are not commonly used in practice in the southern United States (Bettinger et al. 2019).

The basis for the real point pattern of tree boles in our study area involved a ground survey of tree locations, beginning with the determination of three ground control points using a mapping-grade receiver (Nomad 1050, Trimble Inc., USA) equipped with an external antenna (Garmin GPS 19x HVS, Garmin International, USA) and situated on a road next to the seed orchard (Figure 1). The mapping-grade receiver was allowed to warm up for 30 minutes, then position fixes were collected for a 20-minute time period on three different occasions. The mean northing and easting for each measurement period was then used to estimate each control point location. The mean northing and easting coordinates had standard deviations of 0.17 m and 0.45 m, so

these ground control points were considered to be relatively accurate locations. Tree bole locations were then estimated by triangulating the physical distance between trees, the distance from a control point, the azimuth from each tree to a ground control point, and the azimuth from tree to tree (Kiser 2008). These measurements were collected using a measuring tape and a laser rangefinder (TruPulse 360R, Laser Technology Inc., Centennial, CO, USA). The diameter at breast height (DBH) for each tree was also measured. In estimating the distance between two trees or between trees and the ground control point, the distance to the center of a tree stem was determined by adding half of the DBH to the measured distance. As multiple distance measurements were collected between sample trees, tree location was estimated with the optimization function using R (version 1.1.463, RStudio, Inc., Boston, MA, USA) to minimize the error derived from the difference between measured distance and calculated distance. Since the laser rangefinder has a manufacturer's reported error of less than 0.5° in azimuth, the manufacturer's angle error was considered by generating random numbers within this error range (0° to 0.5°) centered on the measured angle value to obtain the calculated distance. The estimated tree locations by optimization were assumed to be the basis for comparison against the GNSS-determined tree locations.

Tree bole locations determined using the three GNSS receivers were collected on four different occasions, at each cardinal position (north, south, east, and west) around a tree, and averaged to investigate whether the data collecting location around trees had significant effects on positional accuracy. In total, there were seven different data collection methods:

Method "All": the mean position of 16 points collected from every cardinal direction

Method “NS”: the mean position of 8 points collected from north and south sides of each tree

Method “EW”: the mean position of 8 points collected from east and west sides of each tree

Method “N”: the mean position of 4 points collected from north side of each tree

Method “S”: the mean position of 4 points collected from south side of each tree

Method “E”: the mean position of 4 points collected from east side of each tree

Method “W”: the mean position of 4 points collected from west side of each tree

The data collection process was time consuming and therefore it was not possible to complete in a single day. Instead, data were collected over a period of three weeks. We visited the study site at a similar time period (between 1 p.m. and 4 p.m.) of the day only when the weather was not severe (rainy, cloudy or windy). In this study, however, the weather conditions were not monitored, as it has been shown that local climatic conditions have little effect on positional accuracy of mapping-grade and recreation-grade GNSS receivers (Bettinger & Fei 2010, Ransom et al. 2010, Merry & Bettinger 2019). During the data collection effort, GNSS receivers were held on top of a monopod with a leveling device, to maintain a constant position. The monopod was located 1 m away from the stem of each tree, and the researcher always stood on the north side of the monopod. One half of each tree’s DBH was added to the 1 m of distance between the tree and the position of the monopod. This distance was used to locate the center of the tree stem from observed spatial data. Before collecting coordinate locations, both the Garmin GNSS receiver and the Trimble GNSS receivers were allowed to warm up for about 5 minutes. The Suunto GPS watch did not need warm-up time because it was always on and ready for collecting spatial data.

The first hypothesis of the study was that the horizontal positions determined using the different GNSS devices and the different methods to estimate tree bole location were not statistically different. The horizontal accuracy of data collected using each GNSS receiver was determined using the root mean square error (RMSE), which can be calculate as

$$RMSE = \sqrt{\frac{\sum_i^n((x_i-x)^2+(y_i-y)^2)}{n}} \quad (1)$$

Where n is the total number of observations in a visit; I is the ith observation of the visit; x_i and y_i are the longitude and latitude, respectively, of the ith observations; and x and y are the assumed true easting and northing of the associated tree location. The RMSE is widely used for horizontal position accuracy with GNSS data (Ransom et al. 2010, Sigrist et al. 1999). In addition to it, the root squared error of the mean (RSEM) was calculated based on the mean center's coordinates. The direction and tendency in collected data was investigated using a standard deviational ellipse described by an orientation angle and an anisotropic ratio (I_a) (Lee et al. 2020, Hung et al. 2019). To test the first hypothesis related to the RMSE and parameters of standard deviational ellipses, we applied the one-way ANOVA and Kruskal-Wallis test using R Studio software (2022.02.0, Rstudio, Inc., Boston, MA, USA). The RSEM and parameters of standard deviational ellipses were calculated with ArcMap GIS software (version 10.7.1, Esri Inc., Redlands, CA, USA).

$$I_a = \left(\frac{R-r}{R}\right)100 \quad (2)$$

The second hypothesis of this study was that the spatial pattern of tree locations determined using the GNSS receivers was completely random. The seed orchard trees planted in a regular pattern allowed us to assess this hypothesis that GNSS-determined positions are representative of a certain spatial pattern. To analyze the observed distributions (patterns) of tree boles, various kinds of distance-based statistical methods were applied including the average nearest neighbor (ANN) analysis, $g(r)$ function, and $\hat{L}(r)$ function so not to omit important information regarding spatial scale (Velázquez et al. 2016, Wiegand et al. 2013). The ANN analysis was applied using ArcMap GIS software (version 10.7.1 Esri Inc., Redlands, Cam USA) to determine whether the observed pattern of tree distribution in the seed orchard follows the CSR process. ANN analysis provides the ANN ratio (or an R-statistic) by comparing the average distance ($\overline{D}_0$) from each object (i.e., tree position determined using a GNSS receiver) to its nearest object (i.e., another tree position) against the expected average distance ($\overline{D}_E$) under CSR. It also provides its significance using *p*-values and z-score indicating whether the observed patterns are statistically departed from the null model of CSR (Wiegand & Moloney 2013) as follows:

$$\overline{D}_0 = \frac{\sum_{i=1}^{n} d_i}{n} \text{ and } \overline{D}_E = \frac{0.5}{\sqrt{n/A}} \quad (3)$$

$$ANN = \frac{\overline{D}_0}{\overline{D}_E} \quad (4)$$

Where d_i is the distance between tree *i* and its nearest neighboring tree, *n* is the total number of trees, and *A* is the study site area.

In this study, the ANN ratio (R) represents how the point patterns of the GNSS-determined positions are distributed. For example, when R = 1, points are considered to be distributed randomly. When R >1, points exhibit a dispersed point pattern (which would most closely emulate a regular pattern). When R <1, points are considered to exhibit a clustered pattern (Clark & Evans 1954).

The $L(r)$ function is a transformed version of 'Ripley's K function ($K(r)$)' and is widely used for SPPA in ecological literature (Gadow et al. 2012, Law et al. 2009, Wiegand & Moloney 2013). The $K(r)$ function describes the pattern based on the quantity of the intensity (λ) and $K(r)$, $\lambda \cdot K(r)$, which is the expected number of further points within distance r of the typical point (Wiegand et al. 2013, Wiegand & Moloney 2013). Since the expected number of points is increased at the rate of r^2 when using the $K(r)$ function, it can be transformed to the $L(r)$ function (Wiegand & Moloney 2013). Calculated from $K(r)$, the $L(r)$ function (Besag 1977) is derived as follows:

$$K(r) = \frac{A}{n^2} \sum_{i=1}^{n} \sum_{j}^{n} {w_{ij}}^{-1} I_r(u_{ij}) \quad (5)$$

$$L(r) = \sqrt{\frac{K(r)}{\pi}} \quad (6)$$

Further, the $L(r)$ function can be normalized as below:

$$\hat{L}(r) = L(\mathrm{r}) - r \quad (7)$$

Where A is the study area, r is the radius, n is the number of individuals, $I_r(u_{ij})$ is an indicator function (which is either 1 when $u_{ij} < r$ or 0 when $u_{ij} > r$), and w_{ij} is a weight value for Ripley edge correction. In this study, the $\hat{L}(r)$ function was applied because it provides more interpretable graphs than $K(r)$ and $L(r)$ (Gadow et al. 2012). Since $\hat{L}(r)$ has a value of 0 under CSR, it is easier to be assessed against the observed pattern (Wiegand & Moloney 2013). A positive value at distance r indicates that there are more points than the expected number of points, indicating a tendency toward clustering. Otherwise, a negative value at distance r means that there are less points than expected, indicating a tendency toward dispersing.

The pair correlation ($g(r)$ function) was also applied to analyze the observed patterns. The $g(r)$ function is closely related to the $K(r)$ function because both are second-order statistics. However, the $g(r)$ function is discernable in that it is a non-cumulative function, accounting the expected point density within a ring with radius (r) and width (dr) centered in the typical point (Wiegand et al. 2013). Although cumulative functions including $K(r)$ and $L(r)$ function were still frequently used, we applied the $g(r)$ function because it provides better assessments when it is compared to cumulative functions (Gadow et al. 2012, Hui et al. 2007, Law et al. 2009). When it comes to the cumulative function, effects observed at short spatial scales can obscure the effects observed at larger spatial scales (Wiegand & Moloney 2013). The $g(r)$ can be calculated from $K(r)$ (Stoyan & Stoyan 1996):

$$g(r) = \frac{dK(r)}{dr} / 2\pi r \quad (8)$$

The $g(r)$ provides value of about 1 when the data represent a CSR pattern, which is relevant to the independent of the intensity of the pattern (Gadow et al. 2012). Therefore, $g(r)$ is considered as a summary statistic that discerns whether the observed pattern is clustered or dispersed (Wiegand & Moloney 2013). For example, if the pattern has a tendency toward dispersion, it will have fewer nearby points at small distance than the expectation under CSR, so it will result in a value less than 1. Otherwise, when the pattern has a tendency toward clustering, it will have more nearby points, which is equivalent to a value larger than 1. These summary statistics are frequently used for SPPA in ecology (Hui et al. 2007, Perry et al. 2006, Velázquez et al. 2016, Wiegand & Moloney 2013). They count the number of points at or within neighborhoods of other features based on the information of inter-point distances to derive spatial information (Gadow et al. 2012, Velázquez et al. 2016).

Monte Carlo simulation was conducted for summary statistics ($g(r)$, $K(r)$, and $\hat{L}(r)$) to produce pseudo significance levels via repeated randomization. A significant departure from the null hypothesis of CSR was estimated by 200 Monte Carlo simulations and the highest and lowest values of these simulations represent approximately 95% upper and lower confidence limits of the null model of CSR. Two hundred simulations were considered sufficient to generate envelopes for determining whether the null model can be rejected or not (Velázquez et al. 2016). The Ripley edge correction was utilized in SPPA for this study and we conducted SPPA using the “spatstat” package in R, which is a standard toolbox for this subject area (Law et al. 2009).

Results and Discussion

With respect to the first hypothesis of this study, the horizontal positional accuracy was analyzed for different tree bole position measurement methods and GNSS receiver types. For the Garmin receiver, occasionally it provided a sub-meter accurate horizontal position, but on average, horizontal position accuracy (as reported using RMSE) for representing the locations of trees was 10–12 m (Table 3.1). The greatest positional error measured was 28 m, and the coefficient of variation was 25–40%. For the Suunto receiver, occasionally it provided about 1 m accurate horizontal positions, but on average, horizontal position accuracy was 9–13 m, which was consistent with a previous study (Lee et al. 2020). The greatest positional error was 82 m, and the coefficient of variation was 40–90%, suggesting much more variation in determined positions than when the Garmin device was used. For the Trimble receiver, a few submeter accurate horizontal positions were determined, but on average, horizontal position accuracy was 5–8 m. The greatest measured positional error was 19 m, and the coefficient of variation was 30–60%. Therefore, as expected, the mapping-grade receiver provided the most accurate estimates of tree positions with the lowest amount of variation compared the recreation-grade receivers. These findings were statistically significant, with p-values of less than 0.05 (Figure 3.2).

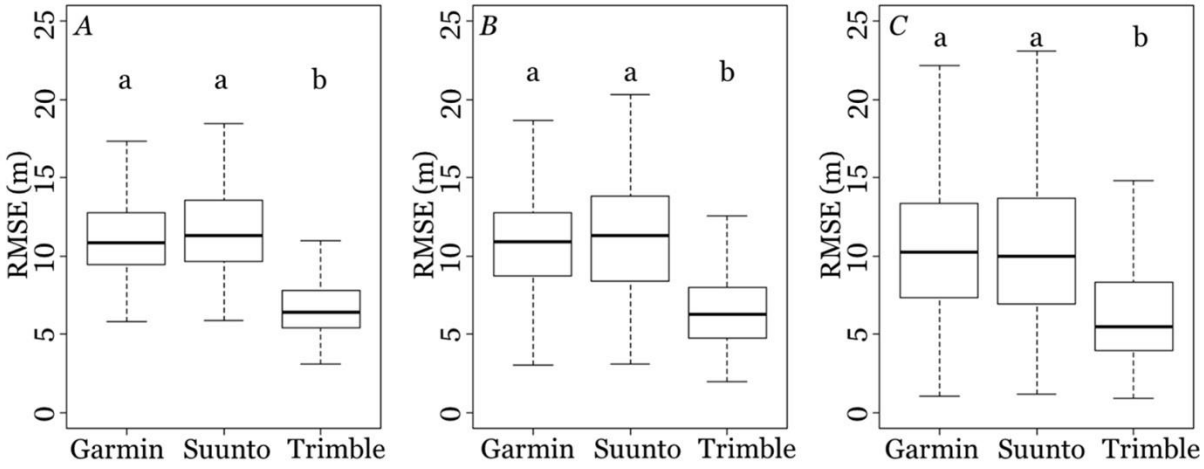

Figure 3.2 Boxplots for horizontal positional accuracy (RMSE) by methods and GNSS receiver types (A mean center of observed points at every cardinal point: *A*; A mean center of observed points at two cardinal points: *B*; A mean center of observed points at each cardinal point: *C*). *Different letters* indicate significant differences between the groups (p-value <0.05).

Table 3.1 A summary of raw data observations for different GNSS receiver types and measurement methods.

Device / metrics	All	Two	NS	EW	Single	N	S	E	W
Garmin Oregon 700									
Mean RMSE (m)	11.31	11.17	11.11	11.22	10.77	9.61	11.81	9.24	12.40
Minimum RMSE (m)	5.92	3.11	5.47	3.11	0.97	1.71	0.97	1.41	2.74
Maximum RMSE (m)	19.84	21.55	18.52	21.55	27.63	20.16	24.85	20.69	27.63
Standard deviation of RMSE (m)	2.93	3.44	3.04	3.81	4.54	3.97	4.26	3.89	5.16
n	97	194	97	97	388	97	97	97	97
Suunto watch GPS	All	Two	NS	EW	Single	N	S	E	W
Mean RMSE (m)	12.34	11.91	12.03	11.79	11.22	9.04	13.52	10.97	11.34
Minimum RMSE (m)	5.96	3.15	3.27	3.15	1.06	1.06	3.67	1.34	2.53
Maximum RMSE (m)	44.04	58.85	42.08	58.85	82.31	40.79	59.20	82.31	30.95
Standard deviation of RMSE (m)	5.12	6.05	4.99	6.98	7.26	5.27	6.90	10.02	5.13
n	97	194	97	97	388	97	97	97	97
	All	Two	NS	EW	Single	N	S	E	W

Trimble Juno T41									
Mean RMSE (m)	6.87	6.71	6.41	7.00	6.36	5.21	6.95	5.22	8.04
Minimum RMSE (m)	3.14	1.95	1.95	2.02	0.91	1.12	0.91	0.92	2.97
Maximum RMSE (m)	12.77	16.11	14.80	16.11	18.86	18.86	17.59	14.89	17.25
Standard deviation of RMSE (m)	2.00	2.51	2.67	2.31	3.29	3.02	3.47	2.82	2.97
n	97	194	97	97	388	97	97	97	97

Regarding measurement methods that might improve horizontal positional accuracy, it was expected that determining a tree bole position using multiple cardinal positions would provide better horizontal positional accuracy regardless of GNSS receiver used. Interestingly, however, the highest and lowest mean RMSE values were observed when a tree bole position was determined at a single cardinal point regardless of GNSS receiver (Figure 3.3). When tree bole positions were determined from the East or North sides of a tree, the lowest positional error was observed. Otherwise, the highest positional errors were observed when tree boles were located South or West of each measurement point. Regarding the positional errors obtained by the average from all cardinal points and the average from two cardinal points (North and South; East and West), there were no significant differences (Figure 3.3).

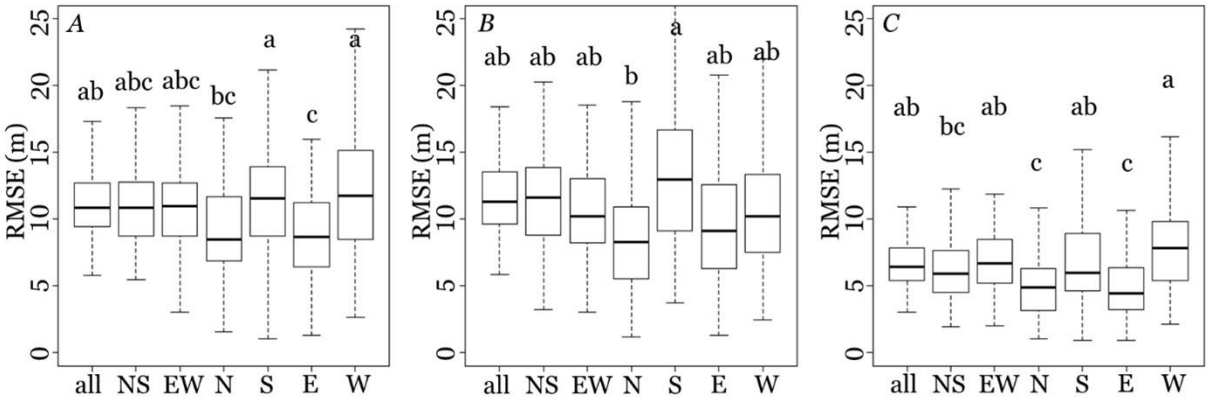

Figure 3.3 Boxplots for horizontal positional accuracy (RMSE) of observed points using different methods within each GNSS receiver type (A mean center of observed points every cardinal points: all; a mean center of observed points at the North and South: NS; a mean center of observed points at the East and West: EW; a mean center of observed points at the North: N; a mean center of observed points at the South: S; a mean center of observed points at the East: E; a mean center of observed points at the West: W; Garmin Oregon 700: *A*; Suunto GPS watch: *B*; Trimble Juno T41: *C*). Different letters indicate significant differences between the groups (*p*-value <0.05).

These results suggested that determining a tree bole location using multiple cardinal positions might not be helpful and does not influence horizontal positional accuracy in a forested area. Various factors related to measurement methods have been tested in prior studies to improve the performance of GNSS receivers. For example, Weaver et al. (2015) investigated the effect of holding position for GNSS receivers on horizontal position accuracy and confirmed holding a GNSS receiver vertically provided improved horizontal positional accuracy compared to holding it at an angle or horizontally. Further, Bettinger and Merry (2012a) suggested that the number of

fixes to determine the location of tree did not influence horizontal position accuracy, since random trends were observed in different forest types. However, in one case the observation time was considered the most important factor for improving horizontal positional accuracy of GNSS receivers (Næsset & Gjevestad 2008). While our short data collection period may have affected horizontal positional accuracy, the method for collecting positional information in this study represented well the way it is applied in a real-world, practical setting. All this aside, it is interesting to note that due to the difficulties encountered in determining accurate tree positions in a forested environment, it has been suggested that more traditional survey techniques be employed to better represent the true location of individual trees (Edson & Wing 2012). Alternatively, if time and cost were not an issue, the use of survey-grade GNSS receivers or RTK (and other) real-time augmentation methods may better accomplish the mission than using basic mapping-grade or recreation-grade GNSS receivers.

When evaluating the mean center coordinates of the average position determined for each tree using the RSEM, the highest and lowest positional error was also observed when the tree bole locations were determined at single cardinal point (Table 3.2). The mean center of tree locations determined by each GNSS receiver was located to the South of true tree locations, where the difference from the actual tree bole location had a negative northing regardless of measurement method. Further, most of the mean center X coordinates were biased to the West of the actual tree locations, where the difference from the actual tree location had a negative easting regardless of measurement method and GNSS receiver type. The bias in determined positions was also observed in a previous study using a GPS watch and mapping-grade receiver, where the X coordinates were biased to the West of true tree locations regardless of GNSS receiver grade,

season, and forest type, but the reason was not confirmed (Lee et al. 2020). The RSEM values provide a different picture of the horizontal accuracy of the GNSS devices since they somewhat correct for directional error (deviations on two sides of true tree bole positions provide a better estimated representation of the location of trees) while RMSE values ignore directional issues and simply report distance deviation regardless of the direction. For the Garmin receiver, RSEM values ranged from 5–13 m, error was often to the South and West of true tree bole positions, the angle of rotation of the estimated ellipse was East-Southeast, and the area of the estimated ellipse was rather large (Table 3.2). For the Suunto receiver, RSEM values ranged from 5–11 m, error was often to the South and West of true tree bole positions, the angle of rotation of the estimated ellipse was Northeast-East, and the area of the estimated ellipse was generally larger than that estimated for the Garmin device. For the Trimble receiver, RSEM values ranged from 3–7 m, error was often to the South and West of true tree bole positions, the angle of rotation of the estimated ellipse was Southeast, and the area of the estimated ellipse was smaller than that estimated for the other devices. The anisotropic ratios for tree locations determined by the Trimble receiver were lower, indicating it generally had lower bias in direction than the other two devices. In concert with the previously reported results, the mapping-grade receiver provided the most accurate estimates of tree bole positions with the lowest amount of variation.

Table 3.2 A summary of the elliptical parameters estimated from positions determined by different GPS equipment using different measurement methods (RSEM = root squared error of the mean; Mean X coordinate = the mean of difference between observed X coordinates and control X coordinate; Mean Y coordinate = the mean of difference between observed Y coordinates and control Y coordinate; I_a = the anisotropic ratio).

Device / metrics	All	Two	NS	EW	Single	N	S	E	W
Garmin Oregon 700									
Mean RSEM (m)	7.54	7.54	7.39	7.70	7.54	6.21	9.39	5.62	10.34
Mean X coordinate (m)	-1.45	-1.45	-1.26	-1.65	-1.45	-3.38	0.86	0.82	-4.11
Mean Y coordinate (m)	-7.40	-7.40	-7.28	-7.53	-7.40	-5.21	-9.35	-5.56	-9.49
Angle of rotation (°)	108.57	104.20	106.23	100.65	101.42	100.17	113.60	109.84	59.46
I_a (%)	37.38	30.80	39.50	22.19	21.19	32.10	26.11	33.30	14.27
Area of ellipse (m^2)	110.32	153.92	144.15	160.69	242.97	202.78	207.68	199.62	226.92
Suunto watch GPS	All	Two	NS	EW	Single	N	S	E	W
Mean RSEM (m)	7.85	7.85	7.78	7.94	7.85	5.00	11.00	6.97	9.48
Mean X coordinate (m)	-0.09	-0.09	0.17	-0.35	-0.09	-1.62	1.96	1.84	-2.54

Mean Y coordinate (m)	-7.85	-7.85	-7.78	-7.93	-7.85	-4.74	-10.83	-6.73	-9.13
Angle of rotation (°)	95.92	88.05	95.16	66.30	87.20	107.97	83.87	24.27	61.67
I_a (%)	32.30	24.37	42.00	13.39	13.10	37.31	40.28	13.57	16.17
Area of ellipse (m^2)	127.59	198.80	160.41	225.73	362.79	237.93	300.93	532.02	200.14
Trimble Juno T41	All	Two	NS	EW	Single	N	S	E	W
Mean RSEM (m)	4.55	4.55	4.01	5.09	4.55	3.22	5.21	3.52	6.89
Mean X coordinate (m)	-0.66	-0.66	-0.73	-0.59	-0.66	-1.78	0.32	0.62	-1.79
Mean Y coordinate (m)	-4.50	-4.50	-3.94	-5.06	-4.50	-2.68	-5.20	-3.47	-6.65
Angle of rotation (°)	121.77	134.35	128.96	138.14	148.90	154.33	121.33	168.06	114.41
I_a (%)	21.19	16.71	22.81	9.11	10.81	16.18	24.07	19.58	5.73
Area of ellipse (m^2)	27.78	47.36	50.35	42.07	95.24	79.60	100.10	69.78	81.24

Regarding the second hypothesis of this study, the ANN analysis of the point pattern of true tree bole locations (control point pattern) suggested it had a dispersed pattern (regular pattern), and that it was significantly different from the CSR (Table 3.3). The ANN ratio for the control point pattern indicated that it had longer average distance to the nearest tree compared to the expected average distance under CSR (ANN ratio = 1.49). Statistically, observed point patterns from other methods were internally similar when the tree bole locations were measured at two cardinal

points (North and South) using the Garmin receiver and when the tree bole locations were determined at two sides (East and West), and South and East using Suunto GPS watch (Table 3.3). Therefore, we assumed these point patterns might be meaningful to proceed further with spatial point pattern analyses such as $g(r)$ function, $K(r)$ function and $\hat{L}(r)$ function. In addition, we investigated observed point patterns to decide, which point patterns should proceed with further analyses (Figure 3.4, 3.5, and 3.6).

However, most observed patterns seemed to not resemble the control point pattern; thus, we decided to choose the point patterns measured by method "All", which represented lines of trees regardless of GNSS receiver. Lastly, three observed point patterns by GNSS receiver were selected based on mean RMSE from the smallest value. Therefore, we analyzed point patterns measured by method "NS", "S", and "N" for the Garmin receiver. Regarding the Suunto GPS watch, point patterns observed by method "N", "E", and "W" were selected. The point patterns from the Trimble receiver included points patterns determined by method "NS", "N", and "E". In sum, a total of 15-point patterns including the control point pattern were selected for further spatial analysis such as $g(r)$ function, $K(r)$ function and $\hat{L}(r)$ function.

Table 3.3 A summary of average nearest neighbor (ANN) analysis for different GNSS receivers and measurement methods.

True tree location		1.49	9.82	<0.01
Device	Measurement methods	ANN ratio	*z*-score	*p*-value
		Garmin Oregon 700		
	All	1.09	1.69	0.09
	NS	1.16	3.01	<0.01
	EW	1.10	1.79	0.07
	N	1.06	1.14	0.25
	S	1.03	0.53	0.59
	E	1.04	0.81	0.42
	W	1.12	2.28	0.02
		Suunto GPS Watch		
	All	1.05	0.98	0.33
	NS	1.02	0.45	0.65
	EW	1.20	3.80	<0.01
	N	1.01	0.26	0.79
	S	1.16	2.93	<0.01
	E	1.20	3.81	<0.01
	W	1.12	2.19	0.03
		Trimble Juno T41		
	All	1.03	0.50	0.62
	NS	0.98	-0.32	0.75
	EW	1.08	1.55	0.12
	N	1.03	0.53	0.60
	S	0.95	-0.92	0.36
	E	1.05	0.97	0.33
	W	0.90	-1.96	0.05

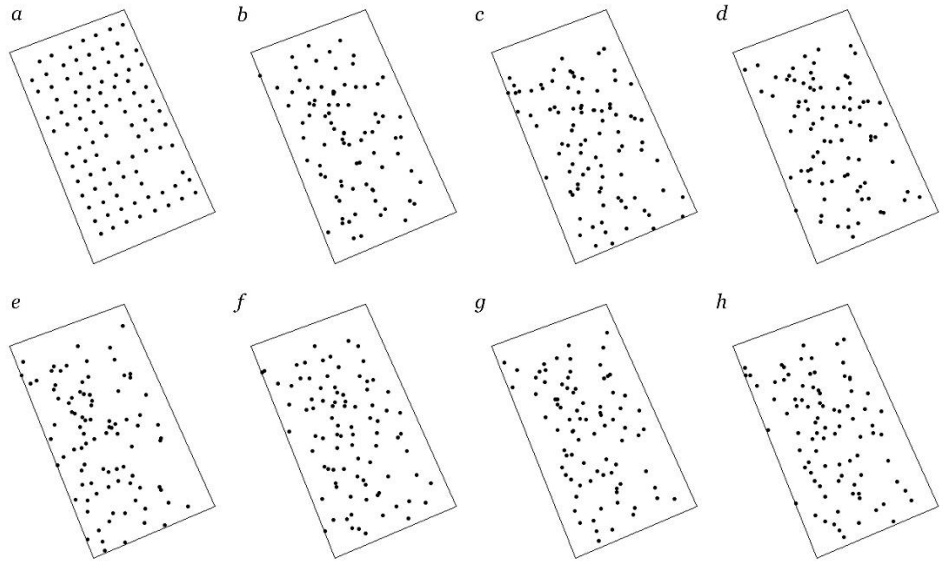

Figure 3.4 The point patterns observed by Garmin receiver depending on measurement method (a: true location, b: North, c: South, d: East, e: West, f: North and South, g: East and West, h: All).

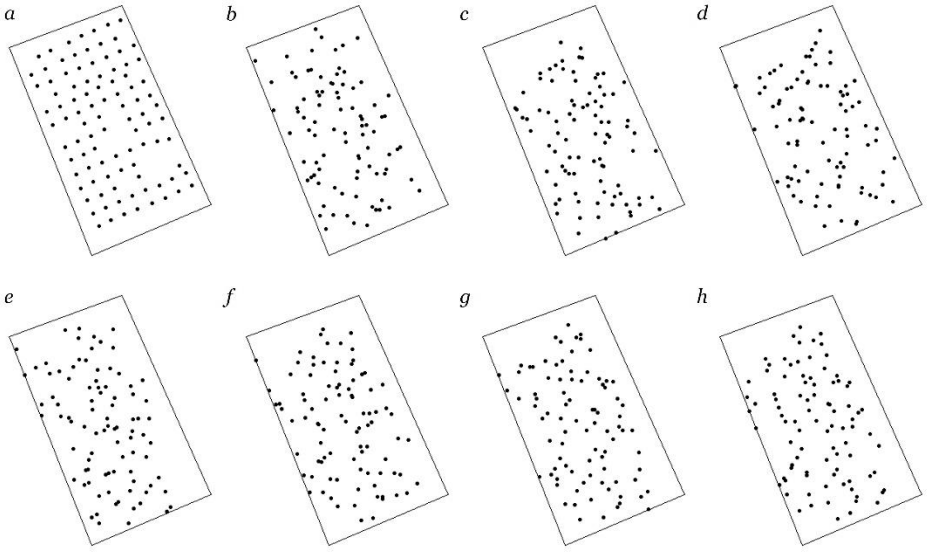

Figure 3.5 The point patterns observed by the Suunto GPS watch depending on measurement method (a: true location, b: North, c: South, d: East, e: West, f: North and South, g: East and West, h: All).

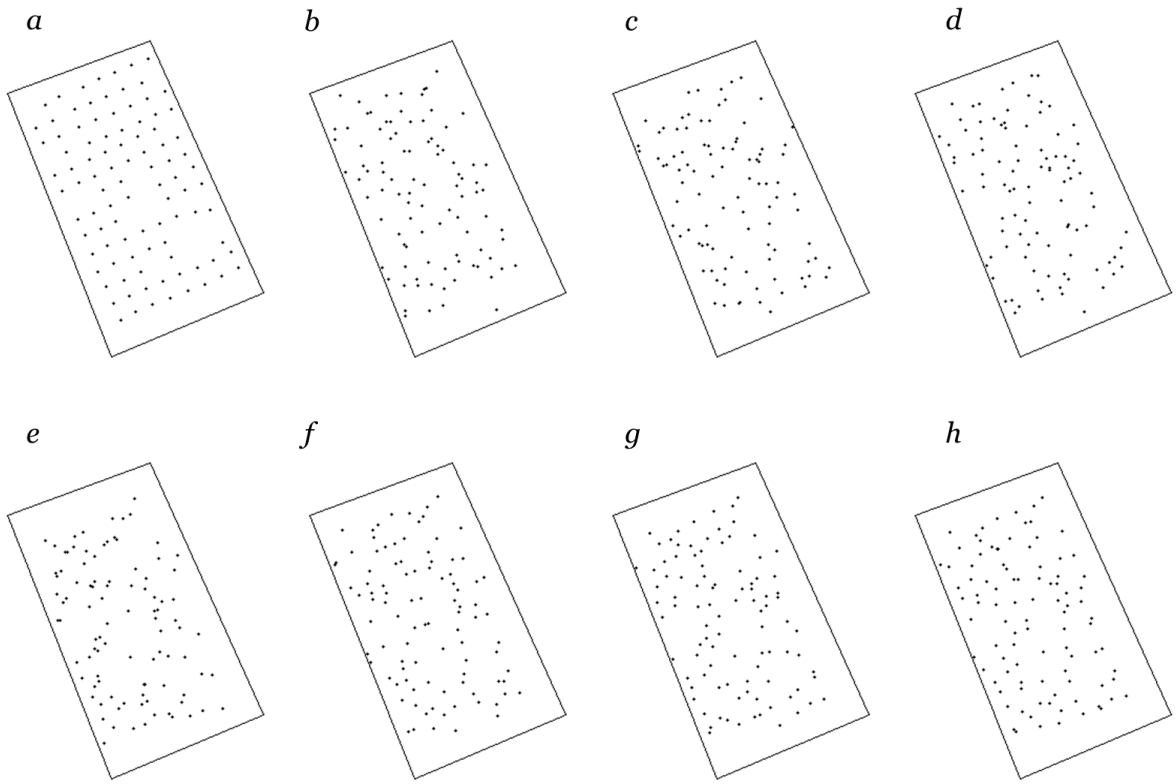

Figure 3.6 The point patterns observed by the Trimble GNSS receiver depending on measurement method (a: true location, b: North, c: South, d: East, e: West, f: North and South, g: East and West, h: All).

The control point pattern represented a statistically significant dispersed pattern (regular pattern) at distances of 3 to 7 m, which is consistent with the actual average tree spacing of 6.12 m (Figure 3.7, 3.8, 3.9 a). At a larger distance scale, there was no evidence of either aggregation or regularity when $K(r)$ and $\hat{L}(r)$ functions were applied (Figure 3.7, 3.8 a). Regarding the observed point pattern from using GNSS receivers and methods, the $K(r)$ lines did not represent significant deviation from the expected line, which indicates the point patterns follow complete randomness (Figure 3.7). However, statistically significant clustered patterns were observed at the wider

distance range regardless of GNSS receivers and methods except the point pattern observed by the Garmin receiver using method "E" (Figure 3.7). The $\hat{L}(r)$ function also detected clustered patterns at larger distance range, but the dispersed pattern (regular pattern) was not observed in any observed point patterns (Figure 3.8). The $\hat{L}(r)$ function suggested that point patterns observed with the Garmin and Trimble receivers using measurement method "E" followed the complete randomness across distance ranges (Figure 3.8 *j* and *o*). Unlike $K(r)$ and $\hat{L}(r)$ function, the $g(r)$ function detected some evidence of a clustered pattern at certain distances from the control point pattern in addition to the evidence of regularity at the distance scale of around 5 m (Figure 3.9 *a*). For example, the suggestive evidence of aggregation was confirmed at around 7, 9, 15, and 20 m of distance scale. Regarding the observed point patterns, a significant dispersed pattern (regular pattern) was not detected. Rather, $g(r)$ function lines for observed point patterns showed almost no deviation from the expected values indicating a random distribution (Figure 3.9). In addition, a statistically significant clumpy distribution was observed at various distances regardless of GNSS receiver and method employed. We had assumed that direction of error would be similar with data collected by each device during a short period of time, but this was not necessarily the case (Figure 3.10).

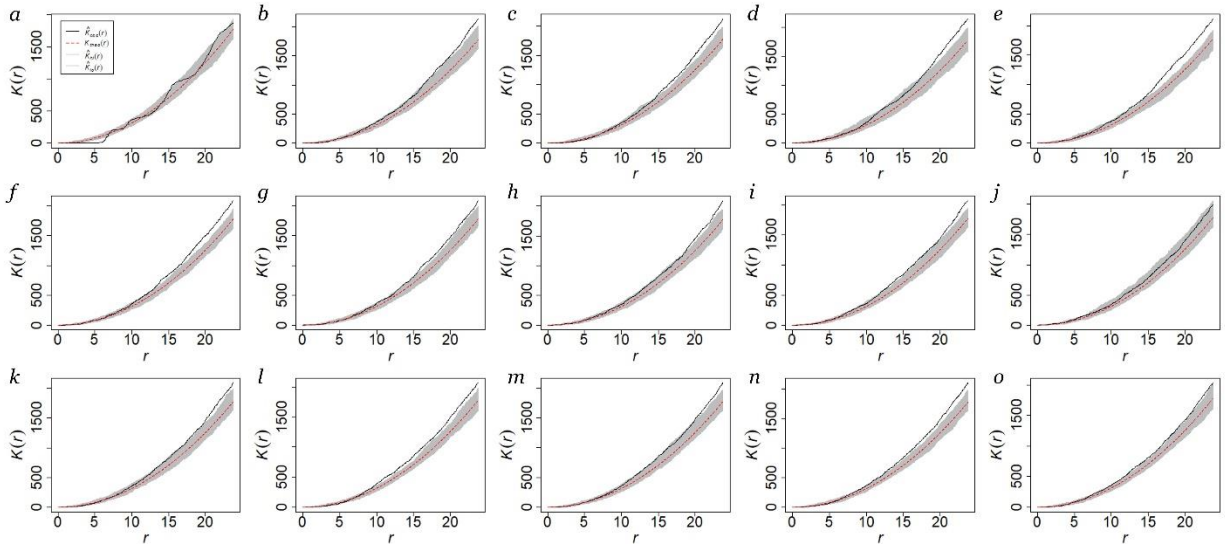

Figure 3.7 Ripley's K functions ($K(r)$) for point patterns observed by different GNSS receivers and measurement methods (*a*: True tree location; *b, c, d, e*: Garmin receiver; *f, g, h, i, j, k*: Suunto GPS watch; *l, m, n, o*: Trimble receiver; *b, f, l*: method "All"; *c, m*: method "NS"; *g*: method "EW"; *d, h, n*: method "N"; *i*: method "S"; *e, j, o*: method "E"; *k*: method "W"). Horizontal axes are the distances *r* between pairs of individuals. Heavy lines show the observed statistic, and the horizontal red dotted lines show the value of $K(r)$ expected from a Poisson process. Gray lines are approximate 95% confidence envelopes for the hypothesis of complete spatial randomness, obtained from 200 independent randomizations of the locations of the trees.

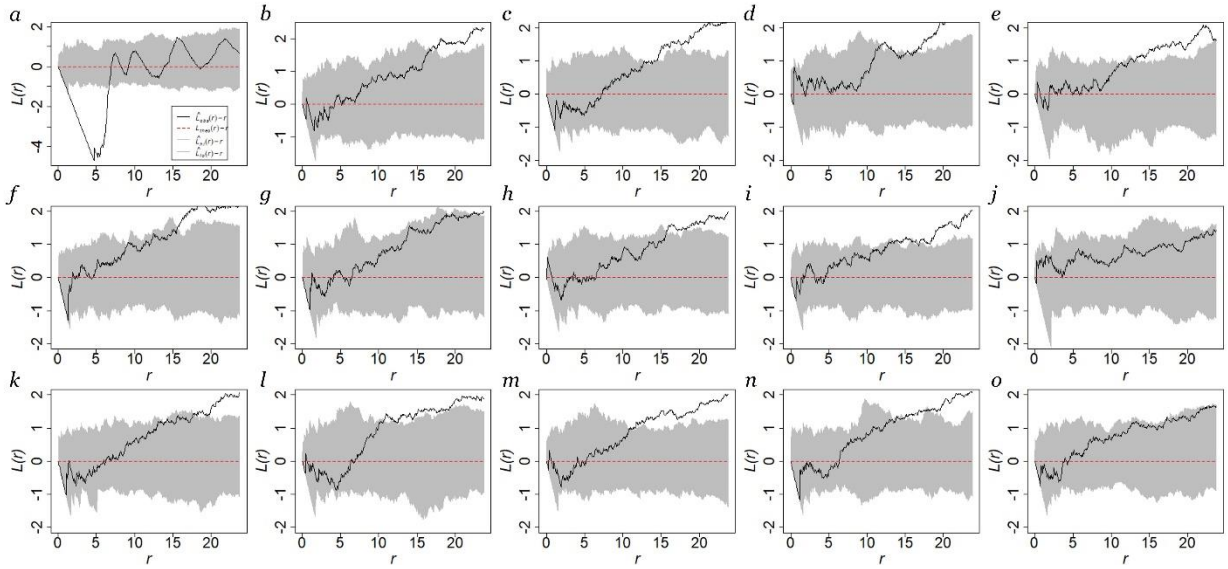

Figure 3.8 The normalized $L(r)$ functions ($\hat{L}(r)$) for point patterns observed by different GNSS receivers and measurement methods (*a*: True tree location; *b, c, d, e*: Garmin receiver; *f, g, h, i, j, k*: Suunto GPS watch; *l, m, n, o*: Trimble receiver; *b, f, l*: method "All"; *c, m*: method "NS"; *g*: method "EW"; *d, h, n*: method "N"; *i*: method "S"; *e, j, o*: method "E"; *k*: method "W"). Horizontal axes are the distances r between pairs of individuals. Heavy lines show the observed statistic, and the horizontal red dotted lines show the value of $\hat{L}(r)$ expected from a Poisson process. Gray lines are approximate 95% confidence envelopes for the hypothesis of complete spatial randomness, obtained from 200 simulations.

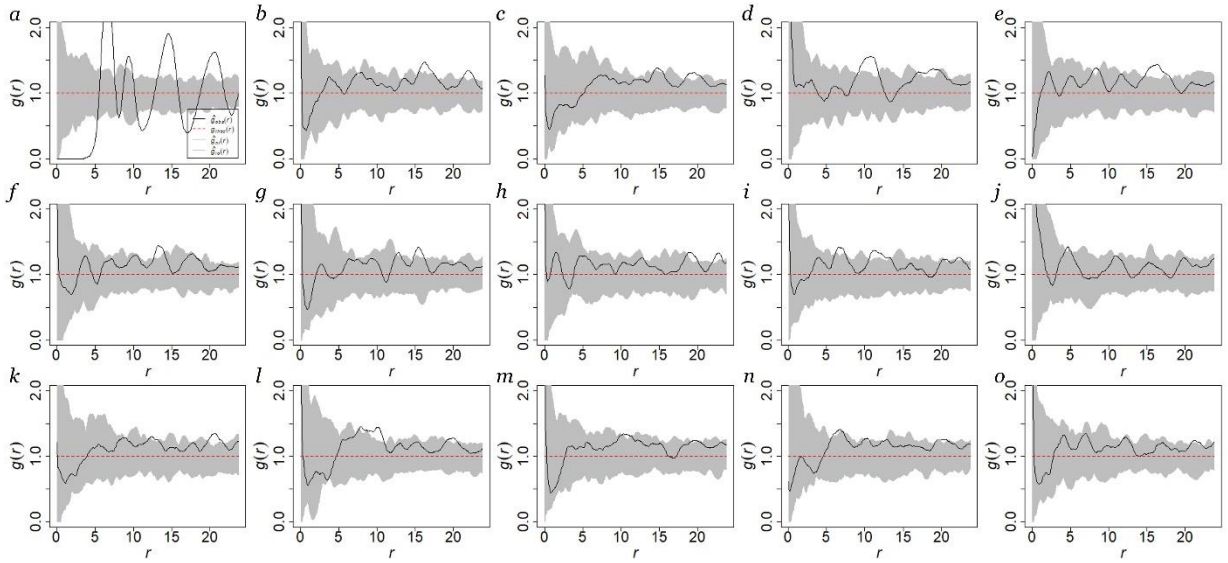

Figure 3.9 Pair correlation ($g(r)$ function) for point patterns observed by different GNSS receivers and measurement methods (*a*: True tree location; *b, c, d, e*: Garmin receiver; *f, g, h, i, j, k*: Suunto GPS watch; *l, m, n, o*: Trimble receiver; *b, f, l*: method "All"; *c, m*: method "NS"; *g*: method "EW"; *d, h, n*: method "N"; *i*: method "S"; *e, j, o*: method "E"; *k*: method "W"). Horizontal axes are the distances *r* between pairs of individuals. Heavy lines show the observed statistic, and the horizontal red dotted lines show the pair correlation function expected from a Poisson process. Gray lines are 95% Monte Carlo simulation envelopes obtained from 200 simulations.

In sum, each of the basic mapping-grade and recreation-grade GNSS receivers we tested provided a pattern of determined tree bole positions that did not reflect the original pattern of the trees in the seed orchard. In fact, the determined tree positions provided an ANN ratio that was close to 1, reflecting a tendency toward the representation of a random pattern of trees rather than a regular arrangement of trees. Based on the ANN ratio, the pattern of determined tree

positions from the Garmin and Suunto devices probably better reflected the original pattern of the tree boles in the seed orchard, yet still did not represent the pattern adequately when applying other summary statistics. Further research in this mission to use GNSS receivers to denote the location of trees in a forested setting seems necessary. If one chooses to accept the mission, it might involve determining whether the use of a RTK GNSS system or other augmentation methods such as DGPS and SLAM can overcome the limitations associated with unaugmented GNSS position fixes collected with autonomous recreation-grade GNSS receivers can develop relatively accurate databases of individual tree bole locations within forests that also maintain the fidelity of the actual tree pattern.

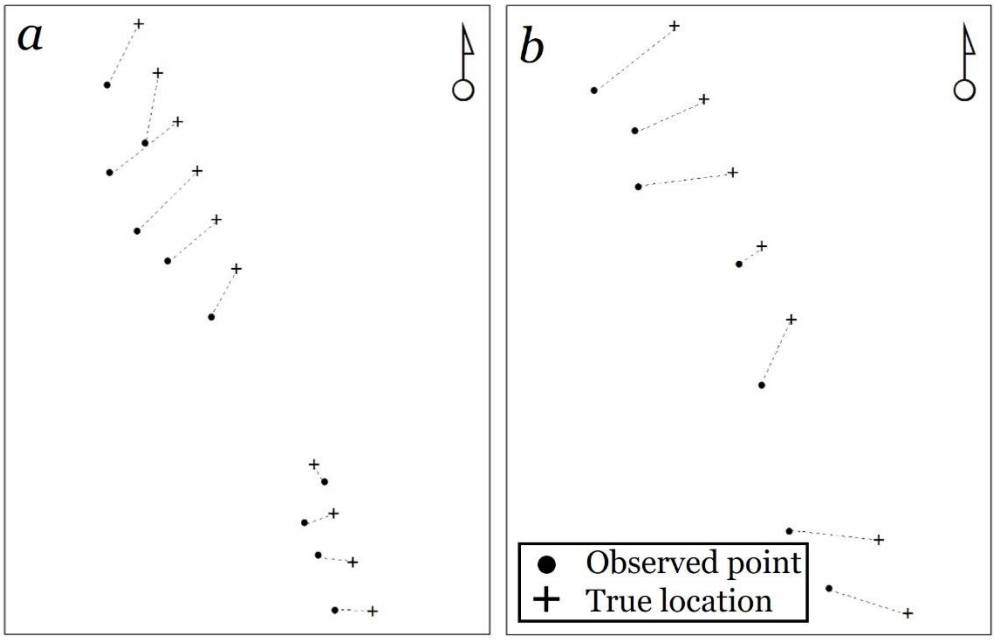

Figure 3.10 The direction of error for data collected by Trimble receiver using "All" method within short period of time (a: collected on February 22nd, 2021; b: collected on March 6th, 2021).

Conclusions

In this study, various methods to determine tree bole locations using GNSS receivers were investigated using horizontal positions (point locations) determined by GNSS receivers. In addition, various summary statistics were applied to assess whether the pattern of the control points and the observed points (the GNSS-determined positions) was indeed regular at a distance range, which is equivalent to the average tree spacing (around 6 m) in a pine seed orchard. Given that the range of horizontal position error was greater than the spacing between the real trees, it was not unexpected that the tree bole locations determined by the three GNSS receivers were not representative of the actual regular pattern of tree boles. The results of the spatial point pattern analysis only indicated a significant regular pattern of trees from the very careful field measurement of the control points. These results and ranges of horizontal position error are relevant to other efforts, which use non-augmented GNSS technology in forested areas. These results suggest that even acceptable ranges of horizontal positional error from unaugmented, basic GNSS technology can be associated with a self-destruction of the actual spatial point pattern of trees in a forested setting.

Acknowledgements

We thank the Warnell School of Forestry and Natural Resources at the University of Georgia for supporting this research.

References

Aguirre, O., Hui, G., Gadow, K.v. and Jiménez, J., 2003. An analysis of spatial forest structure using neighbourhood-based variables. Forest Ecology and Management, 183, 137-145.

Atkinson, P.M., Foody, G.M., Gething, P.W., Mathur, A. and Kelly, C.K., 2007. Investigating spatial structure in specific tree species in ancient semi-natural woodland using remote sensing and marked point pattern analysis. Ecography, 30(1), 88-104.

Besag, J., 1977. Contribution to the discussion on Dr. Ripley's paper. Journal of the Royal Statistical Society, Series B, 39, 93-195.

Bettinger, P. and Fei, S., 2010. One year's experience with a recreation-grade GPS receiver. Mathematical and Computational Forestry & Natural-Resource Sciences, 2(2), 153-160.

Bettinger, P. and Merry, K., 2012a. Static horizontal positions determined with a consumer-grade GNSS receiver: One assessment of the number of fixes necessary. Croatian Journal of Forest Engineering, 33(1), 149-157.

Bettinger, P. and Merry, K.L., 2011. Global navigation satellite system research in forest management: A summary of horizontal, vertical, static, and dynamic accuracy assessments. LAP Lambert Academic Publishing, Saarbrücken, Germany. 64 p.

Bettinger, P. and Merry, K.L., 2012b. Influence of the juxtaposition of trees on consumer-grade GPS position quality. Mathematical and Computational Forestry & Natural-Resource Sciences, 4(2), 81-91.

Bettinger, P., Merry, K., Bayat, M. and Tomaštík, J. 2019. GNSS use in forestry–A multi-national survey from Iran, Slovakia and southern USA. Computers and Electronics in Agriculture, 158, 369-383.

Carrer, M., Castagneri, D., Popa, I., Pividori, M. and Lingua, E., 2018. Tree spatial patterns and stand attributes in temperate forests: The importance of plot size, sampling design, and null model. Forest Ecology and Management, 407, 125-134.

Clark, P.J. and Evans, F.C., 1954. Distance to nearest neighbor as a measure of spatial relationships in populations. Ecology, 35(4), 445-453.

Danskin, S.D., Bettinger, P., Jordan, T.R. and Cieszewski, C., 2009. A comparison of GPS performance in a southern hardwood forest: Exploring low-cost solutions for forestry applications. Southern Journal of Applied Forestry, 33(1), 9-16.

Diggle, P.J., 2013. Statistical analysis of spatial and spatio-temporal point patterns. Monographs on Statistics and Applied Probability 128. CRC Press, Boca Raton, FL.

Dohn, J., Augustine, D.J., Hanan, N.P., Ratnam, J. and Sankaran, M., 2017. Spatial vegetation patterns and neighborhood competition among woody plants in an East African savanna. Ecology, 98(2), 478-488.

Edson, C. and Wing, M.G., 2012. Tree location measurement accuracy with a mapping-grade GPS receiver under forest canopy. Forest Science, 58(6), 567-576.

Fajardo, A., Goodburn, J.M. and Graham, J., 2006. Spatial patterns of regeneration in managed uneven-aged ponderosa pine/Douglas-fir forests of western Montana, USA. Forest Ecology and Management, 223, 255-266.

Fan, Y., Feng, Z., Mannan, A., Khan, T.U., Shen, C. and Saeed, S., 2018. Estimating tree position, diameter at breast height, and tree height in real-time using a mobile phone with RGB-D SLAM. Remote Sensing, 10(11), Article 1845.

Fauzi, M.F., Idris, N.H., Din, A.H.M., Osman, M.J. and Ishak, M.H.I., 2016a. Indigenous community tree inventory: Assessment of data quality. The International Archives of the Photogrammetry, Remote Sensing and Spatial Information Sciences, 42(4), 307-314.

Fauzi, M., Idris, N., Yahya, M., Din, A., Lau, A. and Ishak, M. 2016b. Tropical forest tree positioning accuracy: A comparison of low cost GNSS-enabled devices. International Journal of Geoinformatics, 12(2), 59-66.

Gadow, K.v. and Hui, G.Y., 2002. Characterizing forest spatial structure and diversity. In Sustainable Forestry in Temperate Regions, Björk, L. (ed.). SUFOR, University of Lund, Lund, Sweden, pp. 20-30.

Gadow, K.v., Zhang, C.Y., Wehenkel, C., Pommerening, A., Corral-Rivas, J., Korol, M., Myklush, S., Hui, G.Y., Kiviste, A. and Zhao, X.H., 2012. Forest structure and diversity. In Continuous cover forestry. pp. 29-83. Springer, Dordrecht, The Netherlands.

Garzon-Lopez, C.X., Jansen, P.A., Bohlman, S.A., Ordonez, A. and Olff, H., 2014. Effects of sampling scale on patterns of habitat association in tropical trees. Journal of Vegetation Science, 25(2), 349-362.

Green, L.Y., Mikhailova, E.A., Post, C.J., Darnault, C.C.J.G., Bridges, W.C. and Schlautman, M.A., 2016. A cloud-based spatial-temporal inventory for sustainable urban soil management. Urban Ecosystems, 19(2), 811-822.

Hui, G., Li, L., Zhao, Z. and Dang, P., 2007. Comparison of methods in analysis of the tree spatial distribution pattern. Acta Ecologica Sinica, 27(11), 4717-4728.

Hung, I., Unger, D., Kulhavy, D. and Zhang, Y., 2019. Positional precision analysis of orthomosaics derived from drone captured aerial imagery. Drones, 3(2), Article 46.

Illian, J., Penttinen, A., Stoyan, H. and Stoyan, D., 2008. Statistical analysis and modelling of spatial point patterns. John Wiley & Sons Ltd., West Sussex, England.

Khot, L.R., Tang, L., Blackmore, S.B. and Nørremark, M., 2006. Navigational context recognition for an autonomous robot in a simulated tree plantation. Transactions of the ASABE, 49(5), 1579-1588.

Kiser, J., 2008. Chapter 1, Surveying. In Part 650, Engineering field handbook. U.S. Department of Agriculture, Natural Resources Conservation Service, Washington, D.C.

Law, R., Illian, J., Burslem, D.F., Gratzer, G., Gunatilleke, C.V.S. and Gunatilleke, I.A.U.N., 2009. Ecological information from spatial patterns of plants: insights from point process theory. Journal of Ecology, 97(4), 616-628.

Lee, T., Bettinger, P., Cieszewski, C.J. and Gutierrez Garzon, A.R., 2020. The applicability of recreation-grade GNSS receiver (GPS watch, Suunto Ambit Peak 3) in a forested and an open area compared to a mapping-grade receiver (Trimble Juno T41). PLoS ONE, 15(4), e0231532.

Lewis, J.S., Rachlow, J.L., Garton, E.O. and Vierling, L.A., 2007. Effects of habitat on GPS collar performance: using data screening to reduce location error. Journal of Applied Ecology, 44(3), 663-671.

Merry, K., and Bettinger, P. 2019. Smartphone GPS accuracy study in an urban environment. PLoS ONE, 14(7): e0219890.

Moustakas, A., Wiegand, K., Getzin, S., Ward, D., Meyer, K.M., Guenther, M. and Mueller, K.H., 2008. Spacing patterns of an *Acacia* tree in the Kalahari over a 61-year period: How clumped becomes regular and *vice versa*. Acta Oecologica, 33(3), 355-364.

Næsset, E. and Gjevestad, J.G., 2008. Performance of GPS precise point positioning under conifer forest canopies. Photogrammetric Engineering & Remote Sensing, 74(5), 661-668.

Perry, G.L., Miller, B.P. and Enright, N.J., 2006. A comparison of methods for the statistical analysis of spatial point patterns in plant ecology. Plant Ecology, 187(1), 59-82.

Pommerening, A., 2002. Approaches to quantifying forest structures. Forestry, 75(3), 305–324.

Pommerening, A., 2008. Analysing and modelling spatial woodland structure. Bangor University, Wales, UK (DSc dissertation), University of Natural Resources and Applied Life Sciences, Vienna, Austria.

Pommerening, A. and Grabarnik, P., 2019. Individual-based methods in forest ecology and management. Springer Nature Switzerland, Cham.

Ransom, M.D., Rhynold, J. and Bettinger, P., 2010. Performance of mapping-grade GPS receivers in southeastern forest conditions. RURALS: Review of Undergraduate Research in Agricultural and Life Sciences, 5(1), Article 2.

Ripley, B., 1981. Spatial statistics. John Wiley & Sons, Inc., New York.

Seidler, T.G. and Plotkin, J.B., 2006. Seed dispersal and spatial pattern in tropical trees. PLoS Biology, 4(11), e344.

Sigrist, P., Coppin, P. and Hermy, M., 1999. Impact of forest canopy on quality and accuracy of GPS measurements. International Journal of Remote Sensing, 20(18), 3595-3610.

Stoyan, D. and Stoyan, H., 1996. Estimating pair correlation functions of planar cluster processes. Biometrical Journal, 38(3), 259-271.

Tait, R.J., Allen, T.J., Sherkat, N. and Bellett-Travers, M.D., 2009. An electronic tree inventory for arboriculture management. Knowledge-Based Systems, 22(7), 552-556.

Trochta, J., Král, K., Janík, D. and Adam, D., 2013. Arrangement of terrestrial laser scanner positions for area-wide stem mapping of natural forests. Canadian Journal of Forest Research, 43(4), 355-363.

Uria-Diez, J. and Pommerening, A., 2017. Crown plasticity in Scots pine (*Pinus sylvestris* L.) as a strategy of adaptation to competition and environmental factors. Ecological Modelling, 356, 117-126.

Vacchiano, G., Castagneri, D., Meloni, F., Lingua, E. and Motta, R., 2011. Point pattern analysis of crown-to-crown interactions in mountain forests. Procedia Environmental Sciences, 7, 269-274.

Velázquez, E., Martínez, I., Getzin, S., Moloney, K.A. and Wiegand, T., 2016. An evaluation of the state of spatial point pattern analysis in ecology. Ecography, 39(11), 1042-1055.

Weaver, S.A., Ucar, Z., Bettinger, P. and Merry, K., 2015. How a GNSS receiver is held may affect static horizontal position accuracy. PLoS ONE, 10(4), e0124696.

Wiegand, T., He, F. and Hubbell, S.P., 2013. A systematic comparison of summary characteristics for quantifying point patterns in ecology. Ecography, 36(1), 92-103.

Wiegand, T. and Moloney, K.A., 2013. Handbook of spatial point-pattern analysis in ecology. CRC Press, Boca Raton, FL.

Woodall, C., 2002. Point pattern analysis of FIA data. In Proceedings of the Third Annual Forest Inventory and Analysis Symposium, McRoberts, R.E., Reams, G.A., Van Deusen, P.C. and Moser, J.W., (eds.). U.S. Department of Agriculture, Forest Service, North Central Research Station, St. Paul, MN. General Technical Report NC-230. pp. 162-170.

Xu, J., Gu, H., Meng, Q., Cheng, J., Liu, Y., Sheng, J., Deng, J. and Bai, X., 2019. Spatial pattern analysis of *Haloxylon ammodendron* using UAV imagery-A case study in the

Gurbantunggut Desert. International Journal of Applied Earth Observation and Geoinformation, 83, Article 101891.

CHAPTER 4

The effects of nearby trees on the positional accuracy of GNSS receivers in a forested environment

Abstract

Global Navigational Satellite System (GNSS) technologies have been developed to address demand for enhanced positional accuracy. Smartphones are the most prevalent consumer-grade GNSS receiver today and have garnered attention thanks to improved positional accuracy and usability that can be accessed at an affordable price. In a forested environment, multipath error can deteriorate the positional accuracy, depending on state of nearby vegetation. Therefore, this study was conducted to investigate the impacts of the size and location of vegetation on positional accuracy of GNSS receivers to determine whether the errors observed are systematic. Twenty-six control points within the Whitehall Forest GPS Test site in Athens, Georgia were used to evaluate positional accuracy of three different types of GNSS receivers (mapping-grade, consumer-grade GNSS receiver, and a smartphone). Thirty-five forest variables were developed from information around each control point to conduct a correlation analysis with observed horizontal position error in the positions determined by each device. In this study, we confirmed that the positional error of the smartphone was significantly lower than the consumer-grade GNSS receiver, and similar, but significantly different than the positional error observed by the mapping-grade receiver. We confirmed significant correlations between forest variables and horizontal position error regardless of the GNSS receiver employed, yet trends were not consistent. The effect of the *size* of nearby trees on horizontal position error could not be generalized, however the *location* of nearby trees on horizontal position error could.

Introduction

Since the United States (NAVSTAR GPS) and Russian (GLONASS) global positioning systems were begun, Global Navigational Satellite Systems (GNSS) have developed relatively rapidly over the last 50 years. Today, GNSS constellations include NAVSTAR GPS, GLONASS, GALILEO (European Union), BeiDou (China), NAVIC (India), and QZSS (Japan) and when combined, they currently have over 120 satellites in use for navigational purposes above Earth. These GNSS constellations utilize a variety of electromagnetic frequencies to transmit signals to GNSS receivers. These options facilitate many precise-positioning applications (such as navigation, timing, and remote sensing) through improved satellite visibility and ambiguity resolution of signals (Li et al. 2015, Paziewski 2020). Advancements in associated GNSS technologies (GNSS antenna chipsets and augmentation systems) have also acted to enhance the accuracy of horizontal positions determined by GNSS receivers.

GNSS receivers are used by people to navigate and map land and water features and are often categorized as belonging to three grades (survey, mapping, and consumer) depending on their general ability to correctly determine and position and their general cost. Even though survey-grade receivers provide the highest level of positional accuracy, their acquisition cost and their extended time to determine positions hinder their general use in the forestry practice, except in cases where property corners or other important landscape positions need to be mapped or located with a very high degree of accuracy. Indeed, in a recent survey only 2.8% of foresters in the southern United States indicated that they utilized survey-grade GNSS receivers in their normal work activities (Bettinger et al. 2019). Mapping-grade and consumer-grade GNSS

receivers are much more generally used in the practice of forestry for navigation and mapping purposes (Bettinger et al. 2019). These types of GNSS receivers are more affordable than survey-grade receivers and include moderately priced (up to about $5,000) devices dedicated to data collection and navigation as well as more common smartphones and tablets (Bettinger et al. 2019, Keefe et al. 2019). New developments in GNSS technologies have made it possible to use lower grade GNSS receivers to obtain relatively accurate (2-10 m) horizontal position information (Paziewski 2020). In addition, the positional accuracy of landscape features determined by mapping- and consumer-grade receivers can be improved by using them in conjunction with other technologies such as RFID (radio frequency identification), UWB (ultra-wideband) and localization techniques such as INS (inertial navigation system) and RTK (real-time kinematic) (Keefe et al. 2019, Zangenehnejad and Gao, 2021).

Among consumer-grade GNSS receivers, smartphones have attracted the attention of researchers and forestry practitioners as an alternative GNSS receiver because they can address user desires for lower-cost, more portable, wearable devices (Lachapelle et al. 2018, Paziewski 2020, Zangenehnejad and Gao, 2021) that facilitate alternative uses (telecommunication, applications). About 331.2 million smartphones were shipped to people around the world during the third quarter of 2021, and the demand is expected to continue to be strong despite supply chain issues associated with the Covid-19 pandemic (IDC Corporate USA 2021, Menard et al. 2011, Zangenehnejad and Gao 2021). Some have therefore suggested that the smartphone should be considered as the most prevalent, general type of GNSS receiver in the market today (Paziewski 2020, Tomaštík and Varga 2021).

With the massive popularity of smartphones among society, the need to evaluate the feasibility of using them as GNSS receivers to collect positional information is important. Studies concerning smartphone positioning accuracy have significantly increased in the past few years with the development of mass-market GNSS chipsets and the accessibility of raw GNSS measurements (Paziewski 2020). Low-cost, mass-market GNSS chipsets within smartphones have been studied, as well as chipsets that can accommodate dual frequency multi-constellation signals, allowing one to track modernized GNSS signals (i.e. L5/E5) (Paziewski 2020). These advances may facilitate enhanced positional accuracy by potentially mitigating ionospheric effects on signal propagation (Tomaštík and Varga 2021, Zangenehnejad and Gao 2021). With the advent of the Application Programming Interface 24 (API 24) in 2016, raw GNSS measurements including pseudoranges, carrier phases, Doppler GNSS measurement, navigation messages, and hardware clocks may be accessible to users and developers (Paziewski 2020, Tomaštík and Varga 2021). This information would then allow one to investigate the potential augmentation improvements of various post-processing algorithms that have been designed for higher grade GNSS receivers (Tomaštík and Varga 2021).

According to previous studies, the GNSS chipset typically equipped within smartphones has a few unique characteristics compared to the GNSS chipsets installed in other GNSS receivers. It seems that smartphones have been designed to be sensitive to weaker GNSS signals compared to other GNSS receivers, and smartphones may be able to utilize an Assisted GPS (A-GPS) technology, which uses the Internet or Wi-Fi signals to acquire satellite information, such as the almanac and satellite-specific ephemeris, from network providers (Tomaštík and Varga 2021, Yoon et al. 2016, Zandbergen and Barbeau 2011). This additional information may be

advantageous to the use of smartphones, by reducing the signal search space and the time required to determine a position, and this information can potentially increase positional accuracy even in indoor conditions (Tomaštík and Varga 2021). However, smartphones may also have inherent weaknesses, as some employ duty cycling, which makes the satellite signal data collection process within smartphones operate in a discontinuous manner (Paziewski 2020, Yoon et al. 2016). This function was designed to prevent an adverse rate of battery drainage, but it causes discontinuities in phase observables, which can negatively affect the ability of a smartphone device to precisely determine a position (Gogoi et al. 2019). Due to this and perhaps other hardware and software limitations, smartphones generally have a lower carrier-to-noise ratio (C/N_0) when collecting positional information, compared to the higher grade GNSS receivers (Humphreys et al. 2016, Paziewski 2020, Zhang et al. 2018).

Multipath may be the largest source of error when GNSS receivers are used within a forest (Danskin et al. 2009). Some studies have tried to reduce the impact of multipath error by using an anechoic chamber, a choke ring antenna, or a radio frequency shield box or plate (Danskin et al. 2009, Fortunato et al. 2019, Gogoi et al 2019, Li and Geng 2019, Tomaštík and Varga 2021). However, it is almost impossible to mitigate the impact of multipath error when navigating or working in a forest, as the arrangement of nearby obstructions (trees) and the arrangement of the satellite constellation are constantly changing as one moves around. Because of this, most studies (except Danskin et al. 2009) have been conducted under open area or low multipath conditions to reduce the multipath error and attain the highest positional accuracy. There have been attempts to investigate the effects of nearby vegetation (forest age, composition, and juxtaposition of trees) on positional accuracy determined by GNSS receivers, yet only weak correlations with

horizontal positional accuracy were observed (Bettinger and Merry 2012, Murgaš et al. 2018). None of these studies involved the use of smartphones. Tomaštík and Varga (2021) assumed that the distance of a tree stem to the position being determined by a GNSS receiver would hinder GNSS signal reception as trees were closer to the receiver. Therefore, one can argue that the impact of multipath when using smartphones in forested areas has not yet been thoroughly examined, and that it is essential to investigate the horizontal position accuracy of smartphones in environments where they may often be used (Zangenehnejad and Gao 2021).

The first objective of this study was to evaluate the feasibility of three GNSS receivers (a smartphone, a consumer-grade GNSS receiver, and a mapping-grade GNSS receiver) as a reliable GNSS receiver in a forested area, by comparing their positional accuracy. We focused on the practical common use of GNSS receivers in forestry by limiting the observation time (less than a minute) during the field data collection effort. The performance of the GNSS receivers was evaluated based on the static horizontal positional accuracy that practitioners regularly encounter, employing neither post-process algorithms nor external GNSS antennas. The mapping-grade GNSS receiver was evaluated in this study as the control, the type of receiver that professional foresters commonly use for navigation and field data collection activities. The second objective of this study was to investigate the impact of nearby forest conditions on positional accuracy of these GNSS receivers. We developed a suite of forest variables that were based on the location and size of nearby trees. Some of these forest variables were guided by Tobler's First Law that "near things are more related than distant things" (Tobler 1970). We hypothesize that forest vegetation, as described by the size and location of nearby trees, is correlated with the observed horizontal position error one may experience when determining

positions with a GNSS receiver. We therefore investigated whether the distance or direction of trees to a sample point, along with the size of the trees, had an influence on the horizontal accuracy of positions determined by GNSS receivers.

Materials and Methods

The control points for this study were established based on the surveyed control points at the Whitehall Forest GPS Test Site (gps-test-site.uga.edu) in Athens, Georgia (USA). The GPS Test Site contains 3 Online Positioning User Service (OPUS) monuments and 37 permanent control points which were established in 2004 by professional surveyors. The positions of the 3 monuments were determined using positions (epochs, position fixes) collected for 4 hours using an Ashtech Locus survey-grade GNSS receiver. The horizontal position of these 3 monuments is assumed very accurate (under 2 cm), and they have been accepted into the National Spatial Reference System (NSRS). These monuments are marked with aluminum pins about 9 cm in diameter and 1 m long. The horizontal positions of the 37 permanent control points throughout the GPS Test Site were determined by professional surveyors using a Topcon GTS-211D instrument to develop a closed traverse survey. The horizontal positions of these 37 permanent control points are considered to be nearly as accurate as those of the 3 OPUS monuments.

Two of the 37 permanent control points were selected and used as centers around which we established several other temporary control points. These 2 permanent control points were located within an older, deciduous, uneven-aged forest consisting of *Quercus* spp., *Carya* spp., *Ostrya virginiana*, and other tree species, of which the density was 126 trees ha^{-1}, the basal area

was 23.0 m^2 ha^{-1}, and the dominant trees were 70 to 80 years old. Around these 2 permanent control points, 24 temporary control points were established using careful triangulation, providing a total of 26 control points upon which this study is based (Figure 1). Each temporary control point was located on a 6 m grid around one of the 2 permanents control points, up to a radius of 12 m (Figure 4.1).

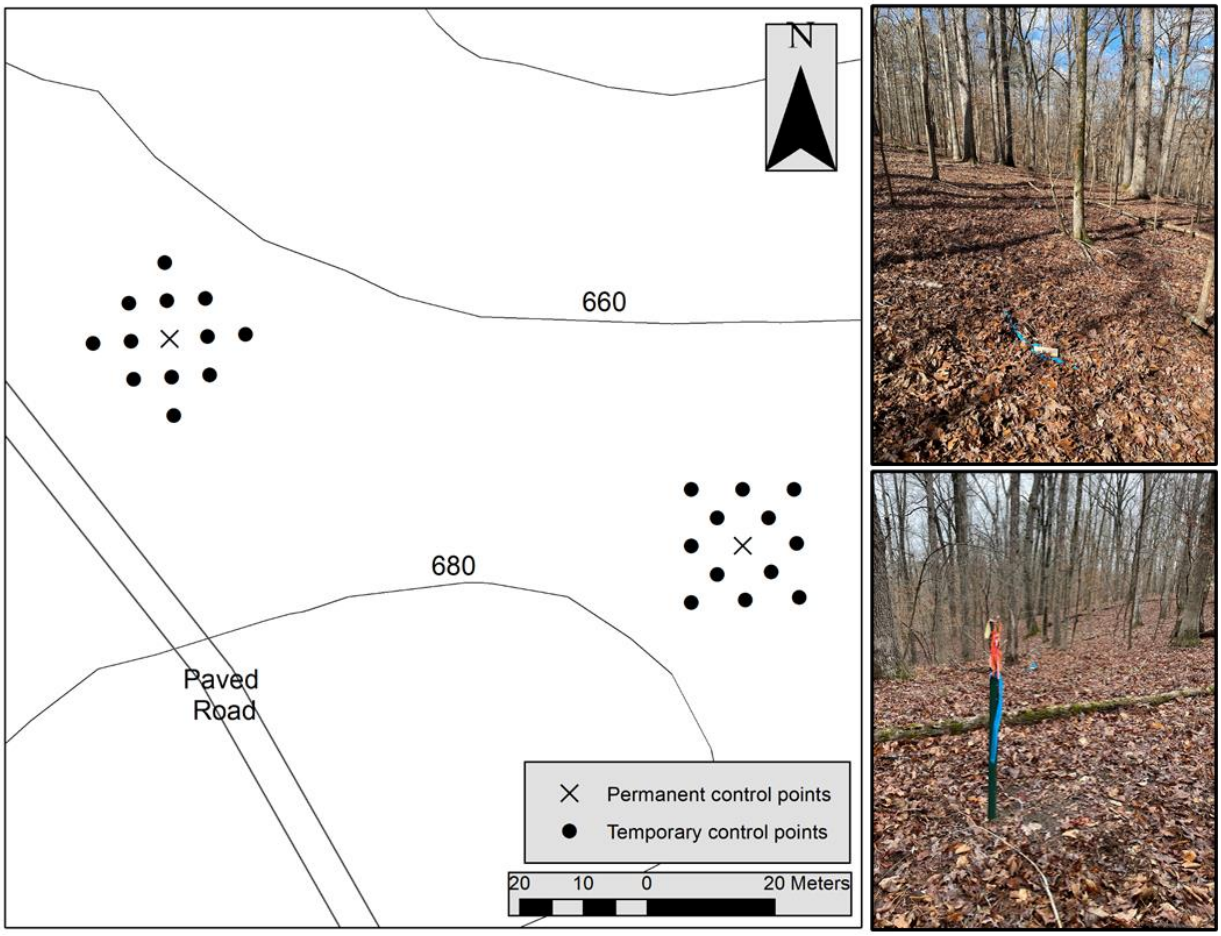

Figure 4.1 The study location of a portion of the GPS Test Site in Athens, Georgia (USA). The temporary control points were placed on a 6 m grid around a permanent control point.

A mapping-grade GNSS receiver and two consumer-grade GNSS receivers were used in this research study to evaluate horizontal position accuracy and tree interactions. The mapping-grade receiver was a Trimble Juno T41 (Trimble Inc., Sunnyvale, CA, USA), which was equipped with a GPS antenna that was manufactured by Inpaq technology Co. Ltd (Chunan, Miaoli, Taiwan) (70×43.18×9 mm). Mapping-grade GNSS receivers have been shown to provide very good horizontal position accuracy (1 to 5 m) under forest canopies, and the acquisition price generally ranges between $1,000 and 10,000 (Bettinger and Merry 2011). With this GNSS receiver, positional data were collected using SOLO Forest software (Trimble Forestry Automation 2012) which allows users to change settings such as the maximum PDOP (positional dilution of precision), minimum SNR (signal to noise ratio), and whether the Wide Area Augmentation System (WAAS) is used. For this study, the maximum PDOP was assumed to be 8, the minimum SNR was assumed to be 4, and WAAS augmentation was enabled. Unlike the consumer-grade GNSS receivers we tested, the mapping-grade GNSS receiver collected points (position fixes) and averaged those to determine a single horizontal position and allowed the user to monitor the standard deviation of the location of the determined positions and the number of position fixes that were recorded. The final, averaged determined position was accepted as a data observation only when the standard deviation was less than 1.5 meters, and the number of position fixes was greater than 25. The data was recorded using the WGS84 coordinate system and exported in a shapefile format for further processing.

Two consumer-grade GNSS receivers, a Garmin Oregon 700 GNSS receiver (Garmin, Olathe, KS, USA) and an iPhone 12 Pro smartphone (Apple Inc., Cupertino, CA, USA) were used in this study. Compared to the mapping-grade GNSS receiver, these consumer-grade receivers did not

allow specific PDOP and SNR settings. Further, these consumer-grade GNSS receivers determined positions using a single point (position fix) rather than the average of multiple points. The Garmin receiver is a traditional handheld GNSS receiver with a GPS antenna made by Cirocomm Technology Corp. (Taoyuan City, Taiwan) (size: 15×15×4 mm). It allows users to choose which satellite system(s) (NAVSTAR GPS and GLONASS) to use and to enable WAAS augmentation. The Garmin receiver had the ability to determine positions through the averaging of multiple position fixes, but this function, and WAAS augmentation, was not enabled in this study as they could not be monitored. Data was exported from the Garmin receiver to an Excel file format using Basecamp software (Garmin, Olathe, KS, USA). Regarding the iPhone 12 Pro, multiple antennas (12) are equipped in the unit, and each has a specific purpose, such as capturing ultra-wide band (UWB) and ultra-high bend (UHB) signals from 5G networks, along with Wi-Fi, cellular, GNSS, or Bluetooth signals. The iPhone 12 Pro can utilize dual frequency GNSS signals, including L1 and L5 for acquiring positional information, using two different antennas equipped at the top and bottom of the unit. The multiple antennas are part of one system, so it was difficult to measure specific size of antennas for capturing L1 and L5 signals precisely. The antennas used to collect L1 and L5 signals are very small (around 10×10 mm). According to the manufacturer's manual, the iPhone can utilize satellite signals from a wide collection of satellite systems, including NAVSTAR GPS, GLONASS, GALILEO, QZSS, and BeiDou. However, the iPhone 12 Pro did not provide the raw GNSS measurements, thus information such as carrier frequency and noise level were not available. The data was collected using the Avenza Maps application (Avenza System Inc., Toronto, Canada). This application allows users to collect waypoints by tapping the screen of the smartphone. Data is exported to a

Keyhole Markup Language (KML) file. Both consumer-grade GNSS receivers recorded data using the WGS84 coordinate system.

Each of the 26 control points was visited 20 times during a leaf-off season (February and March 2021). The order of visit was randomized each time. At a visit to a control point, the order of the data collection effort was also randomized for the 3 GNSS receivers. A leveling monopod was used to place GNSS receivers on top of each control point and to maintain a constant position during the data collection effort. Data were collected during similar time ranges each day to have similar satellites distributed around sky, and the researcher always stood on the north side of monopod when data was being collected. Even though we made efforts to reduce any effects inducing by accepting signals from different satellites or constellations for every visit, it could not be removed. The mapping-grade and consumer-grade receivers that utilized in this study could not modified to receive its signals from specific satellites. Further, collecting spatial data at the same location simultaneously using three GNSS receivers was not possible. So, we changed GNSS receivers promptly to reduce related time delay.

The horizontal accuracy of GNSS receivers was evaluated using the root mean square error (RMSE) of the determined positions, as compared to the true positions of the control points, an assessment commonly employed in this type of study (i.e., Lee et al. 2020, Ransom et al. 2010, Sigrist et al. 1999).

$$RMSE = \sqrt{\frac{\sum_i^n ((x_i - x)^2 + (y_i - y)^2)}{n}}$$

Here, n is the total number of observations in a visit; i is the ith observation of the visit; x_i and y_i are the easting and northing, respectively, of the ith observations; and x and y are the assumed true easting and northing of the associated control point.

Standard deviational ellipses were applied to quantify the directional distribution of determined positions in regard to a related control point (Figure 4.2). The results of this analysis provide the angle (directional distribution), area (distribution), and the mean center (centroid of ellipse representing center tendency) which is equivalent to the root squared error of the mean (RSEM) (Lee et al. 2020).

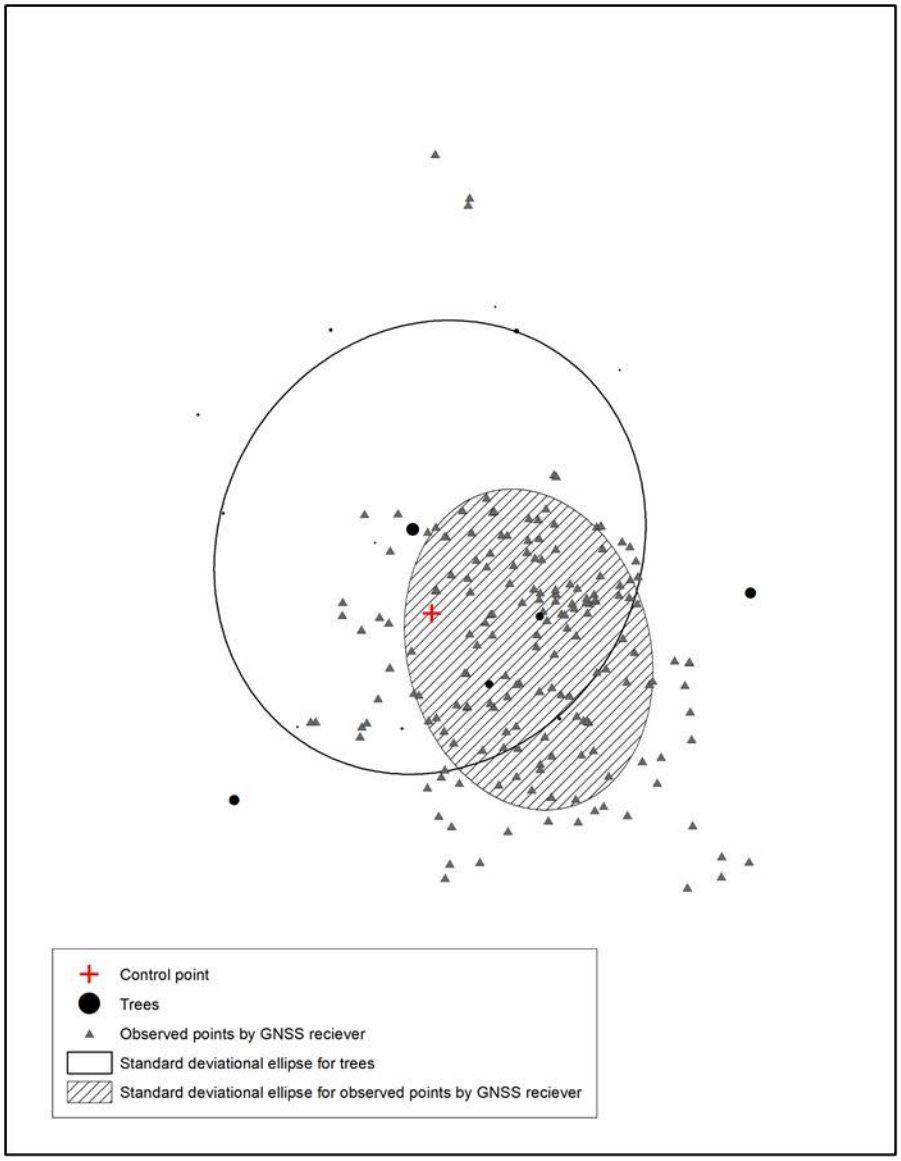

Figure 4.2 The example of standard deviational ellipses. Each standard deviational ellipse was determined based on the location of nearby trees and the observed points by GNSS receiver.

To obtain the forest variables, every tree greater than 1.37 m tall, either dead or alive, was measured if it was located within 20 m from one of the two permanent control points. The location of each tree's stem was determined using a closed traverse survey by measuring

distances and azimuth between trees and temporary and permanent control points. Specifically, the azimuth was measured from a control point to the center of stem using a laser rangefinder (TruPulse 360R, Laser Technology Inc., Centennial, CO, USA). Further, half of the diameter at breast height (DBH) was added to the measured distance to estimate the location of stem center. Each control point (permanent and temporary) was assumed as a center of a plot having a radius of 8 m, which is equivalent a 0.02 ha (0.05 acre) plot, so we had 26 of plots with different groups of nearby trees. Forest condition variables were summarized only for those trees within 8 m from each control point. Thirty-five forest condition variables were developed for assessing the correlation between condition and the observed horizontal position error of the GNSS receivers (Table 4.1). Multivariate regression analysis using R (version 3.6.1, RStudio, Inc., Boston, MA, USA) was conducted to evaluate the association of forest condition variables and horizontal position error observed by the GNSS receivers.

Table 4.1 A summary of forest variables used in the correlation analysis.

Forest variables	Description
1. Tree count	The total number of trees (living and dead) within 8 m or less from a control point
2. Average distance to trees [Ave. Dist.]	The average distance (m) between a control point and the center of trees 8 m or less from the control point
3. Average DBH [Ave. DBH]	The average DBH (cm) of trees 8 m or less from a control point
4. Standard deviation of DBH [SD. DBH]	The standard deviation of the DBH of trees 8 m or less from a control point
5. Coefficient of variation of DBH [CV. DBH]	The coefficient of variation of the DBH of trees 8 m or less from a control point
6. Average basal area of trees [Ave. BA]	The average basal area (m^2) of trees 8 m or less from a control point
7. Standard deviation of basal area [SD. BA]	The standard deviation of the basal area of trees 8 m or less from a control point
8. Coefficient of variation of basal area [CV. BA]	The coefficient of variation of the basal area of trees 8 m or less from a control point
9. Distance to the mean center of an ellipse formed by nearby trees [Dist. MC]	The distance (m) from a control point to the mean center of the ellipse formed by trees 8 m or less from the control point
10. Latitude (north-south) distance to the mean center of an ellipse formed by nearby trees [Lat. MC]	The difference (m) in the *Y* coordinate of the control point and the *Y* coordinate of the mean center of the ellipse formed by trees 8 m or less from the control point
11. Departure distance to the mean center of an ellipse formed by nearby trees [Dep. MC]	The difference (m) in the *X* coordinate of the control point and the *X* coordinate of the mean center of the ellipse formed by trees 8 m or less from the control point
12. Distance to the mean center of an ellipse formed by nearby trees, weighted by DBH [Dist. MC_{DBH}]	The distance (m) from a control point to the mean center of the ellipse formed by trees 8 m or less from the control point, weighted by the DBH of those trees
13. Latitude (north-south) distance to the mean center of an ellipse formed by nearby trees, weighted by DBH [Lat. MC_{DBH}]	The difference (m) in the *Y* coordinate of the control point and the *Y* coordinate of the mean center of the ellipse formed by trees 8 m or less from the control point, weighted by the DBH of those trees
14. Departure (east-west) distance to the mean center of an ellipse formed by nearby trees, weighted by DBH [Dep. MC_{DBH}]	The difference (m) in the *X* coordinate of the control point and the *X* coordinate of the mean center of the ellipse formed by trees 8 m

	or less from the control point, weighted by the DBH of those trees
15. Distance to the mean center of an ellipse formed by nearby trees, weighted by basal area [Dist. MC_{BA}]	The distance (m) from a control point to the mean center of the ellipse formed by trees 8 m or less from the control point, weighted by the basal area of those trees
16. Latitude (north-south) distance to the mean center of an ellipse formed by nearby trees, weighted by basal area [Lat. MC_{BA}]	The difference (m) in the *Y* coordinate of the control point and the *Y* coordinate of the mean center of the ellipse formed by trees 8 m or less from the control point, weighted by the basal area of those trees
17. Departure (east-west) distance to the mean center of an ellipse formed by nearby trees, weighted by basal area [Dep. MC_{BA}]	The difference (m) in the *X* coordinate of the control point and the *X* coordinate of the mean center of the ellipse formed by trees 8 m or less from the control point, weighted by the basal area of those trees
18. Latitude (north-south) distance to largest tree [Lat. $Tree_1$]	The difference (m) in latitude between the control point and the largest tree within 8 m of the control point
19. Departure (east-west) distance to largest tree [Dep. $Tree_1$]	The difference (m) in departure between the control point and the largest tree within 8 m of the control point
20. Largest tree basal area / distance to the largest tree [BA/Dist. $Tree_1$]	The basal area (m^2) of the largest tree within 8 m of a control point divided by the distance (m) to this largest tree from the control point
21. Largest tree basal area / latitude (north-south) distance to the largest tree [BA/Lat. $Tree_1$]	The basal area (m^2) of the largest tree within 8 m of a control point divided by the difference (m) in latitude between the control point and the largest tree
22. Largest tree basal area / departure (east-west) distance to the largest tree [BA/Dep. $Tree_1$]	The basal area (m^2) of the largest tree within 8 m of a control point divided by the difference (m) in departure between the control point and the largest tree
23. Average of two largest tree basal areas / average distance to the two largest trees [BA/Dist. $Tree_2$]	The average basal area (m^2) of the 2 largest trees within 8 m of a control point divided by the average distance (m) to the 2 largest trees from the control point
24. Average of two largest tree basal areas / average latitude (north-south) distance to the two largest trees [BA/Lat. $Tree_2$]	The average basal area (m^2) of the 2 largest trees within 8 m of a control point divided by the average latitude distance (m) to the 2 largest trees from the control point
25. Average of two largest tree basal areas / average departure (east-west) distance to the two largest trees	The average basal area (m^2) of the 2 largest trees within 8 m of a control point divided by

[BA/Dep. $Tree_2$]	the average departure distance (m) to the 2 largest trees from the control point
26. Average of three largest tree basal areas / average distance to the three largest trees [BA/Dist. $Tree_3$]	The average basal area (m^2) of the 3 largest trees within 8 m of a control point divided by the average distance (m) to the 3 largest trees from the control point
27. Average of three largest tree basal areas / average latitude (north-south) distance to the three largest trees [BA/Lat. $Tree_3$]	The average basal area (m^2) of the 3 largest trees within 8 m of a control point divided by the average latitude distance (m) to the 3 largest trees from the control point
28. Average of three largest tree basal areas / average departure (east-west) distance to the three largest trees [BA/Dep. $Tree_3$]	The average basal area (m^2) of the 3 largest trees within 8 m of a control point divided by the average departure distance (m) to the 3 largest trees from the control point
29. Average $(\text{basal area})^2$ [Ave. BA^2]	The average basal area (m^2) of trees 8 m or less from a control point, squared
30. Average (Latitude × $(\text{basal area})^2$) [Ave. Lat. BA^2]	The average of the latitude (north-south) distance (m) from each tree within 8 m of a control point to the control point, times the basal area (m^2) squared of the tree
31. Average (departure × $(\text{basal area})^2$) [Ave. Dep. BA^2]	The average of the departure (east-west) distance (m) from each tree within 8 m of a control point to the control point, times the basal area (m^2) squared of the tree
32. Ellipse area [Area $_{tree}$]	The average area (m^2) of the standard deviational ellipse formed by trees within 8 m of a control point
33. Overlapping ellipse area [Overlap Area]	The area of overlap (m^2) between the ellipse formed by trees within 8 m of a control point, and the ellipse formed by the observed positions from a GNSS receiver at that same control point
34. Overlapping ellipse percent from the perspective of the observed GNSS positions [Overlapped Area $_{GNSS\ receiver}$]	The area of overlap (m^2) between the ellipse formed by trees within 8 m of a control point, and the ellipse formed by the observed positions from a GNSS receiver at that same control point, divided by the size of the ellipse formed by the observed positions from a GNSS receiver at that same control point
35. Overlapping ellipse percent from the perspective of the trees within 8 m of a control point [Overlapped Area $_{tree}$]	The area of overlap (m^2) between the ellipse formed by trees within 8 m of a control point, and the ellipse formed by the observed positions from a GNSS receiver at that same control point, divided by the size of the ellipse

	formed by the trees within 8 m of that same control point

Results

Within 8 m of each control point, we found an average number of 14.5 trees and average DBH of 17.04 cm (Table 4.2). Within these plots, the average distance of trees from each control point ranged from 4.60 to 6.03 m, with an overall average of 5.31 m. Although somewhat variable, more trees seemed to be located slightly to the West and South directions from each control point, as evidenced by the negative average departure (east-west difference) and negative average latitude (north-south difference) in Table 4.2. The average horizontal positional error (RMSE) observed by the GNSS receivers, for each control point, ranged from 2.28 to 9.77 m (Table 4.3). The minimum and maximum average RMSE values for the consumer-grade GNSS receiver were 5.75 m and 9.77 m. When the smartphone was used, the minimum and maximum average RMSE were 3.04 m and 5.64 m. With the mapping-grade GNSS receiver, the minimum and maximum average RMSE were 2.28 m and 6.19 m. In general, the smallest average positional error was obtained using the mapping-grade GNSS receiver, however the performance of the smartphone was very similar in this respect. The largest average positional error was obtained using the consumer-grade GNSS receiver (Garmin Oregon 700). The average RMSE from every control point determined by the consumer-grade GNSS receiver, smartphone, and mapping-grade GNSS receiver was 8.11 m (± 4.61 m), 3.91 m (± 2.36 m), and 3.45 m (± 2.18 m), respectively (Figure 4.3). From this information, we observed a significance difference in the average RMSE by GNSS receiver type.

Table 4.2 A summary of tree characteristics within 8 m of each control point.

Control point	Number of trees	Average of distance (m)	Average DBH (cm)	Average of departure (m)	Average of latitude (m)
Every control point	14.5	5.31	17.04	-0.05	-0.10
1	15	5.17	18.34	-0.26	-0.43
2	10	5.23	19.05	0.50	1.41
3	14	6.03	18.16	-1.05	-0.21
4	11	4.73	11.40	0.34	1.41
5	11	5.90	19.30	-0.20	-1.37
6	11	4.75	20.19	0.94	-0.10
7	10	5.23	18.82	1.02	-0.51
8	12	5.32	16.33	0.01	1.10
9	19	5.56	15.34	0.03	2.06
10	14	5.43	19.28	0.09	-0.09
11	12	5.63	19.00	-0.10	0.23
12	15	5.05	16.03	0.64	0.25
13	15	5.71	20.14	0.32	-0.00
14	14	4.84	17.04	0.00	-0.42
15	17	4.82	12.42	0.42	-0.99
16	18	5.98	18.54	0.53	0.13
17	18	5.10	15.04	-1.02	0.98
18	16	5.31	12.29	-0.63	0.99
19	17	4.99	14.27	0.33	-0.09
20	17	5.79	20.04	0.55	-0.37
21	18	5.37	19.99	-0.63	0.16
22	18	5.39	13.69	-1.11	-1.88
23	15	5.06	13.94	0.06	-1.58
24	17	5.65	19.51	-0.31	-0.60
25	12	4.60	19.35	-1.78	-0.96
26	11	5.39	15.65	-0.08	-1.83

Table 4.3 The positional error (root mean square error, RMSE) and the area of standard deviational ellipses observed by different GNSS receivers at each control point.

Control point	RMSE (m)			Area of standard deviational ellipses (m^2)		
	Garmin Oregon 700	*iPhone 12 Pro*	*Trimble Juno T41*	*Garmin Oregon 700*	*iPhone 12 Pro*	*Trimble Juno T41*
1	7.99	3.56	3.20	173.75	34.44	27.77
2	7.55	3.52	3.47	113.17	30.58	33.00
3	8.40	4.32	2.55	158.84	49.23	23.30
4	8.93	3.79	4.08	164.55	48.46	43.62
5	8.76	3.21	4.22	159.56	23.83	54.06
6	8.57	3.82	3.04	148.69	47.90	27.15
7	9.17	4.41	3.65	134.44	34.96	31.69
8	5.91	3.42	3.75	132.12	30.66	44.66
9	5.75	3.04	3.17	107.74	32.75	36.44
10	9.21	4.14	4.46	107.31	49.19	46.20
11	6.89	3.74	3.60	107.78	33.09	42.34
12	9.23	4.24	3.32	190.69	53.32	39.46
13	7.53	3.20	3.32	131.01	22.57	34.68
14	7.68	3.52	6.19	257.47	42.20	50.17
15	7.29	3.26	3.23	169.93	36.35	33.59
16	7.72	3.95	2.79	125.35	41.56	26.32
17	7.86	4.17	3.97	192.17	33.52	64.14
18	8.76	3.46	2.98	189.15	36.54	37.55
19	8.70	4.32	3.00	174.13	49.93	34.58
20	8.54	4.03	2.96	142.38	51.55	28.66
21	6.95	3.56	2.72	140.27	32.51	27.45
22	8.67	4.86	3.21	226.93	58.52	42.30
23	8.37	3.78	3.34	171.95	35.35	48.04
24	8.33	4.08	3.23	158.38	42.78	47.04
25	9.77	4.76	2.28	221.55	52.88	19.85
26	8.27	5.64	4.01	421.08	63.29	45.77

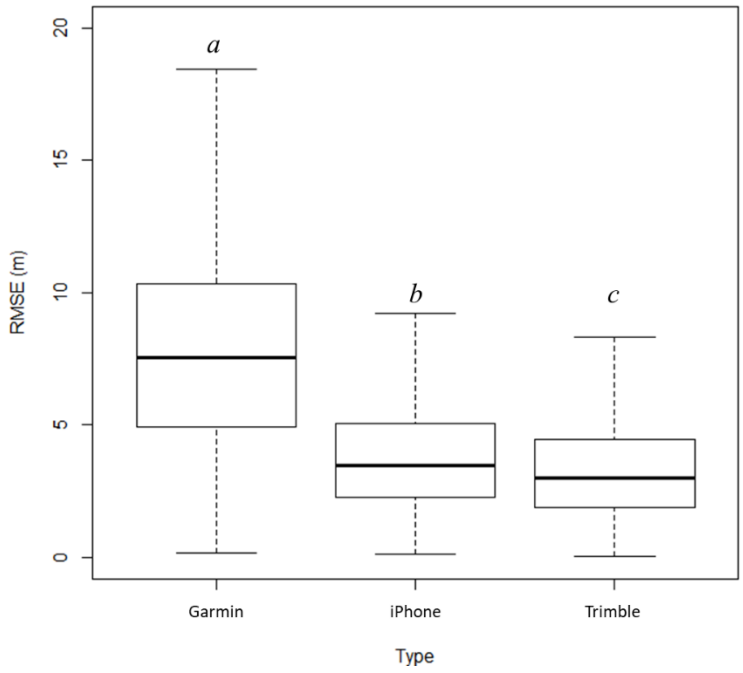

Figure 4.3 Boxplot for horizontal positional accuracy (RMSE, root mean square error) by GNSS receiver types. *Different letter* indicates statistically significant differences (p-value < 0.001).

Parameters related to the distribution of observed points also indicated some significant differences between GNSS receivers (Figure 4.4). For example, the RSEM indicating the distance between mean center of observed GNSS-determined positions and related control points and the area of standard deviational ellipse for GNSS-determined positions suggested no significance differences were observed between the smartphone and the mapping-grade GNSS receiver. However, the RSEM and standard deviational ellipse area for observed GNSS-determined positions using the consumer-grade GNSS receiver were significantly different than both of the other devices. The larger area of standard deviational ellipse from the observed GNSS-determined positions of the consumer-grade GNSS receiver suggested that the observed

points were more likely distributed wider around the control point. This also suggested that the consumer-grade GNSS receiver had larger variance in positional error.

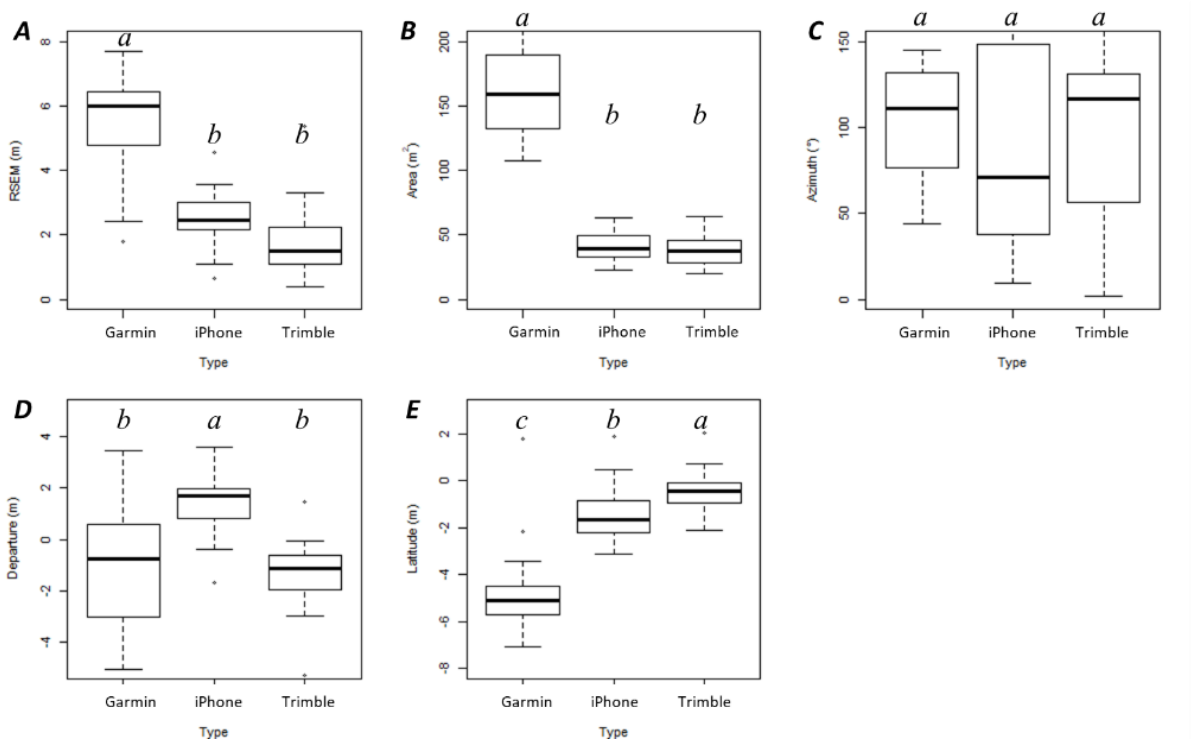

Figure 4.4 Boxplot for directional distribution observed by GNSS receivers (*A*: RSEM (root squared error of the mean, calculated based on the mean center); *B*: Area of ellipse (m^2); *C*: Rotation (º); *D*: Departure (m); *E*: Latitude (m)). The *different letters* indicate significant differences ($p < 0.05$).

We observed no statistically significant difference in the rotation representing the directional distribution of the observed GNSS positions, regardless of the GNSS receiver types due to its wide variance (Table 4.4, Figure 4.4). This meant that the directional distribution might be the most susceptible parameter that could be influenced by environmental factors regardless of

GNSS receivers. The average departure was negative for observed GNSS positions collected by the consumer-grade and mapping-grade GNSS receivers (Table 4.4), indicating observed positions were often slightly (about 1 m) to the West of the control points. When the smartphone was used, the average departure was positive meaning that the mean center for the distribution of observed GNSS positions was located East (about 1.5 m) of each control point. Otherwise, the average latitude was negative regardless of GNSS receiver, indicating that the mean center for the distribution of observed GNSS positions was South of each control point, nearly 5 m South on average in the case of the consumer-grade GNSS receiver.

Standard deviational ellipses were modeled for observed GNSS-determined positions at each control point, and even though the average size (area) of these was not statistically significant between the smartphone and the mapping-grade GNSS receiver, statistically significant differences in the size of these ellipses were observed between the consumer-grade GNSS receiver and the other two receivers. Not surprisingly, the maximum area of an ellipse at any one control point (about 421 m^2) was observed using data collected by the consumer-grade GNSS receiver (Table 4.3). The minimum ellipse area (about 20 m^2), indicating high precision amongst observed GNSS-determined positions, was observed by the mapping-grade GNSS receiver.

Table 4.4 The summary of elliptical metrics from measurements obtained by different GNSS receivers.

Metric	*Garmin Oregon 700*	*iPhone 12 Pro*	*Trimble Juno T41*
RSEM (m)			
Average	5.51	2.52	1.75
St. deviation	1.42	0.79	1.06
Minimum	1.78	0.64	0.40
Maximum	7.70	4.55	5.35
Area (m^2)			
Average	170.01	41.08	38.07
St. deviation	63.73	10.57	10.44
Minimum	107.31	22.57	19.85
Maximum	421.08	63.29	64.14
Rotation (◦)			
Average	105.59	87.99	97.54
St. deviation	29.08	50.97	57.93
Minimum	44.10	9.23	2.10
Maximum	144.79	170.67	167.23
Departure (m)			
Average	-0.86	1.49	-1.29
St. deviation	2.36	1.15	1.28
Minimum	-5.05	-1.69	-5.27
Maximum	3.42	3.58	1.46
Latitude (m)			
Average	-4.84	-1.47	-0.44
St. deviation	1.68	1.16	0.86
Minimum	-7.06	-3.15	-2.10
Maximum	1.77	1.90	2.05

RSEM = root squared error of the mean; Area = the area of standard deviational ellipse; Rotation = the directional distribution of observed points; Departure = the difference between observed X coordinates and control X coordinate; Latitude = the difference between observed Y coordinates and control Y coordinate.

The correlations between positional error (RMSE) and forest variables indicated that in general there was weak to moderate correlation between these regardless of GNSS receiver employed (Table 4.5). However, two forest variables indicated a significant correlation with positional error with all three GNSS receivers. First, the difference between the *X* coordinate of a control point and the *X* coordinate of the mean center of the ellipse formed by trees 8 m or less from the control point, weighted by the DBH of those trees, was statistically significantly and positively correlated with error in positions determined by the smartphone and the consumer-grade GNSS receiver, and statistically significantly and negatively correlated with error in positions determined by the mapping-grade GNSS receiver. Second, the area of overlap between the ellipse formed by trees within 8 m of a control point, and the ellipse formed by the observed positions from a GNSS receiver at that same control point, divided by the size of the ellipse formed by the observed positions from a GNSS receiver at that same control point, was statistically significantly and negatively correlated with error in positions determined by all three devices. In this latter case, as the overlapping area of the ellipse formed by trees within 8 m of a control point and the ellipse formed by GNSS-determined positions increased, positional error decreased. The location of nearby trees with respect to positions being determined, either shifted away (low overlap of ellipses) or directly in the vicinity (high overlap in ellipses), does seem to affect positional error. Further, in this latter case, the strongest correlation was observed amongst the positions determined by the three devices.

Table 4.5 A summary of Pearson correlation coefficients for RMSE and forest variables (†*p*-value < 0.05; ‡ *p*-value < 0.01; ⁂*p*-value <0.001).

Forest variable	*Garmin Oregon 700*	*iPhone 12 Pro*	*Trimble Juno T41*
Tree count	-0.26	-0.13	-0.28
Ave. Dist.	-0.40	-0.08	-0.17
Ave. DBH	0.00	-0.04	-0.11
SD. DBH	-0.10	0.11	-0.12
CV. DBH	-0.13	0.13	-0.02
Ave. BA	-0.13	-0.14	-0.22
SD. BA	-0.01	0.07	-0.18
CV. BA	0.20	0.47 †	0.05
Dist. MC	0.05	0.27	-0.17
Lat. MC	0.45 †	0.50 ‡	0.01
Dep. MC	0.08	0.26	-0.20
Dist. MC_{DBH}	-0.24	0.17	0.16
Lat. MC_{DBH}	0.41 †	0.27	0.09
Dep. MC_{DBH}	0.58 ‡	0.45 †	-0.46 †
Dist. MC_{BA}	-0.14	-0.06	0.15
Lat. MC_{BA}	0.39 †	0.14	0.07
Dep. MC_{BA}	0.61 ⁂	0.34	-0.37
Lat. $Tree_1$	-0.42 †	-0.21	-0.03
Dep. $Tree_1$	-0.24	-0.13	0.05
BA/Dist. $Tree_1$	-0.12	-0.28	-0.10
BA/Lat. $Tree_1$	-0.04	0.56	0.03
BA/Dep. $Tree_1$	-0.14	0.07	0.58 ‡
BA/Dist. $Tree_2$	-0.23	0.03	-0.14
BA/Lat. $Tree_2$	0.21	0.13	0.24
BA/Dep. $Tree_2$	-0.17	-0.29	0.22
BA/Dist. $Tree_3$	-0.28	-0.10	0.18
BA/Lat. $Tree_3$	0.06	-0.18	0.20
BA/Dep. $Tree_3$	0.01	0.04	0.46 †
Ave. BA^2	0.01	0.03	-0.21
Ave. Lat. BA^2	-0.22	-0.18	-0.09
Ave. Dep. BA^2	-0.38	-0.19	0.16
$Area_{tree}$	-0.13	0.04	-0.03
Overlapped Area	-0.70 ⁂	0.20	0.10
Overlapped $Area_{GNSS\ receiver}$	-0.88 ⁂	-0.68 ⁂	-0.85 ⁂
Overlapped $Area_{tree}$	-0.59 ‡	0.12	0.07

BA = Basal area

DBH = Diameter at breast height

Dep = Departure, or east-west difference from true control point position

Dist = Distance from true control point position

MC = The mean center of objects

Lat = Latitude, or north-south difference from true control point position

However, different trends in statistically significant correlations were observed between the three devices. For instance, nine of the forest variables were found to be significantly correlated with the positional error inherent in the data collected by the consumer-grade GNSS receiver, and four forest variables were found to be significantly correlated with the positional error inherent in the data collected by the smartphone and the mapping-grade GNSS receiver. These results indicated that the horizontal position error of the consumer-grade GNSS receiver was more likely affected by the forest variables we measured than the smartphone and the mapping-grade GNSS receiver.

Discussion

Based on the results of our study, the positional data collected by the smartphone had a similar level of horizontal positional accuracy and variance in forested conditions as compared to a mapping-grade GNSS receiver, even though it technically is classified as a consumer-grade GNSS receiver. The horizontal positional accuracy of the smartphone in this study fell into the range of accuracy obtained from previous studies involving smartphones, but again our study indicated that sub-meter positional accuracy was not attainable by any of the devices employed in forested conditions. Zhang et al. (2018) pointed out that sub-meter positional accuracy was

rarely achievable without the use of post-processing and an external antenna to reduce the effects of multipath. But, according to previous studies, even with the aid of post-processing or external antennas, the positional accuracy of a smartphone may be significantly lower than that obtained by higher grade devices under similar conditions (Murgaš et al. 2018, Tomaštík et al. 2021, Tomaštík and Varga 2021, Zang et al. 2018). Yet compared to a more common consumer-grade GNSS receiver, the smartphone had significantly higher positional accuracy with a lower level of variance. And, the horizontal position accuracy of the smartphone was similar to the mapping-grade receiver we employed, which was relevant to the results of previous studies.

The duty cycling and limitations of GNSS chipsets equipped within smartphones are considered major reasons why smartphones cannot attain the positional accuracy of higher grade GNSS receiver (Gogoi et al. 2019, Paziewski 2020, Zangenehnejad and Gao 2021). Duty cycling, the initiation, use, and termination of work on a particular circuit, was implemented in devices such as smartphones to reduce battery usage, but it hinders continuity of signal accepting (Paziewski 2020). Gogoi et al. (2019) confirmed that duty cycling increased the noise observed in GNSS signals, which deteriorates positional accuracy. Fortunately, duty cycling might be disabled in certain recent Android smartphones, and this advancement is expected to lead to enhanced positional accuracy of smartphones in the future by allowing better continuity of phase measurements (Paziewski 2020).

The GNSS chipsets within smartphones and other devices have been developed to address the general need for greater positional accuracy at an affordable cost to the end-user. According to the manufacturer's manual, it was confirmed that the smartphone we tested (iPhone 12 Pro)

could utilize multiple GNSS constellations and frequencies, as could the mapping-grade GNSS receiver we tested (Trimble Juno T41). The ability to obtain signals from multiple GNSS constellations may improve positional accuracy by reducing signal search time (Paziewski 2020). However, determining a position through a multi-constellation system may not always guarantee higher positional accuracy because it could induce noise and signals may be deteriorated by a large number of extreme errors (Tomaštík and Varga 2021, Wang et al. 2012). There are two main manufacturers for smartphone GNSS chipsets, the first dual-frequency chipset was released by Broadcom in 2018, and later that same year Qualcomm also released a dual-frequency chipset (Zangenehnejad and Gao 2021). The dual-frequency chipset may enhance positional accuracy by allowing the system to compensate for perceived ionospheric effects (Tomaštík and Varga 2021, Tomaštík et al. 2021, Zangenehnejad and Gao 2021). However, specific information about GNSS chipset equipped within the iPhone 12 Pro was not available to the public so we could not confirm whether the iPhone 12 Pro benefitted from these advances. The iPhone 12 Pro was equipped with multiple antennas and two of them were designed for accepting satellite signals. These GNSS chipsets were installed at the top and bottom of the smartphone and designed to detect a specific frequency such as L1 and L5. In the past, the GNSS chipset designed for smartphones may have been considered as a limitation (Fortunato et al. 2019), yet two GNSS chipsets designed to detect specific frequencies might be helpful in attaining better positional accuracy.

As it has been suggested that the GNSS chipset in smartphones may be susceptible to multipath error (Paziewski 2020, Tomaštík and Varga 2021); therefore, investigating the correlation between horizontal positional accuracy and forest variables (proxies for the juxtaposition of trees

with respect to survey points) was necessary to fill a knowledge gap. According to previous studies, horizontal position accuracy can change in response to the forest type within which the technology is being used (Lee et al. 2020, Tomaštík and Varga 2021). In this study, we observed a few significant correlations between forest variables and horizontal position error regardless of GNSS receiver. However, the assumption that the size of nearby tree stems would influence horizontal positional accuracy of GNSS receivers was not confirmed. With regard to the departure (east-west position) of the mean center weighted by DBH (Dep. MC_{DBH}), which had a significant correlation regardless of GNSS receivers, different trends of correlations were observed depending on the grade of GNSS receivers, again rendering the hypothesis that the *size* of nearby trees has a consistent, significant effect of positional accuracy of GNSS determined positions moot. Data from the consumer-grade GNSS receiver indicated positive moderate correlation, meaning that the farther the center of a tree was from a control point, the higher positional error was observed. Otherwise, the mapping-grade GNSS receiver had negative moderate correlation, indicating the near vicinity of mean center of tree stems induced the greater positional error. However, regardless of GNSS receiver employed, the percentage of overlap area between the ellipses formed by nearby trees and the ellipses formed by GNSS-determined positions (Overlapped $Area_{GNSS\ receiver}$) was found to be important, thereby may indicate that there is indeed an effect on the positional accuracy of GNSS-determined positions and the *location* of nearby trees.

Even though we developed a number of forest variables based on tree characteristics and their distribution around each control point, we found it complicated to define or generalize trends in correlations between positional accuracy and forest variables. We confirmed that multipath,

likely induced by nearby vegetation, deteriorated the horizontal positional accuracy in the forested study area but how it affected positional accuracy could not be generalized (Bettinger and Merry 2012, Tomaštík and Varga 2021). With this work we also could confirm that the traditional consumer-grade GNSS receiver (Garmin Oregon 700) was more likely affected by the multipath issue, through correlation analysis of the forest variables we developed, compared to the mapping-grade GNSS receiver and the smartphone, simply based on the number of forest variables having significant correlation with positional error. Interestingly, the smartphone had the same number of forest variables with significant correlations with positional accuracy as the mapping-grade GNSS receiver. This suggests that smartphone GNSS technology may be approaching the technological sophistication (hence accuracy levels) obtainable with much more expensive field data collection equipment.

This study focused on the effect of horizontal structure of nearby vegetation. As satellite signals emitted from outer space travel through Earth's atmosphere, the quality of signals may be more affected by the vertical structure of nearby vegetation (the last 30-60 m of travel before being used) which may be related to the shape of tree crowns and tree architecture. As removing multipath error may be almost impossible in a real environment, a further study to scrutinize the impact of nearby vegetation seems necessary. Our study suggests that the raw GNSS measurements, such as SNR, should be examined, and that new forest variables should be developed in an attempt to help explain the impact of nearby vegetation on horizontal position accuracy of GNSS devices.

Conclusion

The feasibility of a smartphone (iPhone 12 Pro) for mapping positions within a forested environment was investigated by comparing the horizontal position error with similar data from a consumer-grade GNSS receiver and a mapping-grade GNSS receiver. It was noteworthy that the smartphone illustrated significantly lower horizontal position error than a consumer-grade GNSS receiver, but significantly higher positional error than a mapping-grade GNSS receiver. However, the range of horizontal positional error for the smartphone was closer to the range of positional error observed by a mapping-grade GNSS receiver. Recent advances in GNSS chipset technology, especially for smartphones, might further enhance their positioning performance, but as with all new technology, these issues need to be constantly assessed. In this study we also investigated the potential correlation between forest variables that might induce multipath error and the observed horizontal position error. We found significant correlations between forest variables and horizontal position error regardless of the GNSS receiver employed, yet more correlations were observed with respect to the horizontal position error of the consumer-grade GNSS receiver. This suggests that the horizontal position error of the consumer-grade GNSS receiver was more likely affected by forest variables than was the horizontal position error of the smartphone and the mapping-grade GNSS receiver. In addition, it was confirmed that the location, but not the size, of nearby trees may be the primary factor in deteriorating the horizontal positional accuracy. Given these results, generalizing the multipath effect of nearby vegetation on horizontal position accuracy might be more complicated than we assumed.

References

Bettinger, P. and Merry, K.L., 2011. Global navigation satellite system research in forest management. LAP Lambert Academic Publishing, Saarbrücken, Germany. 64 p.

Bettinger, P. and Merry, K.L., 2012. Influence of the juxtaposition of trees on consumer-grade GPS position quality. Mathematical and Computational Forestry & Natural-Resource Sciences, 4(2), 81-91.

Bettinger, P., Merry, K., Bayat, M. and Tomaštík, J., 2019. GNSS use in forestry-A multi-national survey from Iran, Slovakia and southern USA. Computers and Electronics in Agriculture, 158, 369-383.

Danskin, S., Bettinger, P. and Jordan, T., 2009. Multipath mitigation under forest canopies: A choke ring antenna solution. Forest Science, 55(2), 109-116.

Fortunato, M., Critchley-Marrows, J., Siutkowska, M., Ivanovici, M.L., Benedetti, E. and Roberts, W., 2019. Enabling high accuracy dynamic applications in urban environments using PPP and RTK on android multi-frequency and multi-GNSS smartphones. In 2019 European navigation conference (ENC). IEEE, New York. pp. 1-9.

Gogoi, N., Minetto, A., Linty, N. and Dovis, F., 2019. A controlled-environment quality assessment of android GNSS raw measurements. Electronics, 8(1), Article 5.

Humphreys, T.E., Murrian, M., van Diggelen, F., Podshivalov, S. and Pesyna Jr., K.M., 2016. April. On the feasibility of cm-accurate positioning via a smartphone's antenna and GNSS chip. In 2016 IEEE/ION position, location and navigation symposium (PLANS). IEEE, New York. pp. 232-242.

IDC Corporate USA, 2021. Smartphone market share. https://www.idc.com/promo/smartphone-market-share (accessed 17 March 2022).

Keefe, R.F., Wempe, A.M., Becker, R.M., Zimbelman, E.G., Nagler, E.S., Gilbert, S.L. and Caudill, C.C., 2019. Positioning methods and the use of location and activity data in forests. Forests, 10(5), Article 458.

Lachapelle, G., Gratton, P., Horrelt, J., Lemieux, E. and Broumandan, A., 2018. Evaluation of a low cost hand held unit with GNSS raw data capability and comparison with an android smartphone. Sensors, 18(12), Article 4185.

Lee, T., Bettinger, P., Cieszewski, C.J. and Gutierrez Garzon, A.R., 2020. The applicability of recreation-grade GNSS receiver (GPS watch, Suunto Ambit Peak 3) in a forested and an open area compared to a mapping-grade receiver (Trimble Juno T41). PLoS ONE. 15(4), Article e0231532.

Li, G. and Geng, J., 2019. Characteristics of raw multi-GNSS measurement error from Google Android smart devices. GPS Solutions, 23(3), Article 90.

Li, X., Zhang, X., Ren, X., Fritsche, M., Wickert, J. and Schuh, H., 2015. Precise positioning with current multi-constellation global navigation satellite systems: GPS, GLONASS, Galileo and BeiDou. Scientific Reports, 5, Article 8328.

Menard, T., Miller, J., Nowak, M. and Norris, D., 2011. Comparing the GPS capabilities of the Samsung Galaxy S, Motorola Droid X, and the Apple iPhone for vehicle tracking using FreeSim_Mobile. In 2011 14th International IEEE Conference on Intelligent Transportation Systems (ITSC). IEEE, New York. pp. 985-990.

Murgaš, V., Sačkov, I., Sedliak, M., Tunák, D. and Chudý, F., 2018. Assessing horizontal accuracy of inventory plots in forests with different mix of tree species composition and development stage. Journal of Forest Science, 64(11), 478-485.

Paziewski, J., 2020. Recent advances and perspectives for positioning and applications with smartphone GNSS observations. Measurement Science and Technology, 31(9), Article 091001.

Ransom, M.D., Rhynold, J. and Bettinger, P., 2010. Performance of mapping-grade GPS receivers in southeastern forest conditions. RURALS: Review of Undergraduate Research in Agricultural and Life Sciences, 5(1), Article 2.

Sigrist, P., Coppin, P. and Hermy, M., 1999. Impact of forest canopy on quality and accuracy of GPS measurements. International Journal of Remote Sensing, 20(18), 3595-3610.

Tobler, W.R., 1970. A computer movie simulating urban growth in the Detroit region. Economic Geography, 46, 234-240.

Tomaštík, J., Chudá, J., Tunák, D., Chudý, F. and Kardoš, M., 2021. Advances in smartphone positioning in forests: dual-frequency receivers and raw GNSS data. Forestry, 94(2), 292-310.

Tomaštík, J. and Varga, M., 2021. Practical applicability of processing static, short-observation-time raw GNSS measurements provided by a smartphone under tree vegetation. Measurement, 178, Article 109397.

Trimble Forestry Automation, 2012. Solo Forest™ data sheet. Trimble Forestry Automation, Corvallis, OR.

Wang, L., Groves, P.D. and Ziebart, M.K., 2012. Multi-constellation GNSS performance evaluation for urban canyons using large virtual reality city models. The Journal of Navigation, 65(3), 459-476.

Yoon, D., Kee, C., Seo, J. and Park, B., 2016. Position accuracy improvement by implementing the DGNSS-CP algorithm in smartphones. Sensors, 16(6), Article 910.

Zandbergen, P.A. and Barbeau, S.J., 2011. Positional accuracy of assisted GPS data from high-sensitivity GPS-enabled mobile phones. The Journal of Navigation, 64(3), 381-399.

Zangenehnejad, F. and Gao, Y., 2021. GNSS smartphones positioning: Advances, challenges, opportunities, and future perspectives. Satellite Navigation, 2, Article 24.

Zhang, X., Tao, X., Zhu, F., Shi, X. and Wang, F., 2018. Quality assessment of GNSS observations from an Android N smartphone and positioning performance analysis using time-differenced filtering approach. GPS Solutions, 22(3), Article 70.

CHAPTER 5

Conclusion

GNSS technologies are essential components in forestry and forest management. Positioning and mapping functions of GNSS technologies are integral to various types of forest management activities, and over time positional accuracy has improved. It is expected that the importance of GNSS technologies not only in forestry but also in society will continue to increase in the future. Therefore, this dissertation presented three studies conducted along one main line: the analysis of GNSS point locations in forested areas.

Chapter 2 evaluated the applicability of a GPS watch by comparing its positional accuracy to a mapping-grade GNSS receiver in various forest conditions, seasons, and meteorological conditions. Although many studies have evaluated the positional accuracy of GNSS receivers in forested conditions, this study was the first to apply the standard deviational ellipse method to assess accuracy, which is not a common measurement in the forestry field. The standard deviational ellipse method quantifies the spatial distribution of points (locations) observed by GNSS receivers. The results when using the standard deviational ellipse method confirmed that the points (locations) observed by GNSS receivers tended to be biased to a certain direction (Western side) from the true locations. This study also confirmed that the positional accuracy of GPS watches (a non-traditional consumer-grade receiver) was significantly affected by the season of the year not by forest cover type. In addition, the positional accuracy of the GPS watch represented a similar level of positional accuracy to the mapping-grade receiver during the

leaf-off season. These findings suggested that the density of canopy coverage might have more influence on positional accuracy rather than differences in forest type. Lastly, it was confirmed that the positional accuracy of GNSS receivers applied in this study was significantly affected by the local air temperature and absolute humidity. However, there was a possibility that the environmental conditions at the nearby airport could be different from the conditions in the forested area, which is a limitation of this study. This study still contributed to science by evaluating the applicability of a non-traditional GNSS receiver in forested areas and by illustrating the applicability of standard deviational ellipse method to analyze the distribution of points (location) observed by GNSS receivers.

Chapter 3 concerned the ability of GNSS point locations to adequately represent the true positions and spatial patterns of trees in a forest, as these positions are increasingly being used in research and popular culture to represent phenomena and relationships of interest to society. This study was conducted within a pine seed orchard where the trees were established in a regular pattern. The positional accuracy of various GNSS receivers was evaluated in these conditions, and various point pattern analysis methods were applied on the observed points (trees) patterns and true tree locations. This study confirmed that the measurement methods significantly affect the positional accuracy regardless of GNSS receiver type. These results suggested that a greater number of observations around a control (true location) does not guarantee higher positional accuracy regardless of GNSS receiver type. The standard deviational ellipse method revealed that the observed points (locations) were biased to the South and West side of the true locations. Further, the point patterns described by the locations of trees captured by GNSS receivers failed to represent the real pattern of those trees. This study contributed to science by suggesting the

usage of non-augmented GNSS technology, which is typical in the forestry practice today for collecting field data, even when representing acceptable ranges of positional error, might misrepresent the actual spatial pattern of trees in forested area. In addition, this study suggested technological enhancements might be necessary to maintain the fidelity of spatial data in forested conditions.

Chapter 4 involved understanding whether there are structural conditions of a forest that can be correlated with horizontal position error observed with GNSS point locations. Within a study area, various forest variables were developed based on the vicinity and size of nearby vegetation to true ground locations. These forest variables were used to examine the correlations with positional error observed from point locations captured by GNSS receivers. This study confirmed that a smartphone, which is considered the most prevalent GNSS receiver today, had a similar level of positional error to a mapping-grade receiver. In comparison to a consumer-grade receiver (traditional handheld type), the smartphone provided significantly lower positional error across the study site. Regardless of GNSS receiver type, the observed points described using GNSS receivers were predominantly biased to the South. Two forest variables seemed to be important in explaining the positional error of GNSS point locations. One related to the mean spatial center of nearby trees, and the other related to the amount of overlap in the standard deviational ellipses of the GNSS point locations and the nearby trees. This study contributed to science by further suggesting that the spatial distribution of nearby trees may be correlated with GNSS point accuracy. Also, this study confirmed that the location of nearby trees might have more influence on the positional error of GNSS receivers rather than the size of nearby trees.

In this dissertation, a consumer-grade GNSS receiver was tested for the various applications in forested areas. This dissertation provides evidence that consumer-grade GNSS receivers (which include smartphones) might someday obviate the need for replacing mapping-grade GNSS receivers in certain landscape conditions to achieve a similar level of positional accuracy. Further, the work conducted here casts doubt on the ability to apply spatial analysis to GNSS measurements that were collected without the use of space-based or ground-based augmentation systems, as the spatial pattern of trees collected under normal field practices may not represent correctly the true spatial pattern of trees in nature. This dissertation provided evidence of the effect of nearby vegetation contributing to multipath, and the outcomes might be more complicated than expected. GNSS technologies continue to improve, and perhaps one day GNSS receivers will be able to provide positional information in forests, without additional augmentation, similar to traditional surveying methods. While it is enjoyable to incorporate new technology into forestry field practices, proper evaluation of the technology seems necessary.

References

Aguirre, O., Hui, G., von Gadow, K. and Jiménez, J. 2003. An analysis of spatial forest structure using neighbourhood-based variables. Forest Ecology and Management, 183(1-3), 137-145.

Akbulut, R., Ucar, Z., Bettinger, P., Merry, K. and Obata, S. 2017. Effects of forest thinning on static horizontal positions collected with a mapping-grade GNSS receiver. Mathematical and Computational Forestry & Natural-Resource Sciences, 9(1), 14-21.

Atkinson, P.M., Foody, G.M., Gething, P.W., Mathur, A. and Kelly, C.K. 2007. Investigating spatial structure in specific tree species in ancient semi-natural woodland using remote sensing and marked point pattern analysis. Ecography, 30(1), 88-104.

Besag, J. 1977. Contribution to the discussion on Dr Ripley's paper. Journal of the Royal Statistical Society, Series B, 39, 193-195.

Bettinger, P. and Fei, S. 2010. One year's experience with a recreation-grade GPS receiver. Mathematical and Computational Forestry & Natural-Resource Sciences, 2(2), 153-160.

Bettinger, P. and Merry, K.L. 2011. Global navigation satellite system research in forest management: A summary of horizontal, vertical, static, and dynamic accuracy assessments. LAP Lambert Academic Publishing, Saarbrücken, Germany.

Bettinger, P. and Merry, K.L. 2012. Influence of the juxtaposition of trees on consumer-grade GPS position quality. Mathematical and Computational Forestry & Natural-Resource Sciences, 4(2), 81-91.

Bettinger, P. and Merry, K. 2012. Static horizontal positions determined with a consumer-grade GNSS receiver: One assessment of the number of fixes necessary. Croatian Journal of Forest Engineering, 33(1), 149-157.

Bettinger, P. and Merry, K. 2018. Follow-up study of the importance of mapping technology knowledge and skills for entry-level forestry job postings, as deduced from recent job advertisements. Mathematical and Computational Forestry & Natural-Resource Sciences, 10(1), 15-23.

Bettinger, P., Merry, K., Bayat, M. and Tomaštík, J. 2019. GNSS use in forestry – A multi-national survey from Iran, Slovakia and southern USA. Computers and Electronics in Agriculture, 158, 369-383.

Bevis, M., Businger, S., Herring, T.A., Rocken, C., Anthes, R.A. and Ware, R.H. 1992. GPS meteorology: Remote sensing of atmospheric water vapor using the Global Positioning System. Journal of Geophysical Research: Atmospheres, 97(D14), 15787-15801.

Cabinet Office, Government of Japan. 2022. Overview of the Quasi-Zenith Satellite System (QZSS). https://qzss.go.jp/en/overview/services/sv01_what.html (accessed June 2, 2022).

Carrer, M., Castagneri, D., Popa, I., Pividori, M. and Lingua, E. 2018. Tree spatial patterns and stand attributes in temperate forests: The importance of plot size, sampling design, and null model. Forest Ecology and Management, 407, 125-134.

China Satellite Navigation Office. 2020. BeiDou Navigation Satellite System Signal in space interface control document. version 1. http://en.beidou.gov.cn/was5/web/search?channelid=249204 (accessed June 2, 2022)

Clark, P.J. and Evans, F.C. 1954. Distance to nearest neighbor as a measure of spatial relationships in populations. Ecology, 35(4), 445-453.

Coster, A., Williams, J., Weatherwax, A., Rideout, W. and Herne, D. 2013. Accuracy of GPS total electron content: GPS receiver bias temperature dependence. Radio Science, 48(2), 190-196.

Danskin, S., Bettinger, P. and Jordan, T. 2009. Multipath mitigation under forest canopies: A choke ring antenna solution. Forest Science, 55(2), 109-116.

Danskin, S.D., Bettinger, P., Jordan, T.R. and Cieszewski, C. 2009. A comparison of GPS performance in a southern hardwood forest: Exploring low-cost solutions for forestry applications. Southern Journal of Applied Forestry, 33(1), 9–16.

Department of Space, Indian Space Research Organisation. 2022. Indian Regional Navigation Satellite System (IRNSS): NavIC. https://www.isro.gov.in/irnss-programme (accessed June 2, 2022).

Diggle, P.J. 2013. Statistical analysis of spatial and spatio-temporal point patterns. Monographs on Statistics and Applied Probability 128. CRC press, Boca Raton, FL.

Dohn, J., Augustine, D.J., Hanan, N.P., Ratnam, J. and Sankaran, M. 2017. Spatial vegetation patterns and neighborhood competition among woody plants in an East African savanna. Ecology, 98(2), 478-488.

Dussault, C., Courtois, R., Ouellet, J.P. and Huot, J. 1999. Evaluation of GPS telemetry collar performance for habitat studies in the boreal forest. Wildlife Society Bulletin, 27(4), 965-972.

Edson, C. and M.G. Wing. 2012. Tree location measurement accuracy with a mapping-grade GPs receiver under forest canopy. Forest Science, 58(6), 567-576.

European Space Agency. 2019. What is Galileo? https://www.esa.int/Applications/Navigation/Galileo/What_is_Galileo (accessed June 2, 2022).

Fajardo, A., Goodburn, J.M. and Graham, J. 2006. Spatial patterns of regeneration in managed uneven-aged ponderosa pine/Douglas-fir forests of Western Montana, USA. Forest Ecology and Management, 223, 255-266.

Fan, Y., Feng, Z., Mannan, A., Khan, T.U., Shen, C. and Saeed, S. 2018. Estimating tree position, diameter at breast height, and tree height in real-time using a mobile phone with RGB-D SLAM. Remote Sensing, 10(11), Article 1845.

Fauzi, M.F., Idris, N.H., Din, A.H.M., Osman, M.J. and Ishak, M.H.I., 2016a. Indigenous community tree inventory: Assessment of data quality. The International Archives of the Photogrammetry, Remote Sensing and Spatial Information Sciences, 42(4), 307-314.

Fauzi, M.F., Idris, N.H., Yahya, M., Din, A., Lau, A. and Ishak, M. 2016. Tropical forest tree positioning accuracy: A comparison of low cost GNSS-enabled devices. International Journal of Geoinformatics, 12(2), 59-66.

Fortunato, M., Critchley-Marrows, J., Siutkowska, M., Ivanovici, M.L., Benedetti, E. and Roberts, W. 2019. Enabling high accuracy dynamic applications in urban environments using PPP and RTK on android multi-frequency and multi-GNSS smartphones. In 2019 European navigation conference (ENC). IEEE, New York.

Gadow, K.V. and Hui, G.Y. 2002. Characterizing forest spatial structure and diversity. Sustainable Forestry in Temperate Regions; Björk, L. (ed). SUFOR, University of Lund, Lund, Sweden, 20-30.

Gadow, K.V., Zhang, C.Y., Wehenkel, C., Pommerening, A., Corral-Rivas, J., Korol, M., Myklush, S., Hui, G.Y., Kiviste, A. and Zhao, X.H. 2012. Forest structure and diversity. In Continuous cover forestry. pp. 29-83. Springer, Dordrecht, The Netherlands.

Garzon-Lopez, C.X., Jansen, P.A., Bohlman, S.A., Ordonez, A. and Olff, H. 2014. Effects of sampling scale on patterns of habitat association in tropical trees. Journal of Vegetation Science, 25(2), 349-362.

Gløersen, Ø., Kocbach, J. and Gilgien, M. 2018. Tracking performance in endurance racing sports: evaluation of the accuracy offered by three commercial GNSS receivers aimed at the sports market. Frontiers in Physiology, 9, Article 1425.

Gogoi, N., Minetto, A., Linty, N. and Dovis, F. 2019. A controlled-environment quality assessment of android GNSS raw measurements. Electronics, 8(1), Article 5.

Green, L.Y., Mikhailova, E.A., Post, C.J., Darnault, C.C., Bridges, W.C. and Schlautman, M.A. 2016. A cloud-based spatial-temporal inventory for sustainable urban soil management. Urban ecosystems, 19(2), 811-822.

GSA. 2019. GNSS Market Report Issue 6, European GNSS Agency (GSA) Publications, Luxembourg. doi:10.2878/031762.

Guerova, G., Jones, J., Douša, J., Dick, G., de Haan, S., Pottiaux, E., Bock, O., Pacione, R., Elgered, G., Vedel, H. and Bender, M. 2016. Review of the state of the art and future prospects of the ground-based GNSS meteorology in Europe. Atmospheric Measurement Techniques, 9(11), 5385-5406.

Hui, G., Li, L., Zhao, Z. and Dang, P. 2007. Comparison of methods in analysis of the tree spatial distribution pattern. Acta Ecologica Sinica, 27(11), 4717-4728.

Humphreys, T.E., Murrian, M., van Diggelen, F., Podshivalov, S. and Pesyna Jr., K.M. 2016. April. On the feasibility of cm-accurate positioning via a smartphone's antenna and GNSS chip. In 2016 IEEE/ION position, location and navigation symposium (PLANS). IEEE, New York. 232-242.

Hung, I., Unger, D., Kulhavy, D. and Zhang, Y. 2019. Positional precision analysis of orthomosaics derived from drone captured aerial imagery. Drones, 3(2), Article 46.

IDC Corporate USA, 2021. Smartphone market share. https://www.idc.com/promo/smartphone-market-share (accessed June 2, 2022).

Illian, J., Penttinen, A., Stoyan, H. and Stoyan, D. 2008. Statistical analysis and modelling of spatial point patterns. John Wiley & Sons Ltd., West Sussex, England.

Ioannides, R.T., Pany, T. and Gibbons, G. 2016. Known vulnerabilities of global navigation satellite systems, status, and potential mitigation techniques. Proceedings of the IEEE, 104(6), 1174-1194.

Ji, G.H., Shin, H. and Won, J.H. 2021. Analysis of multi-constellation GNSS receiver performance utilizing 1-st side-lobe signal on the use of SSV for KPS satellites. IET Radar, Sonar & Navigation, 15(5), 485-499.

Keefe, R.F., Wempe, A.M., Becker, R.M., Zimbelman, E.G., Nagler, E.S., Gilbert, S.L. and Caudill, C.C. 2019. Positioning methods and the use of location and activity data in forests. Forests, 10(5), Article 458.

Khot, L.R., Tang, L., Blackmore, S.B. and Nørremark, M. 2006. Navigational context recognition for an autonomous robot in a simulated tree plantation. Transactions of the ASABE, 49(5), 1579-1588.

Kiser, J. 2008. Chapter 1, Surveying. In Part 650, Engineering field handbook. U.S. Department of Agriculture, Natural Resources Conservation Service, Washington, D.C.

Klimánek, M. 2010. Analysis of the accuracy of GPS Trimble JUNO ST measurement in the conditions of forest canopy. Journal of Forest Science, 56(2), 84-91.

Lachapelle, G., Gratton, P., Horrelt, J., Lemieux, E. and Broumandan, A. 2018. Evaluation of a low cost hand held unit with GNSS raw data capability and comparison with an android smartphone. Sensors, 18(12), Article 4185.

Law, R., Illian, J., Burslem, D.F., Gratzer, G., Gunatilleke, C.V.S. and Gunatilleke, I.A.U.N. 2009. Ecological information from spatial patterns of plants: insights from point process theory. Journal of Ecology, 97(4), 616-628.

Lee, T., Bettinger, P., Cieszewski, C.J. and Gutierrez Garzon, A.R. 2020. The applicability of recreation grade GNSS receiver (GPS watch, Suunto Ambit Peak 3) in a forested and an open area compared to a mapping-grade receiver (Trimble Juno T41). PLoS ONE, 15(3), e0231532.

Lewis, J.S., Rachlow, J.L., Garton, E.O. and Vierling, L.A. 2007. Effects of habitat on GPS collar performance: using data screening to reduce location error. Journal of Applied Ecology, 44(3), 663-671.

Li, G. and Geng, J. 2019. Characteristics of raw multi-GNSS measurement error from Google Android smart devices. GPS Solutions, 23(3), Article 90.

Li, X., Zhang, X., Ren, X., Fritsche, M., Wickert, J. and Schuh, H. 2015. Precise positioning with current multi-constellation global navigation satellite systems: GPS, GLONASS, Galileo and BeiDou. Scientific Reports, 5(1), Article 8328.

Liu, W., Jiao, B., Hao, J., Lv, Z., Xie, J. and Liu, J. 2022. Signal-in-space range error and positioning accuracy of BDS-3. Scientific Reports, 12(1), Article 8181.

Menard, T., Miller, J., Nowak, M. and Norris, D. 2011. Comparing the GPS capabilities of the Samsung Galaxy S, Motorola Droid X, and the Apple iPhone for vehicle tracking using FreeSim_Mobile. In 2011 14th International IEEE Conference on Intelligent Transportation Systems (ITSC). IEEE, New York. pp. 985-990.

Merry, K. and Bettinger, P. 2019. Smartphone GPS accuracy study in an urban environment. PLoS ONE, 14(7), e0219890.

Montenbruck, O., Steigenberger, P. and Hauschild, A. 2015. Broadcast versus precise ephemerides: a multi-GNSS perspective. GPS Solutions, 19(2), 321-333.

Moustakas, A., Wiegand, K., Getzin, S., Ward, D., Meyer, K.M., Guenther, M. and Mueller, K.H. 2008. Spacing patterns of an Acacia tree in the Kalahari over a 61-year period: How clumped becomes regular and vice versa. Acta Oecologica, 33(3), 355-364.

Murgaš, V., Sačkov, I., Sedliak, M., Tunák, D. and Chudý, F. 2018. Assessing horizontal accuracy of inventory plots in forests with different mix of tree species composition and development stage. Journal of Forest Science, 64(11), 478-485.

Næsset, E. and Gjevestad, J.G. 2008. Performance of GPS precise point positioning under conifer forest canopies. Photogrammetric Engineering & Remote Sensing, 74(5), 661-668.

Omr, M., Georgy, J. and Noureldin, A. 2017. Using multiple portable/wearable devices for enhanced misalignment estimation in portable navigation. GPS solutions, 21(2), 393-404.

Ordoñez, C., Martínez, J., de Cos Juez, J.F. and Lasheras, F.S. 2012. Comparison of GPS observations made in a forestry setting using functional data analysis. International Journal of Computer Mathematics, 89(3), 402-408.

Parkinson, B.W., S.T. Powers, G. Green, H. Fruehauf, B. Strom, S. Gilbert, W. Melton, B. Huston, E. Martin, J. Spilker, F. Natali, J. Strada, B. Glazer, D. Schwartz, T. Stansell and others. 2010. The origins of GPS, and the pioneers who launched the system. GPS World, 21(6), 8-18.

Paziewski, J. 2020. Recent advances and perspectives for positioning and applications with smartphone GNSS observations. Measurement Science and Technology, 31(9), Article 091001.

Perry, G.L., Miller, B.P. and Enright, N.J. 2006. A comparison of methods for the statistical analysis of spatial point patterns in plant ecology. Plant Ecology, 187(1), 59-82.

Pham, N.D. 2011. The economics of disruption: $96 billion annually at risk, GPS World. https://www.gpsworld.com/gnss-systemthe-economics-disruption-96-billion-annually-risk-11825/ (accessed June 2, 2022).

Pirti, A. 2005. Using GPS near the forest and quality control. Survey Review, 38(298), 286-298.

Pommerening, A. 2002. Approaches to quantifying forest structures. Forestry, 75(3), 305–324.

Pommerening, A. 2008. Analysing and modelling spatial woodland structure. Bangor University, Wales, UK (DSc dissertation), University of Natural Resources and Applied Life Sciences, Vienna, Austria.

Pommerening, A. and Grabarnik, P. 2019. Individual-based methods in forest ecology and management. Springer Nature Switzerland, Cham.

Ransom, M.D., Rhynold, J. and Bettinger, P. 2010. Performance of mapping-grade GPS receivers in southeastern forest conditions. RURALS: Review of Undergraduate Research in Agricultural and Life Sciences, 5(1), Article 2.

Ripley, B. 1981. Spatial statistics. John Wiley & Sons, Inc., New York.

Roskosmos State Corporation. n.d. About GLONASS. https://www.glonass-iac.ru/en/about_glonass/ (accessed June 2, 2022).

Sanou, D.A. 2013. Analysis of GNSS interference impact on society and evaluation of spectrum protection strategies. Positioning, 4(2), 169-182.

Schipperijn, J., Kerr, J., Duncan, S., Madsen, T., Klinker, C.D. and Troelsen, J. 2014. Dynamic accuracy of GPS receivers for use in health research: a novel method to assess GPS accuracy in real-world settings. Frontiers in Public Health, 10(2), Article 21.

Seidler, T.G. and Plotkin, J.B. 2006. Seed dispersal and spatial pattern in tropical trees. PLoS Biology, 4(11), e344.

Sigrist, P., Coppin, P. and Hermy, M. 1999. Impact of forest canopy on quality and accuracy of GPS measurements. International Journal of Remote Sensing, 20(18), 3595-3610.

Stoyan, D. and Stoyan, H. 1996. Estimating pair correlation functions of planar cluster processes. Biometrical Journal, 38(3), 259-271.

Tait, R.J., Allen, T.J., Sherkat, N. and Bellett-Travers, M.D. 2009. An electronic tree inventory for arboriculture management. Knowledge-Based Systems, 22(7), 552-556.

Teunissen, P.J. and Montenbruck, O. 2017. Springer handbook of global navigation satellite systems (Vol. 10). New York, NY, USA. Springer International Publishing.

Tomaštík, J., Chudá, J., Tunák, D., Chudý, F. and Kardoš, M. 2021. Advances in smartphone positioning in forests: dual-frequency receivers and raw GNSS data. Forestry, 94(2), 292-310.

Tomaštík, J., Tomaštík, J., Saloň, Š. and Piroh, R. 2017. Horizontal accuracy and applicability of smartphone GNSS positioning in forests. Forestry, 90(2), 187-198.

Tomaštík, J. and Varga, M. 2021. Practical applicability of processing static, short-observation-time raw GNSS measurements provided by a smartphone under tree vegetation. Measurement, 178, Article 109397.

Trimble Forestry Automation, 2012. Solo Forest™ data sheet. Trimble Forestry Automation, Corvallis, OR.

Trochta, J., Král, K., Janík, D. and Adam, D. 2013. Arrangement of terrestrial laser scanner positions for area-wide stem mapping of natural forests. Canadian Journal of Forest Research, 43(4), 355-363.

Ucar, Z., Bettinger, P., Weaver, S., Merry, K.L. and Faw, K. 2014. Dynamic accuracy of recreation-grade GPS receivers in oak-hickory forests. Forestry, 87(4), 504-511.

Uria-Diez, J. and Pommerening, A. 2017. Crown plasticity in Scots pine (*Pinus sylvestris* L.) as a strategy of adaptation to competition and environmental factors. Ecological Modelling, 356, 117-126.

U.S. Department of Commerce, National Oceanic Atmospheric Administration. 2022. GPS: The Global Positioning System. www.GPS.gov (accessed June 2, 2022).

Vacchiano, G., Castagneri, D., Meloni, F., Lingua, E. and Motta, R. 2011. Point pattern analysis of crown-to-crown interactions in mountain forests. Procedia Environmental Sciences, 7, 269-274.

Velázquez, E., Martínez, I., Getzin, S., Moloney, K.A. and Wiegand, T. 2016. An evaluation of the state of spatial point pattern analysis in ecology. Ecography, 39(11), 1042-1055.

Wang, L., Groves, P.D. and Ziebart, M.K. 2012. Multi-constellation GNSS performance evaluation for urban canyons using large virtual reality city models. The Journal of Navigation, 65(3), 459-476.

Weaver, S.A., Ucar, Z., Bettinger, P. and Merry, K. 2015. How a GNSS receiver is held may affect static horizontal position accuracy. PLoS ONE, 10(4), e0124696.

Wiegand, T., He, F. and Hubbell, S.P. 2013. A systematic comparison of summary characteristics for quantifying point patterns in ecology. Ecography, 36(1), 92-103.

Wiegand, T. and Moloney, K.A. 2013. Handbook of spatial point-pattern analysis in ecology. CRC Press, Boca Raton, FL.

Wing, M.G. 2008. Consumer-grade global positioning systems (GPS) receiver performance. Journal of Forestry, 106(4), 185-190.

Wing, M.G., Eklund, A. and Kellogg, L.D. 2005. Consumer-grade global positioning system (GPS) accuracy and reliability. Journal of forestry, 103(4), 169-173.

Woodall, C. 2002. Point pattern analysis of FIA data. In Proceedings of the Third Annual Forest Inventory and Analysis Symposium, McRoberts, R.E., Reams, G.A., Van Deusen, P.C. and Moser, J.W., (eds.). U.S. Department of Agriculture, Forest Service, North Central Research Station, St. Paul, MN. General Technical Report NC-230. pp. 162-170.

Xu, J., Gu, H., Meng, Q., Cheng, J., Liu, Y., Sheng, J., Deng, J. and Bai, X. 2019. Spatial pattern analysis of *Haloxylon ammodendron* using UAV imagery-A case study in the Gurbantunggut Desert. International Journal of Applied Earth Observation and Geoinformation, 83, Article 101891.

Yoon, D., Kee, C., Seo, J. and Park, B. 2016. Position accuracy improvement by implementing the DGNSS-CP algorithm in smartphones. Sensors, 16(6), Article 910.

Yuill, R.S. 1971. The standard deviational ellipse; an updated tool for spatial description. Geografiska Annaler: Series B, Human Geography, 53(1), 28-39.

Zandbergen, P.A. and Barbeau, S.J. 2011. Positional accuracy of assisted GPS data from high-sensitivity GPS-enabled mobile phones. The Journal of Navigation, 64(3), 381-399.

Zangenehnejad, F. and Gao, Y. 2021. GNSS smartphones positioning: Advances, challenges, opportunities, and future perspectives. Satellite Navigation, 2, Article 24.

Zhang, X., Tao, X., Zhu, F., Shi, X. and Wang, F. 2018. Quality assessment of GNSS observations from an Android N smartphone and positioning performance analysis using time-differenced filtering approach. GPS Solutions, 22(3), Article 70.